QUANTUM MECHANICS WITH APPLICATIONS TO QUARKONIUM

C. QUIGG

Fermi National Accelerator Laboratory, P.O. Box 500, Batavia, Illinois 60510, U.S.A.

and

Jonathan L. ROSNER

School of Physics and Astronomy, University of Minnesota, Minneapolis, Minnesota 55455, U.S.A.

NORTH-HOLLAND PUBLISHING COMPANY - AMSTERDAM

PHYSICS REPORTS (Review Section of Physics Letters) 56, No. 4 (1979) 167–235. North-Holland Publishing Company

QUANTUM MECHANICS WITH APPLICATIONS TO QUARKONIUM

C. QUIGG

Fermi National Accelerator Laboratory, P.O. Box 500, Batavia, Illinois 60510, U.S.A.

and

Jonathan L. ROSNER

School of Physics and Astronomy, University of Minnesota, Minneapolis, Minnesota 55455, U.S.A.

Received May 1979

Contents:

Abstract:

Some methods of nonrelativistic quantum mechanics which are particularly useful for studying the variation of bound-state parameters with constituent mass and excitation energy are reviewed. These techniques rely upon elementary scaling arguments and on the semiclassical (WKB) approximation. They are of general interest, but are applied here to the study of bound systems of a heavy quark and antiquark. Properties of the interquark interaction are extracted from information about masses and leptonic widths of the ψ and Y families. It is shown how general methods can be applied to the determination of the electric charge of quarks and to the prediction of properties of new families.

1. Introduction

Nonrelativistic quantum mechanics, as embodied in the Schrödinger equation, is the source of much of our understanding of the structure of matter. In a rich variety of circumstances it provides the correct description of physical reality, in that a nonrelativistic treatment is entirely proper or that small relativistic corrections may be treated as well-controlled perturbations. This is the physics of atoms and molecules, of condensed matter, and of university courses in quantum mechanics: the physics of the "heroic age" of the mid-1920's†1. In many other instances, insights gained from the Schrödinger equation have provided indispensible guidance in the relativistic regime. One such episode is the profound influence of studies in potential scattering, as represented in the classic monograph by de Alfaro and Regge [2], upon the evolution of the S-matrix theory of strong interactions. Nuclear and particle physics abound in similar cases. All are characterized by the hope that reliable extrapolations can be made from a solvable nonrelativistic problem to a physically interesting problem which may be difficult to frame with precision or to solve.

Recently a new opportunity to productively employ nonrelativistic methods has presented itself to high energy physicists, in the discovery of the $\psi(3\ \mathrm{GeV}/c^2)$ and $\Upsilon(10\ \mathrm{GeV}/c^2)$ families of heavy neutral mesons. These are interpreted as bound states of a massive quark and antiquark ($Q\bar{Q}$) moving nonrelativistically. The prospect that heavy mesons can be identified as eigenstates of the Schrödinger equation has stimulated considerable activity directed toward the achievement of a predictive spectroscopy of hadrons. Efforts along these lines are encouraged by the special satisfaction that accompanies finding new uses for established techniques or noticing new consequences of familiar ideas.

Many applications of the Schrödinger equation to the new heavy mesons have been based on specific potentials with varying degrees of theoretical justification. Our aim in the present review is somewhat different. We shall show how some general methods, elementary but perhaps not well enough known, can be used to characterize families of mesons and the potentials responsible for them. Many results of specific potential models can be obtained from simple scaling or semiclassical considerations. Thus, we shall explore in this report the way in which various physical properties of heavy mesons can be expected to depend on coupling strength, quark mass, or excitation energy. A number of results promise to give insight into the nature of the interquark interaction: Is it independent of quark species? Does it approach a Coulombic form near the origin as expected from the exchange of a single massless gluon?

Although our recent interest in the Schrödinger equation is motivated by the promise of this program, the present report is not limited to the spectroscopy of heavy mesons. Indeed, for much of the article we shall deal with techniques and results which have more universal applicability. The topics to be discussed have aspects of pedagogical interest, and it will not surprise us to learn that they may illuminate physical issues unrelated to those that concern us. Not until all the techniques have been exhibited and the general results derived shall we present applications to the problems at (our) hand. Most of this report is therefore suited to the general reader, or to the student of undergraduate quantum mechanics.

Let us however briefly summarize the circumstances of the contemporary interest in these methods among high energy physicists. We believe†2 that hadrons are composed of quarks which, if not permanently confined, are at least very difficult to liberate. The nonobservation of free quarks†3

†1 A brief reminiscence of this period is given in ref. [1].

†2 The basis for this belief is summarized in refs. [3] and [4].

†3 Quark searches are reviewed in refs. [4–6]. Recent efforts to detect fractionally charged matter are reported in ref. [7].

suggests that the binding force is formidable, but the success of the quark parton model [8] in describing hard scattering processes argues that quarks nevertheless behave within hadrons as if quasi-free. Although it has not been proved to yield quark confinement, quantum chromodynamics (QCD)†4, the non-Abelian gauge theory of quarks interacting via massless vector quanta called gluons, promises to explain this paradoxical circumstance through the property of asymptotic freedom†5. Asymptotic freedom refers to the fact that in QCD, the strong interaction becomes feeble at large momentum transfers (short distances) so that quarks are weakly bound at small separations, but feel an increasingly strong restoring force at large separations.

On the basis of asymptotic freedom arguments, it was anticipated [13] that bound states of then conjectural heavy quarks might be described by a nonrelativistic analog of the bound e^+e^- system, positronium†6. The spectrum of positronium (Ps) is shown schematically in fig. 1. The ground state, a favorite textbook example [16], is split by the hyperfine interaction into the $J^{PC} = 1^{--}$ orthopositronium and $J^{PC} = 0^{-+}$ parapositronium components with lifetimes that differ by a factor of 1120. We refer to the hadronic counterpart of positronium generically as quarkonium.

At the end of 1974, the ψ/J (3095 MeV/c^2) was discovered [17, 18] in experiments at SLAC and Brookhaven. It was immediately recognized as exceptional because of its tiny decay width (67 keV), which may be understood [13] by analogy with the metastability of orthopositronium. The ψ is composed of a charmed quark and antiquark ($c\bar{c}$). In addition to the second-order electromagnetic decays illustrated in fig. 2(a), two sorts of strong decays may be contemplated. The first of these,

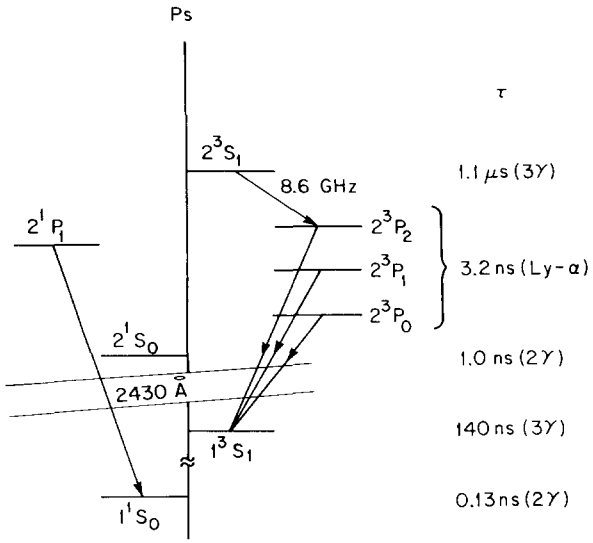

Fig. 1. A schematic representation of the spectrum of positronium. Principal decay modes are indicated. Here and elsewhere we shall use the spectroscopic notation $N^{2S+1}L_J$, where $N = n + l$ is the principal quantum number, n is the radial quantum number, S is the spin (0 or 1), L(=S, P, D, F, ...) deonotes the orbital angular momentum l(=0, 1, 2, 3, ...), and J is the total angular momentum.

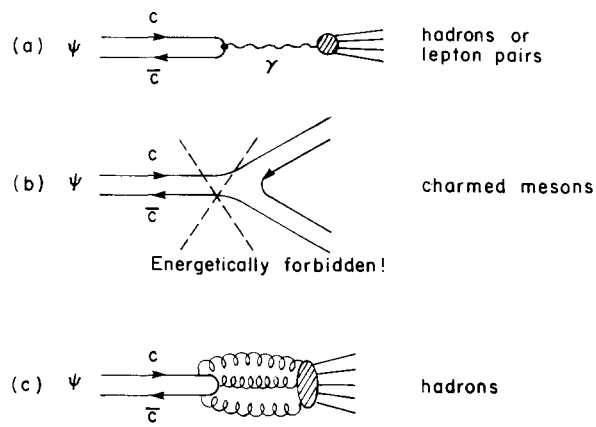

Fig. 2. (a) Second-order electromagnetic decay of ψ. (b) Energetically forbidden dissociation of ψ into charmed mesons. (c) Inhibited strong decay of ψ into ordinary hadrons.

†4 For a review, see ref. [9].

†5 Asymptotic freedom has been reviewed in ref. [10]. For further applications see refs. [11] and [12].

†6 For a general review of positronium, see ref. [14]. A review of hyperfine structure is given in ref. [15].

dissociation into a pair of charmed particles (shown in fig. 2(b)) is energetically forbidden. This kind of decay mechanism is the norm for ordinary hadrons. Finally, as indicated in fig. 2(c), the $c\bar{c}$ pair may annihilate into three (virtual) gluons which materialize into the observed ordinary hadrons. Three gluons, each transforming under the SU(3) color gauge group as a member of an octet, are required to reach the color singlet final state. This decay mechanism is inhibited by the smallness of the heavy quark coupling to gluons.

The experimentally-studied spectrum of the ψ, or charmonium, family is exceedingly rich,†7 as shown in fig. 3(a). Below the threshold for decay into pairs of charmed mesons lie the very narrow states $\psi(3095)$, $\psi'(3684)$, $\chi(3415)$, $\chi(3510)$, and $\chi(3550)$ for which quantum numbers are rather convincingly established. Above charm threshold lie the discrete vector states $\psi(3772)$ and $\psi(4414)$, and a thicket of levels around 4.1 GeV/c^2. In addition, there have been suggestions of states which may be pseudoscalar: X(2830), $\chi(3455)$, X(3600),†8 none of which is unambiguously identified. (See Note added in proof.) The spectroscopic notation for the psions as bound states of a charmed quark and antiquark is indicated in fig. 3(b).

In broad terms, the description of the psions as atomic levels of a nonrelativistic ($c\bar{c}$) system bound by a static potential has met with great success†9. The spectrum resembles a nonrelativistic level scheme, and there have been some predictive triumphs. The principal challenges to the ingenuous model have primarily to do with spin-orbit and hyperfine splittings. To do justice to the quantitative difficulties and

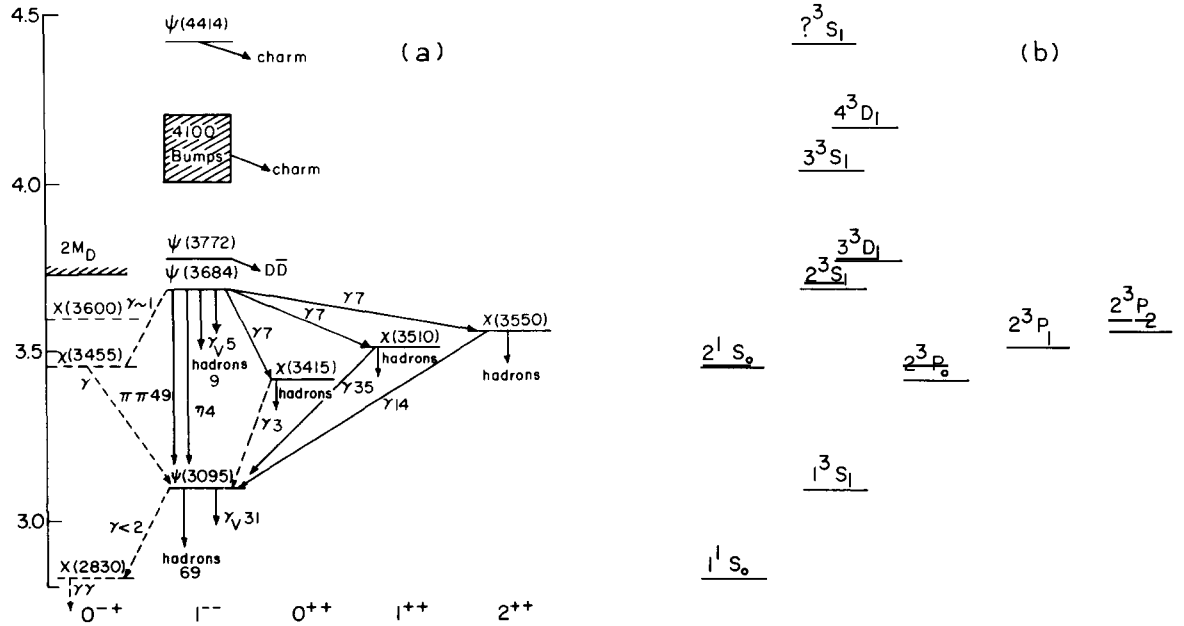

Fig. 3. (a) The spectrum of charmonium ($c\bar{c}$). Branching fractions (in percent) are shown for the important classes of decays. Charm threshold is indicated at twice the D meson mass. (b) Spectroscopic notation for the levels of charmonium. The identification of $^1S_0$ levels is speculative. See Note added in proof.

†7 Summaries of charmonium spectroscopy are given in refs. [19] and [20]. See also ref. [6] for references on individual states.

†8 Evidence for a few examples of the cascade $\psi(3684) \to \gamma + X(3600)$, $X(3600) \to \gamma + \psi(3095)$, with a combined probability of $(2.8 \pm 1.2) \times 10^{-3}$, has been presented in ref. [21]. The data are from the DESY-Heidelberg NaI-Pb Glass detector. See Note added in proof.

†9 Thorough reviews have been given in refs. [22–26]. A recent, but abbreviated, assessment appears in refs. [27] and [28].

proposed resolutions would take us too far afield†10. It will be enough to know that the Schrödinger equation approach does very well on the generalities of the charmonium system, and that the nonrelativistic approximation should be much better for families composed of heavier quarks. For the purposes of this report, we shall confine ourselves to the spin-triplet spectrum, which includes the important vector mesons, and neglect fine structure and hyperfine structure effects.

It is appropriate to ask what are the aspirations of a nonrelativistic quantum mechanics approach to quarkonium spectroscopy. We expect it to serve as a basis for a fertile phenomenology, a means of asking the right experimental questions and understanding how to interpret the answers. It can also provide specific guides to experiment. If the form of the interquark potential is known, there is for the first time in hadron physics the possibility of a predictive, rather than descriptive spectroscopy†11. In addition, many nontrivial predictions can be made even without precise knowledge of the potential. We will be concerned only in passing with adjusting explicit potentials to reproduce detailed features of the data.

The body of this report is organized as follows. In section 2 we review general consequences of the Schrödinger equation and theorems which do not depend upon restrictive conditions on the potential. Section 3 is devoted to the sharper results which hold for potentials which are simple powers of the interquark separation or depend logarithmically upon the separation. Semiclassical results are the subject of section 4. For many of the results discussed in sections 2–4, we relate unfamiliar general results to well-known special cases. In section 5 we turn our attention for the first time to quarkonium spectroscopy. There we review some earlier applications of scaling laws to the ψ and Y families. We compare two specific potentials for the charmonium and upsilon families in section 6. In section 7 we show how charges of the quarks in neutral vector mesons can be deduced from the leptonic decay widths of these mesons in a manner largely independent of details of the potential. In section 8 semiclassical methods are used to count narrow quarkonium levels by estimating the threshold for decays of the form shown in fig. 2(b). In a concluding section we survey the achievements and future promise of quarkonium quantum mechanics.

Encouragement to prepare this report has come from many of our colleagues who have convinced us that the style of quantum mechanics presented here is of interest to physicists of diverse backgrounds. We hope the reader will find in the study of this report as much entertainment and enlightenment as we have found in the writing.

2. The Schrödinger equation – General consequences

In this section we fix notation and derive some useful general consequences of the Schrödinger equation. The theorems that can be proved in potential theory are nearly limitless, as are the identities that can be deduced from the Schrödinger equation. Our principal object will be to find results which are convenient for the discussion of bound-state problems. We shall not discuss the complementary problem of quantum scattering, many aspects of which are summarized in the monograph by de Alfaro and Regge [2]. Almost without exception, the results presented here are not novel, but in only a few cases has it been possible to attribute them to the originators.

†10 An appealing (but perhaps rose-colored) response to the apparently large ^3S–^1S hyperfine splitting is to deny the existence (or at least the identity) of the pseudoscalar candidates. See the discussion in ref. [27], and Note added in proof.

†11 The description of systems containing only light quarks has relied, by contrast, to a much greater extent on group-theoretic interrelations among resonant particles and their decay amplitudes (see, e.g., refs. [4] and [29]). Dynamical descriptions of these systems have been of a cruder nature, though some insights have been gained from specific models (see, e.g., ref. [30]) and from QCD (see ref. [31]).

After introducing our notation, we shall derive (section 2.1) the Feynman–Hellmann theorem on the variation of the energy eigenvalue with parameters of the interaction, a result that we shall frequently apply. We shall then construct (section 2.2) the virial theorem and its generalizations. Of these, the connection between the wavefunction at the origin and the gradient of the potential occurs most often in the applications we discuss. A slightly technical digression (section 2.3) on bound-state normalizations may be omitted by the reader who is not concerned with details. The subsequent discussion of the mass dependence of wavefunctions (section 2.4) is important. We draw upon it many times in the rest of the article. A very brief treatment of quantum mechanical sum rules (section 2.5) is included for completeness, although no later developments build upon it.

The Schrödinger equation [32] in three dimensions is written in the form

$$-\frac{\hbar^2}{2\mu}\nabla^2\Psi(\boldsymbol{r})+[V(\boldsymbol{r})-E]\Psi(\boldsymbol{r})=0, \tag{2.1}$$

where μ is the reduced mass of the two-body system, $\boldsymbol{r}$ is the relative coordinate, $\Psi(\boldsymbol{r})$ is the Schrödinger wavefunction, $V(\boldsymbol{r})$ is the interaction potential, E is the energy eigenvalue, and $\hbar$ is Planck's constant divided by 2π. For the interesting case of a central potential, it is convenient to write

$$\Psi(\boldsymbol{r})=R(r)Y_{lm}(\theta,\phi), \tag{2.2}$$

where $R(r)$ is the radial wavefunction and $Y_{lm}(\theta,\phi)$ is a spherical harmonic†12. With this substitution, the Schrödinger equation separates and the radial wavefunction satisfies

$$-\frac{\hbar^2}{2\mu}\left(\frac{\mathrm{d}^2}{\mathrm{d}r^2}+\frac{2}{r}\frac{\mathrm{d}}{\mathrm{d}r}\right)R(r)-\left[E-V(r)-\frac{l(l+1)\hbar^2}{2\mu r^2}\right]R(r)=0. \tag{2.3}$$

The radial equation can be placed in formal correspondence with the one-dimensional Schrödinger equation by means of the substitution

$$u(r)\equiv rR(r), \tag{2.4}$$

which defines the reduced radial wavefunction. The reduced radial equation is then

$$-u''(r)=\frac{2\mu}{\hbar^2}\left[E-V(r)-\frac{l(l+1)\hbar^2}{2\mu r^2}\right]u(r), \tag{2.5}$$

subject to the boundary conditions

$$u(0)=0, \tag{2.6a}$$

$$u'(0)=R(0). \tag{2.6b}$$

We denote by a prime the derivative of a function with respect to its argument. Equation (2.5) is identical with the one-dimensional equation for an effective potential given by $V(r)+l(l+1)\hbar^2/2\mu r^2$, except that even parity solutions are inconsistent with the boundary conditions (2.6). The Schrödinger wavefunction is normalized,

$$\int \mathrm{d}^3\boldsymbol{r}|\Psi(\boldsymbol{r})|^2=1, \tag{2.7}$$

†12 We adopt the standard normalization $\int \mathrm{d}\Omega\, Y^*_{lm}(\theta,\phi)\, Y_{l'm'}(\theta,\phi)=\delta_{ll'}\delta_{mm'}$. See, for example, the appendix of ref. [33].

so that the reduced radial wavefunction satisfies†13

$$\int_0^\infty dr[u(r)]^2 = 1. \tag{2.8}$$

2.1. The Feynman–Hellmann theorem

As a first consequence of the Schrödinger equation, we show that the larger the constituent mass, the lower a specified bound state lies in a given potential. This result rests on a general theorem due to Feynman and Hellmann [34]. We write the Schrödinger equation in Hamiltonian form as

$$\mathscr{H}(\lambda)|\Psi\rangle = E(\lambda)|\Psi\rangle, \tag{2.9}$$

where λ is any parameter characterizing the interaction, such as potential strength or reduced mass. Then the variation of bound-state energy with the parameter λ is given by

$$\partial E/\partial\lambda = \langle \partial\mathscr{H}/\partial\lambda \rangle, \tag{2.10}$$

where $\langle\ \rangle$ denotes an expectation value. The proof is elementary. Since $E = \langle\mathscr{H}\rangle$,

$$\frac{\partial E}{\partial\lambda} = \frac{\partial}{\partial\lambda}\langle\Psi|\mathscr{H}|\Psi\rangle = \frac{\partial\langle\Psi|}{\partial\lambda}\mathscr{H}|\Psi\rangle + \langle\Psi|\frac{\partial\mathscr{H}}{\partial\lambda}|\Psi\rangle + \langle\Psi|\mathscr{H}\frac{\partial|\Psi\rangle}{\partial\lambda}. \tag{2.11}$$

Using (2.9), we rewrite the first and last terms to obtain

$$\partial E/\partial\lambda = \langle\partial\mathscr{H}/\partial\lambda\rangle + E(\langle(\partial\Psi/\partial\lambda)|\Psi\rangle + \langle\Psi|(\partial\Psi/\partial\lambda)\rangle). \tag{2.12}$$

The term proportional to E may be recognized as

$$E\frac{\partial}{\partial\lambda}\langle\Psi|\Psi\rangle = E\frac{\partial}{\partial\lambda}(1) = 0, \tag{2.13}$$

by virtue of (2.7), which establishes the theorem.

Early applications of this theorem were to physical situations such as molecular configurations for which λ is a parameter of the potential. An important case for our purposes is the variation of bound-state energy with reduced mass. For bound states in a three-dimensional potential, the Hamiltonian is, according to (2.1),

$$\mathscr{H}(\mu) = T(\mu) + V(\boldsymbol{r}) = -(\hbar^2\nabla^2/2\mu) + V(\boldsymbol{r}). \tag{2.14}$$

Consequently we have

$$\frac{\partial\mathscr{H}}{\partial\mu} = -\frac{1}{\mu}\left(-\frac{\hbar^2\nabla^2}{2\mu}\right) = -\frac{1}{\mu}(\mathscr{H} - V(\boldsymbol{r})). \tag{2.15}$$

The Feynman–Hellmann theorem (2.10) now yields

$$\frac{\partial E}{\partial\mu} = -\frac{1}{\mu}(E - \langle V\rangle) < 0, \tag{2.16}$$

which shows that as μ increases, the energy of a specified bound state decreases. Examples of this

†13 For one-dimensional problems, we shall adopt the normalization $\int_{-\infty}^{\infty} dx\,[u(x)]^2 = 1$ except where explicitly stated otherwise.

behavior will be given in section 3. The same result holds in any number of dimensions, for a Hamiltonian of the general form (2.14). For a central potential which is monotonically increasing with r, $V'(r) \geq 0$, the classical turning point r_c, defined through

$$V(r_c) = E, \tag{2.17}$$

will therefore decrease as well. A further application of relation (2.16) will be made in section 2.4.

2.2. The virial theorem and related theorems

Two results of considerable general utility for the study of bound states in a central potential are the virial theorem,

$$\langle T \rangle = E - \langle V \rangle = \langle \tfrac{1}{2} r(\mathrm{d}V/\mathrm{d}r) \rangle \tag{2.18}$$

and the connection between the s-wave wavefunction at the origin and the gradient of the potential,†14

$$|\Psi(0)|^2 = (\mu/2\pi\hbar^2)\langle \mathrm{d}V/\mathrm{d}r \rangle. \tag{2.19}$$

We shall derive these connections in a way that permits powerful generalizations for many simple potentials. It is convenient to define the function

$$\mathscr{L}(r) = (2\mu/\hbar^2)[E - V(r) - l(l+1)\hbar^2/2\mu r^2], \tag{2.20}$$

so that the Schrödinger equation may be written as

$$-u''(r) = \mathscr{L}(r)u(r). \tag{2.21}$$

We then multiply the Schrödinger equation by $r^q\, u'(r)$, where $q \geq -2l$, and integrate from 0 to ∞†15,

$$-\int_0^\infty \mathrm{d}r\, r^q\, u'(r)\, u''(r) = \int_0^\infty \mathrm{d}r\, r^q\, \mathscr{L}(r)\, u(r)\, u'(r). \tag{2.22}$$

Recognizing that $u'u'' = \tfrac{1}{2}(u'^2)'$ and that $uu' = \tfrac{1}{2}(u^2)'$, we integrate both sides by parts, whereupon

$$\begin{aligned} &-r^q[u'(r)]^2\Big|_0^\infty + q\int_0^\infty \mathrm{d}r\, r^{q-1}\,[u'(r)]^2 \\ &\quad = r^q\,\mathscr{L}(r)\,[u(r)]^2\Big|_0^\infty - q\int_0^\infty \mathrm{d}r\, r^{q-1}\,\mathscr{L}(r)\,[u(r)]^2 - \int_0^\infty \mathrm{d}r\, r^q\,\mathscr{L}'(r)\,[u(r)]^2. \end{aligned} \tag{2.23}$$

For bound states the boundary terms vanish at the upper limit of integration, leaving

$$r^q[u'(r)]^2\Big|_0 + q\int_0^\infty \mathrm{d}r\, r^{q-1}\,[u'(r)]^2 = -r^q\,\mathscr{L}(r)\,[u(r)]^2\Big|_0 - q\langle r^{q-1}\,\mathscr{L}(r)\rangle - \langle r^q\,\mathscr{L}'(r)\rangle. \tag{2.24}$$

†14 This relation has been ascribed to unpublished lecture notes of J. Schwinger. We first encountered it in ref. [35].

†15 In this and subsequent manipulations we take the lower limit of integration to be an infinitesimal quantity which is allowed to approach zero at the end.

To evaluate the remaining integral, we integrate again by parts:

$$q\int_0^\infty \mathrm{d}r\, r^{q-1}\,[u'(r)]^2 = qr^{q-1}\,u(r)\,u'(r)\Big|_0^\infty - q\int_0^\infty \mathrm{d}r\, r^{q-1}\,u(r)\,u''(r) - q(q-1)\int_0^\infty \mathrm{d}r\, r^{q-2}\,u(r)\,u'(r), \quad (2.25)$$

where the first term again vanishes at infinity. The second term is seen to be $+q\langle r^{q-1}\mathscr{L}(r)\rangle$, by using (2.21). A final integration by parts yields

$$-q(q-1)\int_0^\infty \mathrm{d}r\, r^{q-2}\,u(r)\,u'(r) = -\frac{q}{2}(q-1)\,r^{q-2}\,[u(r)]^2\Big|_0^\infty + \frac{q(q-1)(q-2)}{2}\langle r^{q-3}\rangle. \quad (2.26)$$

Assembling the pieces and again using the Schrödinger equation (2.21), we obtain

$$\begin{aligned}&[r^q[u'(r)]^2 - q\,r^{q-1}\,u(r)\,u'(r) + \tfrac{1}{2}q(q-1)r^{q-2}[u(r)]^2 - r^q\,u(r)\,u''(r)]_{r=0}\\ &\quad = -2q\langle r^{q-1}\mathscr{L}(r)\rangle - \langle r^q\mathscr{L}'(r)\rangle - \tfrac{1}{2}q(q-1)(q-2)\langle r^{q-3}\rangle. \end{aligned} \quad (2.27)$$

Near the origin, the reduced radial wavefunction for angular momentum l takes the form

$$u_l(r) \sim a_l r^{l+1}, \quad (2.28)$$

so that

$$u_l'(r) \sim (l+1)a_l r^l. \quad (2.29)$$

Evaluating (2.27) in the limit $r \to 0$, we find that

$$(2l+1)^2 a_l^2 \delta_{q,-2l} = -\langle 2qr^{q-1}\mathscr{L} + r^q\mathscr{L}' + \tfrac{1}{2}q(q-1)(q-2)r^{q-3}\rangle, \quad (2.30)$$

which holds for any power $q \geq -2l$.

To recover eq. (2.19) we set $l = 0$, $q = 0$, for which

$$a_0^2 = -\langle \mathscr{L}'(r)\rangle = (2\mu/\hbar^2)\langle \mathrm{d}V/\mathrm{d}r\rangle. \quad (2.31)$$

Next observe that according to (2.6b) and (2.29)

$$u'(0) = a_0 = R(0) = \sqrt{4\pi}\Psi(0), \quad (2.32)$$

so that

$$|\Psi(0)|^2 = (\mu/2\pi\hbar^2)\langle \mathrm{d}V/\mathrm{d}r\rangle. \quad (2.19)$$

The virial theorem follows from (2.30) with the choice $q = 1$: the equation

$$2\langle \mathscr{L}(r)\rangle = -\langle r\mathscr{L}'(r)\rangle \quad (2.33)$$

can be rearranged to read

$$E - \langle V\rangle \equiv \langle T\rangle = \langle \tfrac{1}{2}r(\mathrm{d}V/\mathrm{d}r)\rangle. \quad (2.18)$$

An important special case occurs for power-law potentials of the form

$$V(r) = \lambda r^\nu, \quad (2.34)$$

for which the kinetic, potential, and total energies are related by

$$\langle T\rangle = \tfrac{1}{2}\nu\langle V\rangle = \nu E/(2+\nu), \quad (2.35a)$$

or equivalently,

$$\langle V\rangle = 2E/(2+\nu). \tag{2.35b}$$

Thus for the linear potential ($\nu = 1$) we find

$$\langle r\rangle = (1/\lambda)\langle V\rangle = (2/3\lambda)E. \tag{2.36}$$

For the Coulomb potential ($\nu = -1$), the generalized virial theorem with $q = 2$ leads immediately to[†16]

$$\langle r\rangle = \frac{3\lambda}{4E} + \frac{l(l+1)\hbar^2}{2\mu\lambda} = \frac{3}{2\langle r^{-1}\rangle} + \frac{l(l+1)\hbar^2}{2\mu\lambda}. \tag{2.37}$$

Other practical uses of the general formula (2.30) include the determination of the coefficients a_l and, especially for the Coulomb and linear potentials, the evaluation of other spatial moments of the probability distribution. One-dimensional applications can be read off from (2.27), with the imposition of appropriate boundary conditions.

2.3. Bound state normalization

Consider the Schrödinger equation for a symmetric potential in one dimension, with $2\mu \equiv \hbar^2$ for convenience:

$$\phi''(x) + (E - V(x))\phi(x) = 0, \tag{2.38}$$

subject to the boundary conditions

$$\phi(0) = 1, \qquad \phi'(0) = 0, \tag{2.39a}$$

or

$$\phi(0) = 0, \qquad \phi'(0) = 1. \tag{2.39b}$$

This statement of the problem is chosen in practice for numerical calculations. At an eigenvalue $E = E_n$, $\phi(x) \to 0$ as $|x| \to \infty$.

It is of interest to evaluate the normalization integral

$$I \equiv \int_0^\infty \mathrm{d}x\, [\phi(x)]^2, \tag{2.40}$$

which is needed to construct normalized eigenfunctions. In one dimension these are given by

$$\psi(x) = \phi(x)/\sqrt{2I}. \tag{2.41}$$

For the three-dimensional problem in a symmetric potential, for which boundary conditions (2.39b) are appropriate, the (normalized) reduced radial wavefunction is

$$u(r) = \phi(r)/\sqrt{I}. \tag{2.42}$$

Since according to (2.32) the Schrödinger wavefunction at the origin is given by

[†16] This is an example of a relation given in ref. [33, p. 17]. Other choices of q in eq. (2.30) for the Coulomb problem give moments of r in terms of those determined previously, e.g. $q = 3$ gives $\langle r^2\rangle$ in terms of $\langle r\rangle$; $q = 0$ (for $l \neq 0$) gives $\langle r^{-3}\rangle$ in terms of $\langle r^{-2}\rangle$; $q = -1$ (for $l \neq 0$) gives $\langle r^{-4}\rangle$ in terms of $\langle r^{-3}\rangle$ and $\langle r^{-2}\rangle$; and so on. See ref. [36, vol. I, problem 1, p. 431].

$$\Psi(0) = u'(0)/\sqrt{4\pi}, \tag{2.32'}$$

we find that

$$|\Psi(0)|^2 = 1/4\pi I. \tag{2.43}$$

We now derive a useful expression for the normalization integral. Similar forms may be found in ref. [2].

Define the function

$$\tilde{\phi} \equiv \partial\phi/\partial E, \tag{2.44}$$

and differentiate the Schrödinger equation (2.38) with respect to E,

$$\tilde{\phi}'' + \phi + (E - V)\tilde{\phi} = 0. \tag{2.45}$$

Next multiply (2.38) by $\tilde{\phi}$ and (2.45) by ϕ, and subtract. The result is

$$\phi^2 = \tilde{\phi}\phi'' - \phi\tilde{\phi}'' = [\tilde{\phi}\phi' - \phi\tilde{\phi}']'. \tag{2.46}$$

Therefore the normalization integral (2.40) becomes

$$I = \int_0^\infty \mathrm{d}x\, [\phi(x)]^2 = [\tilde{\phi}\phi' - \phi\tilde{\phi}']_0^\infty. \tag{2.47}$$

With either set of boundary conditions, the contribution at the lower limit is zero. To compute the contribution at $x = \infty$, we express the wavefunction as a linear combination of solutions damped and unbounded at infinity. Let us write

$$\phi(x, E) = c_1(E) f_1(x, E) + c_2(E) f_2(x, E), \tag{2.48}$$

where

$$\lim_{x\to\infty} f_1(x, E) = 0 \tag{2.49}$$

and

$$\lim_{x\to\infty} f_2(x, E) = \pm\infty. \tag{2.50}$$

At an energy eigenvalue, the unbounded solution is absent, so that

$$c_2(E_n) = 0, \tag{2.51}$$

or equivalently

$$\phi(x, E_n) = c_1(E_n) f_1(x, E_n). \tag{2.52}$$

For large values of x, we note from eqs. (2.48)–(2.51) that the function $\tilde{\phi}$ approaches

$$\tilde{\phi}(x, E_n) \approx f_2(x, E_n) \left.\frac{\mathrm{d}c_2}{\mathrm{d}E}\right|_{E=E_n}. \tag{2.53}$$

Thus the normalization integral is given by

$$I_n = c_1(E_n) \left.\frac{\mathrm{d}c_2}{\mathrm{d}E}\right|_{E=E_n} W(f_2, f_1), \tag{2.54}$$

where the Wronskian determinant

$$W(f_2, f_1) \equiv f_2 f_1' - f_1 f_2' \tag{2.55}$$

is independent of x because the Schrödinger equation (2.38) is free of first-derivative terms.

In some cases, notably for the Coulomb problem, eq. (2.54) is suitable for computations. However, all reference to the unphysical solution f_2 can be eliminated from eq. (2.54). To show this, we express the boundary values as

$$\phi(0, E) = c_1(E) f_1(0, E) + c_2(E) f_2(0, E) \tag{2.56}$$

and

$$\phi'(0, E) = c_1(E) f_1'(0, E) + c_2(E) f_2'(0, E), \tag{2.57}$$

both valid for all values of E. As usual, the prime indicates a derivative with respect to the spatial argument. Imposing the even boundary conditions (2.39a), we compute

$$c_{1e}(E) = -f_2'(0, E)/W(f_2, f_1), \tag{2.58}$$

$$c_{2e}(E) = f_1'(0, E)/W(f_2, f_1), \tag{2.59}$$

$$\frac{dc_{2e}}{dE}(E) = \frac{\partial f_1'(0, E)/\partial E}{W(f_2, f_1)} - \frac{f_1'(0, E)\partial W/\partial E}{W(f_2, f_1)^2}. \tag{2.60}$$

The vanishing of c_{2e} at an even eigenvalue E_e implies that

$$f_1'(0, E_e) = 0, \tag{2.61}$$

so that

$$\frac{dc_{2e}}{dE}(E_e) = \frac{\partial f_1'(0, E_e)/\partial E}{W(f_2, f_1)}. \tag{2.60'}$$

It is convenient to evaluate the Wronskian at $x = 0$, for which

$$W(f_2, f_1) = -f_1(0, E_e) f_2'(0, E_e). \tag{2.62}$$

Combining (2.54), (2.58), (2.60') and (2.62), we arrive at the normalization integral for even-parity bound states,

$$I_e = \frac{\partial f_1'(0, E_e)/\partial E}{f_1(0, E_e)}. \tag{2.63}$$

The derivation for odd-parity bound states, which obey the boundary conditions (2.39b), entails similar arithmetic. We now have

$$c_{1o}(E) = f_2(0, E)/W(f_2, f_1), \tag{2.64}$$

$$c_{2o}(E) = -f_1(0, E)/W(f_2, f_1), \tag{2.65}$$

and

$$\frac{dc_{2o}(E)}{dE} = -\frac{\partial f_1(0, E)/\partial E}{W(f_2, f_1)} + \frac{f_1(0, E)\partial W/\partial E}{W(f_2, f_1)^2}. \tag{2.66}$$

The vanishing of c_{2o} at an odd eigenvalue E_o implies that

$$f_1(0, E_o) = 0, \tag{2.67}$$

so that

$$\frac{dc_2}{dE}(E_o) = -\frac{\partial f_1(0, E_o)/\partial E}{W(f_2, f_1)}. \tag{2.66'}$$

The Wronskian is again conveniently evaluated at $x = 0$, this time yielding

$$W(f_2, f_1) = f_2(0, E_o) f_1'(0, E_o). \tag{2.68}$$

Now combining (2.54), (2.64), (2.66') and (2.68) we obtain the normalization integral for odd-parity bound states

$$I_o = -\frac{\partial f_1(0, E_o)/\partial E}{f_1'(0, E_o)}. \tag{2.69}$$

We illustrate the use of eqs. (2.63) and (2.69) by applying them to the bound states of a linear potential,

$$V(x) = |x|, \tag{2.70}$$

for which the damped solution as $x \to +\infty$ is

$$f_1(x, E) = \mathrm{Ai}(x - E). \tag{2.71}$$

The energy eigenvalues are specified by the zeroes of Airy functions,†17 namely

$$\mathrm{Ai}'(-E_e) = 0, \tag{2.72}$$

for even-parity solutions, and

$$\mathrm{Ai}(-E_o) = 0, \tag{2.73}$$

for odd-parity solutions. The even-parity normalization integral is then evaluated from (2.63) as

$$I_e = -\mathrm{Ai}''(-E_e)/\mathrm{Ai}(-E_e), \tag{2.74}$$

which, by virtue of the Schrödinger equation

$$\phi''(x) + (E - |x|)\phi(x) = 0, \tag{2.75}$$

may be recognized as

$$I_e = E_e. \tag{2.76}$$

For the odd-parity normalization integral, (2.69) leads at once to

$$I_o = 1, \tag{2.77}$$

which implies for the three-dimensional problem in a central potential that

$$|\Psi(0)|^2 = 1/4\pi, \tag{2.78}$$

in agreement with (2.19).

†17 A useful summary of the properties of these functions may be found in ref. [37, pp. 446–452].

2.4. Mass dependence of Schrödinger wavefunctions

We continue to deal with the one-dimensional bound-state problem for a symmetric potential, and its straightforward extension to the three-dimensional central potential problem. An important class of applications concerns the dependence of observables upon the mass μ [38, 39]. Here we shall show that for any potential which is monotonically increasing for $x > 0$, the probability that a bound particle lies within a fixed distance from the origin is an increasing function of μ, for the lowest-lying states of even and odd parity. In other words, probability will be shown to flow inward across any arbitrarily chosen boundary, when μ is increased. Probability also flows inward when the potential strength is increased.

Because of the symmetry of the problem, we need only discuss positive values of x. We examine the probability $P(R)$ that a particle be contained within the interval $(0, R)$. In terms of the wavefunction $u(x)$, normalized according to

$$\int_0^\infty dx\,[u(x)]^2 = 1, \tag{2.8}$$

we have

$$P(R) \equiv \int_0^R dx [u(x)]^2, \tag{2.79}$$

so that

$$0 \le P(R) \le 1, \tag{2.80}$$

and

$$P'(R) \ge 0. \tag{2.81}$$

We shall demonstrate that for symmetric potentials satisfying

$$V'(x) \ge 0, \qquad x > 0, \tag{2.82}$$

the function

$$G(R) \equiv \frac{1}{2}\frac{\partial P(R)}{\partial \mu} = \int_0^R dx\, u(x)\, \partial u(x)/\partial \mu \tag{2.83}$$

satisfies

$$G(R) \ge 0, \qquad 0 \le R \le \infty \tag{2.84}$$

for the even-parity and odd-parity ground states. We begin with the Schrödinger equation in the form

$$u''(x) = -\frac{2\mu}{\hbar^2}[E - V(x)]\, u(x), \tag{2.85}$$

and apply $u(x)\,\partial/\partial\mu$:

$$u(x)\frac{\partial u''}{\partial \mu}(x) = -\frac{2}{\hbar^2}\left[E - V(x) + \mu\frac{\partial E}{\partial \mu}\right][u(x)]^2 - \frac{2\mu}{\hbar^2}[E - V(x)]u(x)\frac{\partial u(x)}{\partial \mu}. \tag{2.86}$$

With the aid of the Feynman–Hellmann theorem (2.16), this expression can be simplified to

$$u(x)\frac{\partial u''}{\partial \mu}(x)=\frac{2}{\hbar^2}[V(x)-\langle V\rangle][u(x)]^2+\frac{2\mu}{\hbar^2}[V(x)-E]u(x)\frac{\partial u(x)}{\partial \mu}. \tag{2.87}$$

From this we subtract $\partial u/\partial\mu \times$ eq. (2.85), and integrate from $x=0$ to R:

$$\int_0^R \mathrm{d}x\left[u(x)\frac{\partial u''}{\partial \mu}(x)-u''\frac{\partial u}{\partial \mu}(x)\right]=\frac{2}{\hbar^2}\int_0^R \mathrm{d}x\,[V(x)-\langle V\rangle][u(x)]^2. \tag{2.88}$$

Integration of the left-hand side by parts and application of the boundary conditions

$$u(0)=\text{finite}, \qquad u'(0)=0 \tag{2.89}$$

for even-parity states or

$$u(0)=0, \qquad u'(0)=\text{finite} \tag{2.90}$$

for odd-parity bound states yields

$$u(R)\frac{\partial u'}{\partial \mu}(R)-u'(R)\frac{\partial u}{\partial \mu}(R)=\frac{2}{\hbar^2}\int_0^R \mathrm{d}x\,[V(x)-\langle V\rangle][u(x)]^2\le 0, \tag{2.91}$$

where the inequality is a consequence of (2.82).

The function

$$G'(R)=u(R)\,\partial u(R)/\partial\mu \tag{2.92}$$

vanishes only for $u=0$ or $\partial u/\partial\mu=0$. By evaluating G'' at an extremum of G from (2.91), we discover that

$$G''(R)>0 \quad \text{if } u(R)=0 \text{ (a minimum)}, \tag{2.93a}$$

and

$$G''(R)<0 \quad \text{if } \partial u(R)/\partial\mu=0 \text{ (a maximum)}. \tag{2.93b}$$

Since $G(0)=0=G(\infty)$, the function $G(R)$ can become negative for $0<R<\infty$ only if it possesses a minimum in that interval. By virtue of (2.93a), a minimum occurs only at a node of the wavefunction, $u(x)=0$. The ground-state wavefunctions are nodeless, so (2.84) is established†$_{18}$.

The proof just concluded for the odd-parity case directly establishes the result (2.84) in three dimensions for the s-wave ground state. By applying the same arithmetic to the Schrödinger equation form (2.21) for the three-dimensional problem, we immediately extend the proof to all nodeless wavefunctions, for arbitrary values of the angular momentum l. Thus for all bound states on the leading Regge trajectory for a central potential satisfying $V'(r)\ge 0$, $\partial P(R)/\partial\mu \ge 0$.

The result for the s-wave ground state has important applications to the quarkonium problem, which are detailed in section 7. The inward flow of probability can be established for excited states as well, for specific potentials. This is accomplished in section 3.

†$_{18}$ We thank B. Simon for informing us of a proof by J. Avron, I. Herbst, and B. Simon (unpublished) of a more general theorem which has (2.84) as a special case, and of an unpublished proof by A. Martin which is very similar in spirit to the present one.

A precisely parallel argument leads to a similar result for the variation of $P(R)$ with the potential strength. To carry out the proof, we let $V(x) \to \kappa V(x)$ in the Schrödinger equation (2.85) and substitute $\partial/\partial\kappa$ for $\partial/\partial\mu$ in subsequent steps. The analog of (2.91) is

$$u(R)\frac{\partial u'}{\partial \kappa}(R) - u'(R)\frac{\partial u}{\partial \kappa}(R) = \frac{2\mu}{\hbar^2}\int_0^R \mathrm{d}x\,[V(x) - \langle V\rangle][u(x)]^2 \leq 0. \tag{2.94}$$

The discussion following (2.91) applies, mutatis mutandis, to the present case and shows that $\partial P(R)/\partial\kappa \geq 0$, under the same conditions for which $\partial P(R)/\partial\mu \geq 0$.

2.5. Quantum mechanical sum rules

Many different sum rules find wide-ranging applications in quantum physics. The principal sum rules of atomic physics are summarized in §61, 62 of the monograph by Bethe and Salpeter [33]. Here we content ourselves with remarks of a general character, indicating the methods of derivation for classes of sum rules [40].

The sum of squares of the transition matrix elements of any operator $\mathcal{O}$ satisfies a sum rule

$$\sum_{n\neq \mathrm{i}} |\langle \mathrm{i}|\mathcal{O}|n\rangle|^2 = \langle \mathrm{i}|\mathcal{O}\mathcal{O}^+|\mathrm{i}\rangle - |\langle \mathrm{i}|\mathcal{O}|\mathrm{i}\rangle|^2, \tag{2.95}$$

where the unrestricted sum runs over a complete set of states.

Energy-weighted sum rules are generated by the double commutator $[[\mathscr{H}, \mathcal{O}], \mathcal{O}^+]$. Its matrix element is

$$\begin{aligned}\langle \mathrm{i}|[[\mathscr{H}, \mathcal{O}], \mathcal{O}^+]|\mathrm{i}\rangle &= \sum_n (\langle \mathrm{i}|[\mathscr{H}, \mathcal{O}]|n\rangle\langle n|\mathcal{O}^+|\mathrm{i}\rangle - \langle \mathrm{i}|\mathcal{O}^+|n\rangle\langle n|[\mathscr{H}, \mathcal{O}]|\mathrm{i}\rangle)\\ &= 2\sum_n (E_\mathrm{i} - E_n)|\langle \mathrm{i}|\mathcal{O}|n\rangle|^2.\end{aligned} \tag{2.96}$$

As an illustration, let us consider the one-dimensional problem in which the Hamiltonian is

$$\mathscr{H} = p^2/2\mu + V(x) \tag{2.97}$$

and the operator $\mathcal{O}$ is only a function of the coordinate x. Under these assumptions,

$$[\mathscr{H}, \mathcal{O}] = \left[\frac{p^2}{2\mu}, \mathcal{O}\right] = -\frac{\mathrm{i}\hbar}{2\mu}(p\mathcal{O}' + \mathcal{O}'p), \tag{2.98}$$

where

$$\mathcal{O}' = \mathrm{d}\mathcal{O}/\mathrm{d}x, \tag{2.99}$$

and the double commutator is easily seen to be

$$[[\mathscr{H}, \mathcal{O}], \mathcal{O}^+] = -\frac{\hbar^2}{\mu}|\mathcal{O}'|^2. \tag{2.100}$$

The sum rule (2.96) takes the form

$$\frac{2\mu}{\hbar^2}\sum_n (E_n - E_\mathrm{i})|\langle \mathrm{i}|\mathcal{O}|n\rangle|^2 = \langle \mathrm{i}||\mathcal{O}'|^2|\mathrm{i}\rangle. \tag{2.101}$$

A familiar special case†19 occurs for $\mathcal{O} = x$, in which event

$$\frac{2\mu}{\hbar^2}\sum_n (E_n - E_i)|\langle i|x|n\rangle|^2 = 1. \tag{2.102}$$

It is also possible to generate sum rules weighted by the square of the transition energy by considering

$$\begin{aligned}\langle i|[[\mathcal{H}, \mathcal{O}]|^2|i\rangle &= \sum_n \langle i|[\mathcal{H}, \mathcal{O}]|n\rangle\langle n|[\mathcal{O}^+, \mathcal{H}]|i\rangle \\ &= \sum_n (E_i - E_n)^2|\langle i|\mathcal{O}|n\rangle|^2.\end{aligned} \tag{2.103}$$

A case of special interest is again $\mathcal{O} = x$, with $\mathcal{H}$ given by (2.97), for which

$$|[\mathcal{H}, \mathcal{O}]|^2 = \frac{\hbar^2}{\mu^2}p^2 = \frac{2\hbar^2}{\mu}(\mathcal{H} - V(x)), \tag{2.104}$$

so that

$$(E_i - \langle V\rangle_i) = \frac{\mu}{2\hbar^2}\sum_n (E_i - E_n)^2|\langle i|x|n\rangle|^2. \tag{2.105}$$

By virtue of the virial theorem (2.18), we may express the last result as

$$\frac{\mu}{\hbar^2}\sum_n (E_i - E_n)^2|\langle i|x|n\rangle|^2 = \langle i|xV'|i\rangle. \tag{2.106}$$

Alternatively, we may invoke the Feynman–Hellmann theorem (2.16) to write

$$\sum_n (E_i - E_n)^2|\langle i|x|n\rangle|^2 = -2\hbar^2\partial E_i/\partial\mu, \tag{2.107}$$

which again demonstrates that $\partial E_i/\partial\mu \leq 0$.

These examples illustrate but a few of the powerful and unexpected consequences of quantum-mechanical sum rules. The applications which have been made to the charmonium problem are mentioned very briefly in section 9.

3. Specific results for power-law and logarithmic potentials

A class of simple potentials displays a number of remarkable regularities. In this section we explore the consequences of power-law potentials

$$V(r) = \lambda r^\nu \quad (-2 < \nu < \infty) \tag{3.1}$$

and of the logarithmic potential

$$V(r) = C\ln(r/r_0), \tag{3.2}$$

which behaves in some respects as the $\nu \to 0$, $\lambda \to \infty$, $\lambda\nu \to C$ limit of (3.1). In such potentials the mass dependence of energy levels, distance scales, and wavefunctions all follow from elementary rescaling

†19 An interesting historical discussion of the importance of this ("Thomas–Reiche–Kuhn", ref. [41]) sum rule is given in ref. [42, §6–9, 25.2, and 25.8]. It played an important role in the development by Heisenberg of commutation relations [43].

operations. In addition, the kinetic, potential, and total bound-state energies are related in simple fashion. The virial theorem (2.18) provides the connection

$$\langle T\rangle = E - \langle V\rangle = \tfrac{1}{2}\nu\langle V\rangle \tag{3.3}$$

or

$$\langle T\rangle = \nu E/(2+\nu) \tag{3.4}$$

for power-law potentials, and

$$\langle T\rangle = C/2 \tag{3.5}$$

for the logarithmic potential (3.2).

3.1. Dependence upon mass and coupling strength

We shall perform some elementary operations on the reduced radial Schrödinger equation in a power-law potential,

$$\frac{\hbar^2}{2\mu}u''(r) + \left[E - \lambda r^\nu - \frac{l(l+1)\hbar^2}{2\mu r^2}\right]u(r) = 0, \tag{3.6}$$

to cast it in dimensionless form†20. The dimensionful parameters in (3.6) are $2\mu/\hbar^2$ and λ, which has dimensions

$$[\lambda] = [\hbar^{-\nu}\mu^{1+\nu}], \tag{3.7}$$

when the speed of light is defined to be $c = 1$. Define the scaled measure of length ρ through

$$\rho = (\hbar^2/2\mu|\lambda|)^p r, \tag{3.8}$$

with the parameter p chosen to eliminate all explicit dependence on the mass and coupling strength from eq. (3.6). This is effected by the choice

$$p = -1/(2+\nu), \tag{3.9}$$

and the rescaling of the energy eigenvalue as

$$E = \left(\frac{\hbar^2}{2\mu|\lambda|}\right)^{2p}\left(\frac{\hbar^2}{2\mu}\right)\epsilon. \tag{3.10}$$

With the definition

$$w(\rho) \equiv u(r), \tag{3.11}$$

the Schrödinger equation assumes the dimensionless form

$$w''(\rho) + [\epsilon - \mathrm{sgn}(\lambda)\rho^\nu - l(l+1)/\rho^2]\, w(\rho) = 0. \tag{3.12}$$

These elementary manipulations have a number of useful consequences.

†20 We have reviewed many of these scaling arguments in ref. [44]. They appear in numerous places in the recent literature: see, for example, refs. [22, 23 and 45–47].

3.1.1. Level spacings

We are at liberty to shift the energy eigenvalues by a common amount by adding a constant to the potential. However the mass and coupling strength dependences of the level spacings, which are eigenvalue differences, are prescribed by (3.10) as

$$\Delta E \propto (2\mu/\hbar^2)^{-\nu/(2+\nu)}|\lambda|^{2/(2+\nu)}. \tag{3.13}$$

Thus for the Coulomb problem ($\nu = -1$), $\Delta E \propto \mu|\lambda|^2$; the Rydberg unit is proportional to the reduced mass and to the square of the coupling constant. The result $\Delta E \propto (\lambda/\mu)^{1/2}$ for the harmonic oscillator ($\nu = 2$) may be familiar as well. For the linear potential ($\nu = 1$) popular in quark confinement schemes, $\Delta E \propto (\lambda^2/\mu)^{1/3}$. Notice that for singular potentials ($\nu < 0$), the level spacing ΔE increases with increasing mass μ, while for nonsingular potentials ($\nu > 0$), ΔE is a decreasing function of μ. For a pure power-law potential, not shifted by a redefinition of the zero, all the foregoing results hold for the energy levels (eigenvalues) themselves.

3.1.2. Lengths

According to eq. (3.8), quantities with the dimensions of length scale as

$$L \propto (\mu|\lambda|)^{-1/(2+\nu)}. \tag{3.14}$$

For example, the probability density at the origin, $|\Psi(0)|^2$, has dimensions of inverse volume and so scales as

$$|\Psi(0)|^2 \propto (\mu|\lambda|)^{3/(2+\nu)}. \tag{3.15}$$

For a Coulomb potential, therefore, $|\Psi(0)|^2 \propto (\mu|\lambda|)^3$, while for a linear potential $|\Psi(0)|^2 \propto (\mu\lambda)$. This last result can be recovered at once from eq. (2.19), which yields

$$|\Psi(0)|^2 = (\mu/2\pi\hbar^2)\langle dV/dr\rangle = \mu\lambda/2\pi\hbar^2 \tag{3.16}$$

for the linear potential $V(r) = \lambda r$. Away from the origin, eqs. (2.2), (2.4), (3.8) and (3.11) imply that

$$\left|\Psi\left(\rho\left[\frac{\hbar^2}{2\mu|\lambda|}\right]^{1/(2+\nu)}\right)\right|^2 \propto (\mu|\lambda|)^{3/(2+\nu)}, \tag{3.17}$$

for any fixed value of ρ.

The probability density $|\Psi(0)|^2$ is of interest, for example, in the leptonic decays of massive neutral vector mesons $\mathcal{V}^0$ which are $^3S_1$ bound states of a quark and an antiquark. The decay width is given by [48]

$$\Gamma(\mathcal{V}^0 \to \ell^+\ell^-) = 16\pi\hbar^3\alpha^2 e_Q^2|\Psi(0)|^2/M_{\mathcal{V}}^2, \tag{3.18}$$

where α is the fine-structure constant, e_Q is the quark charge in units of the proton charge, and $M_{\mathcal{V}}$ is the vector meson mass. Using (3.15) we have

$$\Gamma(\mathcal{V}^0 \to \ell^+\ell^-) \propto e_Q^2(\mu|\lambda|)^{3/(2+\nu)}/M_{\mathcal{V}}^2 \tag{3.19a}$$

$$\propto e_Q^2\mu^{-(1+2\nu)/(2+\nu)}|\lambda|^{3/(2+\nu)}, \quad \nu \geq -1, \tag{3.19b}$$

where the second expression follows upon neglect of binding energies. For $\nu > -1$, the scale of $M_{\mathcal{V}}$ will be set by μ for the low-lying levels, because $\Delta E/\mu$ does not grow with increasing μ, according to (3.13). We therefore assume $M_{\mathcal{V}} \approx 2(2\mu) +$ small binding corrections, for constituents of mass 2μ. We shall return in section 5 to a discussion of leptonic widths of vector mesons.

Transition matrix elements of electric and magnetic multipole operators and sizes of bound states with given quantum numbers are other examples of quantities to which the scaling law (3.14) may be applied. Thus electric multipole matrix elements scale as

$$\langle n'|Ej|n\rangle \propto L^j \tag{3.20}$$

while magnetic multipole matrix elements behave as†21

$$\langle n'|Mj|n\rangle \propto L^{j-1}/\mu. \tag{3.21}$$

Since radiative widths are given by

$$\Gamma(Ej \text{ or } Mj) \propto p_\gamma^{2j+1}|\langle n'|Ej \text{ or } Mj|n\rangle|^2 \tag{3.22}$$

with $p_\gamma \sim \Delta E$, we find

$$\Gamma(Ej) \propto \mu^{-[2j(1+\nu)+\nu]/(2+\nu)}|\lambda|^{2(j+1)/(2+\nu)} \tag{3.23}$$

and

$$\Gamma(Mj) \propto \mu^{-[2j(1+\nu)+3\nu+2]/(2+\nu)}|\lambda|^{2(j+2)/(2+\nu)}. \tag{3.24}$$

For potentials less singular than a Coulomb potential near $r=0$ (i.e. for $\nu > -1$), the relative importance of higher multipoles decreases with increasing μ. It is amusing that for $-2 < \nu < -1$ the rapid growth of $p_\gamma \sim \Delta E$ with μ can lead to an increasing prominence of high multipole transitions in the limit of large μ. For any power ν in the interval $-2 < \nu < \infty$, an increase in the coupling constant increases the importance of high multipole transitions.

3.1.3. The infinite square well

An infinite square well potential of width R corresponds to the $\nu \to \infty$ limit of eq. (3.1), provided the coupling strength is written as $R^{-\nu}$:

$$V(r) = \lim_{\nu\to\infty} (r/R)^\nu, \tag{3.25}$$

so that

$$V(r) = \begin{cases} 0, & r < R \\ \infty, & r > R \end{cases}. \tag{3.26}$$

For the potential (3.25), the dependence of the energy eigenvalues upon the mass and well width is given by (3.13) as

$$E \propto \hbar^2/2\mu R^2 \tag{3.27}$$

which behaves as the kinetic energy of a particle of mass μ in a box of length R.

3.1.4. The logarithmic potential

The scaling law (3.13) shows that the energy levels vary more slowly than any power of μ for a potential which varies more slowly than any power of r. A power-law potential of the form (3.1) with $\nu = 0$ is of course trivial and supports no bound states. However, let us consider rescaling the

†21 For simplicity, in discussing magnetic transitions we assume that only one mass scale is important, whether because the two particles bound to one another have equal masses ($=2\mu$), or because one (with mass $\approx\mu$) is much lighter than the other.

Schrödinger equation by the transformation (3.8) with $p = -\frac{1}{2}$, which corresponds to $\nu \to 0$ in eq. (3.9).

We write the potential in the general form

$$V(r) = \lambda U(r), \tag{3.28}$$

where U is dimensionless, for which the rescaled Schrödinger equation reads

$$w''(\rho) + [(E/\lambda) - U([\hbar^2/2\mu\lambda]^{1/2}\rho) - (l(l+1)/\rho^2)]w(\rho). \tag{3.29}$$

The dimensionless energy eigenvalue is simply

$$\epsilon = E/\lambda. \tag{3.30}$$

The differences of eigenvalues are independent of μ if and only if under a scale transformation $\mu \to \sigma\mu$,

$$U(\rho[\hbar^2/2\sigma\mu\lambda]^{1/2}) = U(\rho[\hbar^2/2\mu\lambda]^{1/2}) + f(\sigma). \tag{3.31}$$

The solution to eq. (3.31) may be obtained by differentiating with respect to σ and ρ and separating variables. We find

$$U(r) = \ln(r/r_0), \tag{3.32}$$

$$f(\sigma) = -\tfrac{1}{2}\ln\sigma. \tag{3.33}$$

Thus for the logarithmic potential the level spacings are independent of μ [49]. Moreover, the logarithmic potential is unique in generating level spacings which are independent of μ. The parameter λ sets the scale of the spacings, as shown by (3.30).

To establish this uniqueness in a different way, let us show that the Schrödinger equation can be scaled only for power-law and logarithmic potentials†22. We write the Schrödinger Hamiltonian as

$$\mathscr{H} = (p^2/2\mu) + V(r) + (l(l+1)\hbar^2/2\mu r^2) \tag{3.34}$$

and consider the effect of a dilation, or scale change, for which

$$r \to \kappa r \tag{3.35}$$

and

$$p \to p/\kappa. \tag{3.36}$$

The rescaled Hamiltonian is

$$\mathscr{H}(\kappa) = (p^2/2\mu\kappa^2) + V(\kappa r) + (l(l+1)\hbar^2/2\mu\kappa^2 r^2). \tag{3.37}$$

We ask for the most general condition under which the eigenfunctions and eigenvalues of $\mathscr{H}(\kappa)$ are identical to those of $\mathscr{H}$ except for possible changes in scale and shifts in the zero of energy. Now, $\mathscr{H}(\kappa)$ must be a linear function of $\mathscr{H}$, in order to preserve the quadratic momentum dependence, and hence $V(r)$ must be a linear function of $V(\kappa r)$:

$$V(r) = AV(\kappa r) + B. \tag{3.38}$$

This is the condition upon the scaling behavior of a potential which ensures the desired scaling properties of the Schrödinger equation.

†22 We thank H.J. Lipkin for suggesting this approach.

To find solutions, we consider an infinitesimal scale transformation and expand (3.38) about $\kappa = 1$. We thereby obtain

$$V(r) = A[V(r) + (\kappa - 1)rV'(r)] + B, \tag{3.39}$$

which is more conveniently written in the form

$$\frac{dV}{V(1-A)-B} = \frac{1}{(\kappa-1)}\frac{dr}{r}. \tag{3.40}$$

In this last form the equation is easily seen to admit two solutions. If the coefficient $A \neq 1$, an integration yields

$$\frac{\ln[V(1-A)-B]}{1-A} = \frac{1}{(\kappa-1)}\ln r + \text{constant}, \tag{3.41}$$

i.e. a potential of power-law form (3.1). When the coefficient $A = 1$, the solution is

$$V(r) = -\frac{B}{(\kappa-1)}\ln(r/r_0) \tag{3.42}$$

a logarithmic potential of the form (3.2). This shows that the Schrödinger equation exhibits the desired scaling behavior only for power-law and logarithmic potentials, and establishes the uniqueness of the logarithmic potential in generating eigenvalue differences which are mass-independent.

The dimensionless levels ϵ in the logarithmic potential (3.32) have been calculated numerically (for $r_0\sqrt{2\mu\lambda/\hbar^2} = 1$) in ref. [49]. They are illustrated in fig. 4. [See also table 6 below.] Because of the scaling properties we have just developed, it is straightforward to deduce the levels appropriate to any values of μ, λ and r_0. The rescaling of eigenvalues of power-law potentials according to (3.13) is also elementary.

3.1.5. Summary

The behavior of energy levels under variations of the mass μ is illustrated for three different potentials in fig. 5. The examples chosen are $V(r) = -r^{-1/2}$, $V(r) = \ln r$, and $V(r) = r$, for which

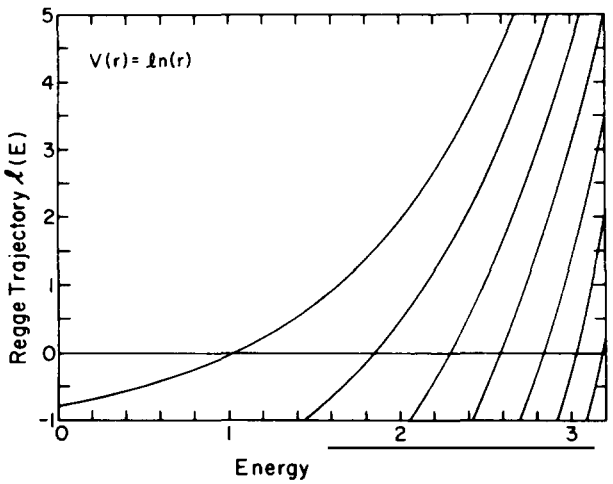

Fig. 4. Energy levels in the potential $V(r) = \ln(r)$. Here $2\mu = 1$.

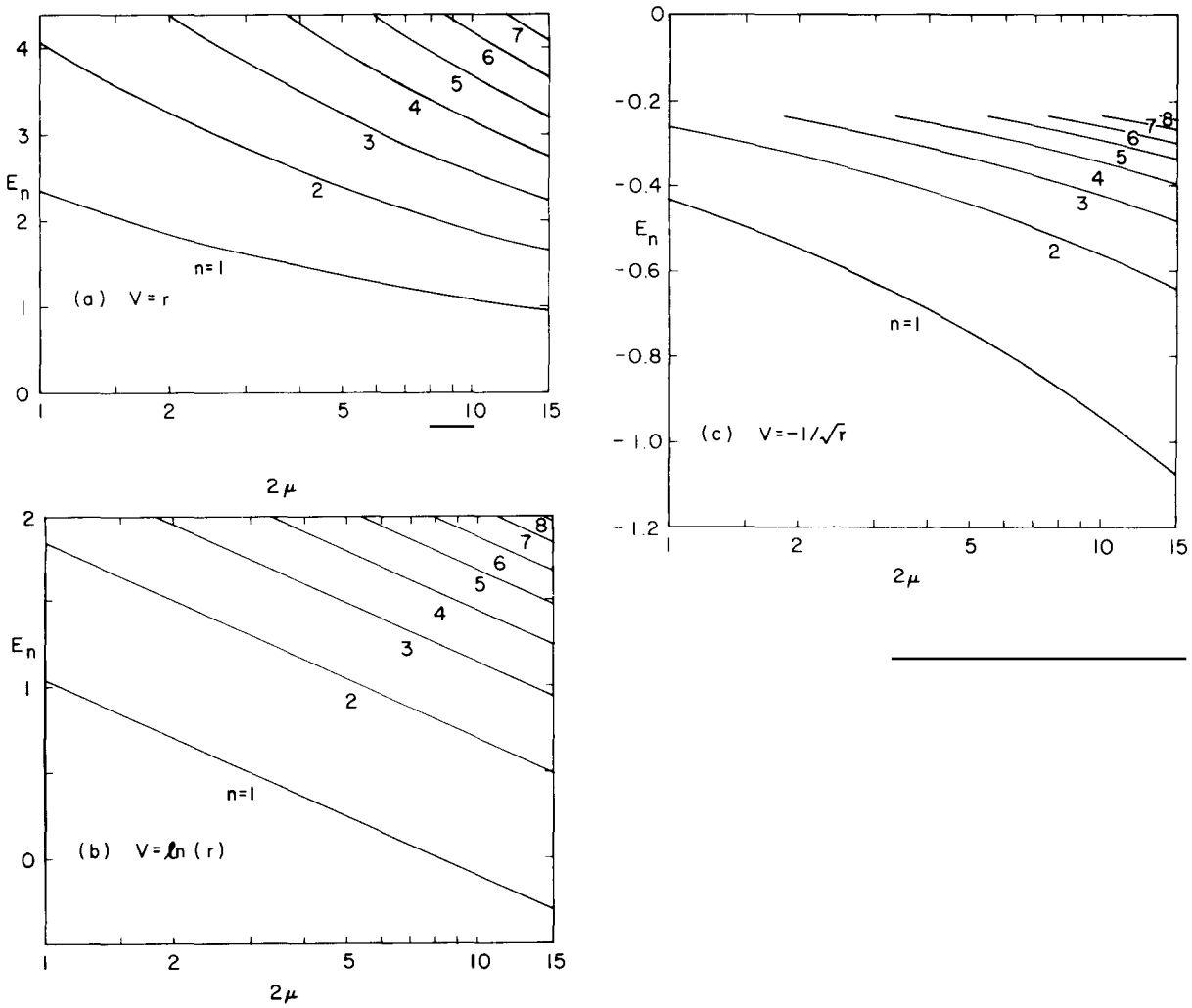

Fig. 5. Comparison of mass dependence of energy levels in three potentials: (a) $V(r) = r$; (b) $V(r) = \ln r$; (c) $V(r) = -r^{-1/2}$.

$\Delta E \sim \mu^{1/3}$, μ^0, and $\mu^{-1/3}$ respectively. All the levels fall deeper into the potential as μ is increased, in conformity with the Feynman–Hellmann theorem (2.16). For the potential with $\nu = -\frac{1}{2}$, singular at the origin, the levels spread apart as they sink into the well. For the linear potential, no such hole exists, but the levels are packed together more densely as μ rises. The logarithmic potential represents an intermediate situation in which the level spacing is independent of the mass and levels fall into the well at a common rate given by

$$E_i(\mu') = E_i(\mu) - \tfrac{1}{2}\ln(\mu'/\mu). \tag{3.43}$$

These differences in deportment will be found very interesting in section 8 when we discuss the calculation of thresholds for the production of pairs of hadrons containing quarks with new flavors. Other aspects of the scaling properties of various specific potentials may be found in table 1.

Table 1
Scaling properties of some physical quantities in various potentials $V(r) = \lambda r^{\nu}$

Potentials	ν	ΔE	length scale	Γ(E1)	Γ(M1)	$\Gamma(\mathcal{V} \to e^+e^-)$
Coulomb	-1	μ	μ^{-1}	μ	μ	μ
Logarithmic	0	μ^0	$\mu^{-1/2}$	μ^{-1}	μ^{-2}	$\mu^{-1/2}$
Linear	1	$\mu^{-1/3}$	$\mu^{-1/3}$	$\mu^{-5/3}$	μ^{-3}	μ^{-1}
Harmonic oscillator	2	$\mu^{-1/2}$	$\mu^{-1/4}$	μ^{-2}	$\mu^{-7/2}$	$\mu^{-5/4}$
Square well	∞	μ^{-1}	μ^0	μ^{-3}	μ^{-5}	μ^{-2}

3.2. Relations among power-law potentials

We have distinguished, in the previous subsection, between power-law potentials (3.1) which are singular at the origin (i.e. with $-2 < \nu < 0$) and those which are nonsingular (i.e. with $\nu > 0$). It is interesting, and perhaps not universally known, that pairwise relations exist between the Schrödinger problems associated with these two families. The best-known example is the relationship of the Coulomb potential with the harmonic oscillator†$_{23}$.

The Schrödinger equation

$$\frac{\hbar^2}{2\mu} u''(r) + \left[E - \lambda r^{\nu} - \frac{l(l+1)\hbar^2}{2\mu r^2}\right] u(r) = 0, \tag{3.6}$$

is related to another equation, identical in form. We introduce a new length variable

$$z = r^{-\nu/\bar{\nu}}, \tag{3.44}$$

with $\bar{\nu}$ a power to be determined, and let

$$u(r) \equiv z^{-[1+(\bar{\nu}/\nu)]/2} v(z). \tag{3.45}$$

The Schrödinger equation assumes the form

$$\frac{\hbar^2}{2\mu}\left(\frac{\bar{\nu}}{\nu}\right)^{-2}\left\{z^{2[(\bar{\nu}/\nu)+1]} v''(z) + \frac{1}{4z^2}\left(1 - \left(\frac{\bar{\nu}}{\nu}\right)^2\right) z^{2[(\bar{\nu}/\nu)+1]} v(z)\right\}$$
$$+ \left\{E - \lambda z^{-\bar{\nu}} - \frac{l(l+1)\hbar^2}{2\mu z^2} z^{2[(\bar{\nu}/\nu)+1]}\right\} v(z) = 0. \tag{3.46}$$

We now multiply by $(\bar{\nu}/\nu)^2 z^{\bar{\nu}}$, and find

$$\frac{\hbar^2}{2\mu} z^{2[(\bar{\nu}/\nu)+1]+\bar{\nu}} v''(z) + \left\{-\lambda\left(\frac{\bar{\nu}}{\nu}\right)^2 + E\left(\frac{\bar{\nu}}{\nu}\right)^2 z^{\bar{\nu}}\right.$$
$$\left. - \frac{\hbar^2}{2\mu z^2}\left[l(l+1)\left(\frac{\bar{\nu}}{\nu}\right)^2 - \frac{1}{4}\left(1 - \left(\frac{\bar{\nu}}{\nu}\right)^2\right)\right] z^{2[(\bar{\nu}/\nu)+1]+\bar{\nu}}\right\} v(z) = 0. \tag{3.47}$$

The choice (3.45) has ensured that this last equation contains no first derivatives. If we now require

†$_{23}$ This connection is mentioned in ref. [50].

that

$$2[(\bar{\nu}/\nu)+1]+\bar{\nu}=0, \tag{3.48}$$

we recover an equation in the Schrödinger form,

$$(\hbar^2/2\mu)v''(z)+[\bar{E}-\bar{\lambda}z^{\bar{\nu}}-(\hbar^2\bar{l}(\bar{l}+1)/2\mu z^2)]v(z)=0, \tag{3.49}$$

where

$$\bar{E}=-\lambda(\bar{\nu}/\nu)^2, \tag{3.50}$$

$$\bar{\lambda}=-E(\bar{\nu}/\nu)^2, \tag{3.51}$$

and

$$\bar{l}(\bar{l}+1)=l(l+1)(\bar{\nu}/\nu)^2-\tfrac{1}{4}(1-(\bar{\nu}/\nu)^2). \tag{3.52}$$

To solve (3.52), we complete the square on both sides of the equation, which yields

$$(\bar{l}+\tfrac{1}{2})^2=(\bar{\nu}/\nu)^2(l+\tfrac{1}{2})^2. \tag{3.53}$$

If u is regular at the origin,

$$u_l(r)\sim r^{l+1}, \tag{2.28}$$

then the choice

$$\bar{l}+\tfrac{1}{2}=-(\bar{\nu}/\nu)(l+\tfrac{1}{2}) \tag{3.54}$$

ensures that

$$v_{\bar{l}}(z)\sim z^{\bar{l}+1} \tag{3.55}$$

is also the solution regular at the origin.

The definition (3.44) and the constraint (3.48) imply that

$$z=r^{1/(1+\bar{\nu}/2)}=r^{1+\nu/2}, \tag{3.56}$$

which indicates that for $-2<\nu<\infty$, the point $r=0$ maps into $z=0$, and the point $r=\infty$ maps into $z=\infty$. We note that ν and $\bar{\nu}$ appear symmetrically in (3.44), (3.48), (3.50), (3.51) and (3.53).

The relation between the Schrödinger equations (3.6) and (3.49) is of special interest because it connects the bound-state spectrum of an infinitely rising potential ($\nu>0$) with that of a singular potential ($-2<\bar{\nu}<0$). The identification (3.44) between ν and $\bar{\nu}$ is plotted in fig. 6.†$_{24}$

3.3 Bound-state normalization

In section 4 we shall compare energy eigenvalues and $|\Psi(0)|^2$ derived semiclassically with exact results. Here we apply the normalization techniques of section 2.3 to specific cases of interest.

3.3.1. Harmonic oscillator ($\nu=2$)

Solutions of the Schrödinger equation

$$\phi''(r)+(E-r^2)\phi(r) \tag{3.57}$$

†$_{24}$ A similar connection has been noted in ref. [47] within the context of the semiclassical approximation.

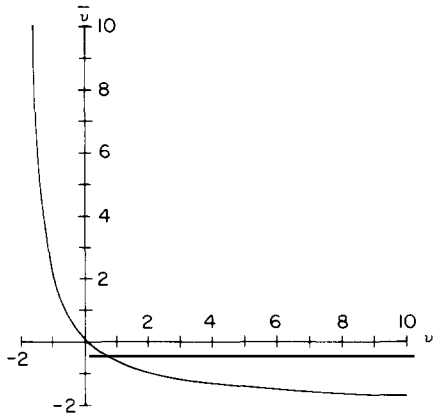

Fig. 6. The relation $\nu\bar{\nu} + 2(\nu + \bar{\nu}) = 0$.

which are damped at infinity are the parabolic cylinder functions†25

$$f_1(r, E) = U(-E/2, r\sqrt{2}), \tag{3.58}$$

for which†26

$$f_1(0, E_n) = \frac{2^{(E-1)/4}}{\sqrt{\pi}} \sin \pi \left[\frac{3-E}{4}\right] \Gamma\left(\frac{E+1}{4}\right) \tag{3.59}$$

and

$$f_1'(0, E_n) = \frac{2^{(E+3)/4}}{\sqrt{\pi}} \cos \pi \left[\frac{3-E}{4}\right] \Gamma\left(\frac{E+3}{4}\right). \tag{3.60}$$

According to the eigenvalue condition

$$f_1(0, E_n) = 0, \tag{2.67}$$

the energy eigenvalues are

$$E_n = 4n - 1; \qquad n = 1, 2, \ldots. \tag{3.61}$$

The normalization integral (2.69) is therefore

$$I_n = -\frac{\partial f_1(0, E_n)/\partial E}{f_1'(0, E_n)} = \frac{\pi}{8} \Gamma(n)/\Gamma(n + \tfrac{1}{2}). \tag{3.62}$$

A similar result can of course be obtained more directly using properties of Hermite polynomials†27.

3.3.2. Coulomb potential ($\nu = -1$)

For this case it is convenient to compute the normalization integral by means of (2.54). Solutions to the Schrödinger equation

$$\phi''(r) + (-\kappa^2 + r^{-1})\phi(r) = 0 \tag{3.63}$$

†25 See ref. [37, p. 687].
†26 See ref. [37, §19.3.5].
†27 See, for example, ref. [51, section 30].

which obey the boundary conditions (2.39b) are of the form†28

$$\phi(r) = r\,e^{-\kappa r}\,{}_1F_1(1-1/2\kappa;2;2\kappa r), \tag{3.64}$$

where the energy eigenvalue is

$$E = -\kappa^2. \tag{3.65}$$

For large values of r the decomposition according to (2.48)–(2.50) into damped and unbounded solutions yields coefficients

$$c_1(E) = (1/2\kappa)\Gamma(1+1/2\kappa), \tag{3.66}$$

$$c_2(E) = \sin(\pi/2\kappa)\Gamma(1/2\kappa)/2\pi\kappa, \tag{3.67}$$

with†29

$$f_1(r,E) \sim -(2\kappa r)^{1/2\kappa}\,e^{-\kappa r}\,e^{-i\pi/2\kappa}, \tag{3.68}$$

$$f_2(r,E) \sim (2\kappa r)^{-1/2\kappa}\,e^{\kappa r}. \tag{3.69}$$

The vanishing of c_2 at energy eigenvalues implies that

$$1/2\kappa = n; \qquad n = 1, 2, \ldots \tag{3.70}$$

so that

$$E_n = -1/4n^2. \tag{3.71}$$

A brief calculation then yields

$$I_n = 2n^3, \tag{3.72}$$

which can also be obtained by elementary means.†30

3.4. Mass dependence of Schrödinger wavefunctions

The scaling behavior of Schrödinger wavefunctions established in eq. (3.17) permits the proof of a very strong

Theorem: For a power-law or logarithmic potential, the function

$$G(R) \equiv \frac{1}{2}\frac{\partial}{\partial\mu}\int_0^R dr\,[u(r)]^2 = \int_0^R dr\,u(r)\,\partial u(r)/\partial\mu \tag{2.83}$$

(i) is non-negative for $0 < R < \infty$, and (ii) vanishes only at the zeroes of the reduced radial wavefunction $u(r)$, for any bound state. To prove the theorem, we use the normalization condition

$$\int_0^\infty dr\,[u(r)]^2 = 1, \tag{2.8}$$

†28 See, for example, ref. [52, vol. II, p. 1664].

†29 See ref. [37, §13.5.1].

†30 See, for example, ref. [33, sec. 3] and ref. [53, appendix d].

and the definitions

$$w(\rho) \equiv u(r) \tag{3.11}$$

and

$$\rho = (2\mu|\lambda|/\hbar^2)^{1/(2+\nu)} r \tag{3.8}$$

to define a scaled wavefunction

$$\tilde{w}(\rho) = (\hbar^2/2\mu|\lambda|)^{1/2(2+\nu)} w(\rho) \tag{3.73}$$

which is independent of μ (and of λ) and satisfies

$$\int_0^\infty d\rho\, [\tilde{w}(\rho)]^2 = 1. \tag{3.74}$$

We may then write

$$u(r) = (2\mu|\lambda|/\hbar^2)^{1/2(2+\nu)} \tilde{w}(\rho), \tag{3.75}$$

which leads, after a brief computation, to

$$\frac{\partial u(r)}{\partial \mu} = \frac{1}{2\mu(2+\nu)} [u(r) + 2ru'(r)] = \frac{1}{2\mu(2+\nu)\, u(r)} \frac{d}{dr} (r[u(r)]^2). \tag{3.76}$$

The integral (2.83) can now be evaluated; it yields

$$G(R) = R[u(R)]^2/2\mu(2+\nu), \tag{3.77}$$

which is non-negative and vanishes only at the zeroes of $u(r)$, as claimed. The case $\nu = 0$ applies to the logarithmic potential, as explained in section 3.1.4.

Thus the probability that a particle lies within a spherical shell of radius R cannot decrease as the mass μ is increased. The result (3.77) shows that probability does not flow past nodes in the reduced radial wavefunction. A similar statement holds for variations of the coupling strength λ. Using (3.75) we can show at once that

$$\mathcal{G}(R) \equiv \frac{1}{2} \frac{\partial}{\partial|\lambda|} \int_0^R dr\, [u(r)]^2 = \int_0^R dr\, u(r) \frac{\partial u(r)}{\partial|\lambda|} = \frac{R[u(R)]^2}{2|\lambda|(2+\nu)} \geq 0. \tag{3.78}$$

The function $G(R)$ is known to be non-negative for s-wave levels in a square well of finite depth [39]. Its minima correspond to the nodes of the radial wavefunction (as required by (2.93a) for the ground state), but it does not vanish at these nodes. Within the well the result analogous to (3.77) is found to be [39]

$$G(R) = AR[u(R)]^2 + B \int_0^R dr\, [u(r)]^2, \tag{3.79}$$

where A and B are non-negative constants. In an infinitely deep square well, the probability distribution depends only on the size of the well, independent of μ. Thus $G(R) \equiv 0$ for all levels, as follows from the $\nu \to \infty$ limit of (3.77).

The most general class of potentials for which $G(R) \geq 0$ for all bound states, or for all s-wave bound states, has not yet been characterized [54]. We expect such potentials to be monotonically increasing functions of the coordinate, and to have some degree of smoothness. One example known to us of a monotonic potential for which $G(R)$ can become negative for an s-wave level is a finite square well nested within an infinite square well [39].

Finally, it is possible to investigate the behavior of $G(R)$ in the classical limit. This is done in section 4.

4. Semiclassical results

Within the framework of the semiclassical (JWKB, WKB) approximation†$_{31}$ the quantum number dependence of energy eigenvalues and of bound-state normalizations becomes particularly simple. The resulting expressions are impressively accurate, as several examples in this section will illustrate.

It will be convenient to discuss first, in section 4.1, results that can be obtained for potentials which are nonsingular at the origin. Singular potentials are dealt with in section 4.2. A critical summary of simple approximations for low-lying states occupies section 4.3. In section 4.4 we discuss very briefly the mass dependence of Schrödinger wavefunctions.

4.1. Potentials finite at the origin

4.1.1. Wavefunctions and quantization condition

We begin by discussing one-dimensional motion in an arbitrary nonsingular potential between the turning points x_1 and x_2 which represent the extremes of classically alowed motion for a particle with energy E:

$$V(x_1) = E, \tag{4.1a}$$

$$V(x_2) = E, \tag{4.1b}$$

as depicted in fig. 7. To the right of the turning point x_1 (in the interval $x_1 \leq x \leq x_2$), the Schrödinger wavefunction can be represented as

$$u(x) = \frac{N}{\sqrt{p(x)}} \cos\left\{\frac{1}{\hbar}\int_{x_1}^{x} \mathrm{d}x'\, p(x') - \frac{\pi}{4}\right\}, \tag{4.2}$$

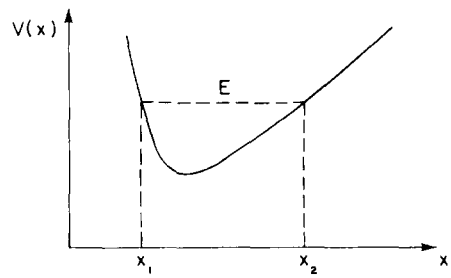

Fig. 7. Motion in an arbitrary one-dimensional potential between classically allowed extremes x_1 and x_2.

†$_{31}$ The literature on this approximation is voluminous. We have drawn some enlightenment from the following very incomplete list: refs. [51, 53, 55–59]. Some more recent observations are contained in ref. [47].

where

$$p(x) \equiv [2\mu(E - V(x))]^{1/2} \tag{4.3}$$

is the local momentum of the particle and N is a normalization factor to be determined. The phase $-\pi/4$ in eq. (4.2) comes from the requirement that the solution "match" one which is exponentially damped as $x \to -\infty$ [53, 56, 57]. It is valid as long as the potential does not vary "too rapidly" near $x = x_1$, but can be expanded in a form

$$V(x) \approx V(x_1) + (x - x_1)V'(x_1) \tag{4.4}$$

valid for a region around x_1 in which $u(x)$ goes through an oscillation or two. The Schrödinger equation then may be solved near x_1 in terms of Airy functions (cf. section 2, eqs. (2.70)–(2.78)) in order to "match" the approximate solution (4.2) with one to the left of x_1.

A similar discussion leads us to another representation for $u(x)$:

$$u(x) = \frac{N'}{\sqrt{p(x)}} \cos\left\{\frac{1}{\hbar}\int_x^{x_2} dx'\, p(x') - \frac{\pi}{4}\right\}, \tag{4.5}$$

which is of the correct form to match an exponentially damped solution on the right.

The solutions (4.2) and (4.5) must agree for $x_1 < x < x_2$. They can be identified only if

$$\frac{1}{\hbar}\int_{x_1}^{x} dx\, p(x) - \frac{\pi}{4} = m\pi - \left[\frac{1}{\hbar}\int_x^{x_2} dx'\, p(x') - \frac{\pi}{4}\right]; \tag{4.6}$$

where $m = 0, 1, 2, \ldots$ and $N' = (-1)^m N$. The condition (4.6) may be written

$$\int_{x_1}^{x_2} dx\, p(x) = (m + \tfrac{1}{2})\pi\hbar; \qquad (m = 0, 1, 2, \ldots) \tag{4.6'}$$

it represents a *quantization condition* which specifies the values of E in eq. (4.3) that can lead to bound states.

In anticipation of the three-dimensional problem which is our principal concern, we again specialize to symmetric potentials

$$V(x) = V(-x) \tag{4.7}$$

in one dimension. Without further loss of generality (for potentials that are finite at the origin) we may choose

$$V(0) = 0. \tag{4.8}$$

For a symmetric potential (4.7), the local momentum satisfies

$$p(x) = p(-x) \tag{4.9}$$

and the turning points are

$$x_1 = -x_2 \equiv -x_c. \tag{4.10}$$

We assume $V'(x) \geq 0$ for $x \geq 0$ so only one pair of turning points occurs. Consequently the quantization

condition takes the form

$$\int_0^{x_c} \mathrm{d}x\, p(x) = (m+\tfrac{1}{2})\pi\hbar/2, \qquad m = 0, 1, 2, \ldots . \tag{4.11}$$

The normalization constant N is fixed by the requirement that[†13]

$$\frac{1}{2} = \int_0^{x_c} \mathrm{d}x\, [u(x)]^2 = N^2 \int_0^{x_c} \frac{\mathrm{d}x}{p(x)} \cos^2\left\{\frac{1}{\hbar}\int_0^x \mathrm{d}x'\, p(x') - \frac{\pi}{4}\right\}. \tag{4.12}$$

The average value of the oscillatory factor in (4.12) may be taken equal to $\frac{1}{2}$, so that

$$N^2 \approx \left[\int_0^{x_c} \mathrm{d}x/p(x)\right]^{-1}. \tag{4.13}$$

The integral in (4.13) is related to the classical probability that the particle be found near the origin. To evaluate it, we differentiate the quantization condition (4.11) with respect to the quantum number m [60]:

$$\frac{1}{2}\frac{\mathrm{d}E_m}{\mathrm{d}m}\int_0^{x_c} \mathrm{d}x\, \frac{2\mu}{p(x)} = \frac{\pi\hbar}{2}, \tag{4.14}$$

so that

$$N^2 = \frac{2\mu}{\pi\hbar}\frac{\mathrm{d}E_m}{\mathrm{d}m}. \tag{4.15}$$

It is now straightforward to compute that

$$[u(0)]^2 = \frac{1}{\pi\hbar}\sqrt{\frac{2\mu}{E_m}}\frac{\mathrm{d}E_m}{\mathrm{d}m}\cos^2(m\pi/2) \tag{4.16}$$

and

$$[u'(0)]^2 = \frac{(2\mu)^{3/2}}{\pi\hbar^3}\sqrt{E_m}\frac{\mathrm{d}E_m}{\mathrm{d}m}\sin^2(m\pi/2). \tag{4.17}$$

The one-dimensional discussion carries over directly to s-waves in three dimensions (for nonsingular central potentials) if we identify s-wave bound states with the odd-parity levels in one dimension, as shown in fig. 8, corresponding to odd values of M. We therefore choose

$$u(r) = \frac{N}{\sqrt{p(r)}}\cos\left\{\frac{1}{\hbar}\int_0^r \mathrm{d}r'\, p(r') - \frac{\pi}{2}\right\}. \tag{4.18}$$

The quantization condition (4.11) then takes the form

$$\int_0^{x_c} \mathrm{d}x\, p(x) = [(2n-1)+\tfrac{1}{2}]\pi\hbar/2, \tag{4.19}$$

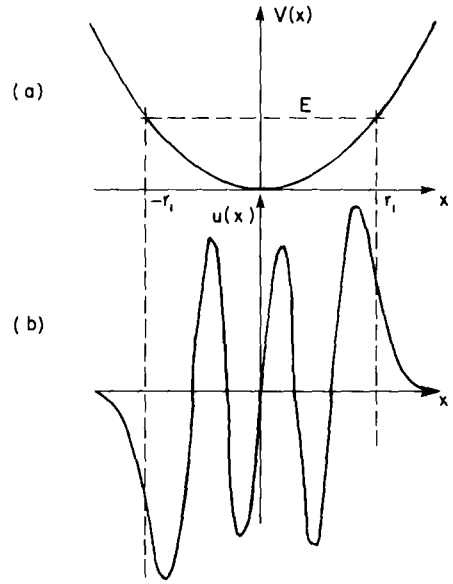

Fig. 8. The one-dimensional problem appropriate to s-waves in three dimensions. (a) Symmetric potential $V(-x) = V(x)$; (b) antisymmetric wave function $u(-x) = -u(x)$. The classical turning points are at $x = \pm r_1$.

where $n = 1, 2, 3, \ldots$ is the principal quantum number in three dimensions. The preceding equation may be rewritten, in three-dimensional notation, as

$$\int_0^{r_c} dr\,[2\mu(E - V(r))]^{1/2} = (n - \tfrac{1}{4})\pi\hbar, \tag{4.20}$$

where r_c is defined by $V(r_c) = E$. A derivation parallel to the one which led to (4.16) and (4.17) yields the useful result [61, 62]

$$|\Psi(0)|^2 = [u'(0)]^2/4\pi = \frac{(2\mu)^{3/2}}{4\pi^2\hbar^3} E_n^{1/2} \frac{dE_n}{dn}. \tag{4.21}$$

This connection has recently been generalized to higher partial waves by Bell and Pasupathy [63], who find†32

$$\left| \frac{d^l R_{nl}(r)}{dr^l} \right|_{r=0}^2 = \frac{1}{\pi}\left[\frac{l!}{(2l+1)!!}\right]^2 \left(\frac{2\mu E_{nl}}{\hbar^2}\right)^{l+1/2} \frac{\partial(2\mu E_{nl}/\hbar^2)}{\partial n}, \tag{4.22}$$

where the radial wavefunction $R_{nl}(r)$ is defined by eqs. (2.2) and (2.3), and n is the radial quantum number, equal to one plus the number of nodes in the radial wavefunction. Writing the radial wavefunction near the origin as

$$R_{nl}(r) \sim a_{nl} r^l \tag{4.23}$$

†32 The authors of ref. [63] derive eq. (4.22) by means of a Thomas–Fermi approximation: when $l = 0$, for example, $\Sigma_{E \le E_n} |\Psi_n(r)|^2 = \int_{|k| < k_F(r)} d^3k/(2\pi)^3$. $E - V(r) = k_F^2(r)/2\mu$. This relation may be differentiated with respect to n to obtain eq. (4.21). As noted in ref. [63], eq. (4.22) also may be obtained by matching solutions in terms of spherical Bessel functions near $r = 0$ to the WKB solutions for larger r.

as implied by eq. (2.28), we may rewrite (4.22) as

$$a_{nl}^2 = \frac{(2\mu E_{nl}/\hbar^2)^{l+1/2}}{\pi[(2l+1)!!]^2}\frac{\partial(2\mu E_{nl}/\hbar^2)}{\partial n}. \tag{4.24}$$

The quantization condition (4.20) and the phase in eq. (4.5) are slightly modified if the potential has an infinite wall at $x = x_2$†33:

$$V(x) = +\infty, \qquad x \geq x_2. \tag{4.25}$$

In this event, the wavefunction must vanish at the wall, so we choose

$$u(x) = \frac{N'}{\sqrt{p(x)}}\cos\left\{\frac{1}{\hbar}\int_x^{x_2} \mathrm{d}x'\, p(x') - \frac{\pi}{2}\right\}. \tag{4.26}$$

For three-dimensional motion, the wavefunction (4.18) remains appropriate, while the quantization condition (4.20) becomes

$$\int_0^{r_c} \mathrm{d}r\,[2\mu(E_n - V(r))]^{1/2} = n\pi\hbar, \tag{4.27}$$

with $n = 1, 2, 3, \ldots$. Similarly, in one dimension, for an infinite square well with walls at x_1 and x_2 the quantization condition is

$$\int_{x_1}^{x_2} \mathrm{d}x\,[2\mu(E_m - V(x))]^{1/2} = (m+1)\pi\hbar, \qquad m = 0, 1, 2, \ldots. \tag{4.28}$$

The result (4.20) may be used to find a unique radially symmetric potential (monotonically increasing with r) once E_n is known. (We imagine E_n to be a continuous function of n for this purpose.) This is related to the problem of determining the shape of a classical potential if one knows the dependence on the energy of the period of oscillation.†34.

We change variables in (4.20), letting V be the independent variable:

$$\int_0^E \mathrm{d}V \frac{\mathrm{d}r}{\mathrm{d}V}\left[\frac{2\mu}{E-V}\right]^{1/2} = 2\pi\hbar\left[\frac{\mathrm{d}E_n}{\mathrm{d}n}\right]^{-1}. \tag{4.29}$$

The monotonicity of V is important here, to ensure that r will be a single-valued function of V.

Now multiply (4.29) by $(\tilde{V} - E)^{-1/2}$, where $\tilde{V} \geq E$ is some fixed constant, and integrate with respect to E from 0 to $\tilde{V}$. Since

$$0 \leq V \leq E \leq \tilde{V}, \tag{4.30}$$

the order of integration on the left-hand side can be reversed, with the result

†33 Consideration of an infinite wall at $r = 0$ leads to an alternative derivation of the quantization condition for a nonsingular potential in three dimensions. See ref. [56].

†34 Cf. problem 23, §1 in ref. [60]. The classical mechanics problem is described in ref. [64, §12].

$$(2\mu)^{1/2}\int_0^{\tilde V} dV\,\frac{dr}{dV}\int_V^{\tilde V}\frac{dE}{(\tilde V-E)^{1/2}(E-V)^{1/2}}=2\pi\hbar\int_0^{\tilde V} dE\,(\tilde V-E)^{-1/2}\left[\frac{dE_n}{dn}\right]^{-1}. \tag{4.31}$$

But the integral with respect to E on the left is just a beta function which has the value π, and we find†35

$$r(V)=\frac{2\hbar}{(2\mu)^{1/2}}\int_0^{V} dE\,(V-E)^{1/2}\left[\frac{dE_n}{dn}\right]^{-1}. \tag{4.32}$$

4.1.2. *Power-law potentials*

For a potential (3.1) with $0<\nu<\infty$ the integral (4.20) can be performed exactly, leading to

$$E_n=\lambda^{2/(2+\nu)}(2\mu/\hbar^2)^{-\nu/(2+\nu)}[A(\nu)(n-\tfrac14)]^{2\nu/(2+\nu)}, \tag{4.33}$$

$$A(\nu)=[2\nu\sqrt{\pi}\,\Gamma(\tfrac32+1/\nu)]/\Gamma(1/\nu),\qquad \nu>0. \tag{4.34}$$

The limit $\nu\to\infty$ corresponds to the square well (if we replace $n-\frac14$ by n as noted above). The semiclassical and exact results for a linear, harmonic oscillator, and infinite square well potential (with $\lambda=2\mu/\hbar^2=1$) are compared in table 2. We shall show below that eq. (4.33) can be generalized to all partial waves by the replacement $n\to n+l/2$.

Table 2
Semiclassical and exact results for s-wave energy levels in potentials $V(r)=\lambda r^\nu$, $\nu>0$. Here $2\mu\lambda/\hbar^2=1$

	E_n(semiclassical, eq. (4.33))	E_n(exact)
$\nu=1$ (linear)		
n	$\left[\frac{3\pi}{2}(n-\frac14)\right]^{2/3}$	$\mathrm{Ai}(-E_n)=0$ [eq. (2.73)]
1	2.32025	2.33811
2	4.08181	4.08795
3	5.51716	5.52056
4	6.78445	6.78671
5	7.94249	7.94413
6	9.02137	9.02265
7	10.03914	10.04017
8	11.00767	11.00852
9	11.93528	11.93602
10	12.82814	12.82878
$\nu=2$ (harmonic oscillator)		
	$4n-1$	$4n-1$ [eq. (3.61)]
$\nu\to\infty$ (infinite square well, radius R: $\lambda=R^{-\nu}$)		
	$(\pi n/R)^2$	$(\pi n/R)^2$

†35 This is the appropriate form for three dimensions. In one dimension the factor of 2 in the numerator of the right-hand side of (4.32) is absent, and the potential is *defined* to be symmetric. The symmetry is a very strong requirement; other (non-symmetric) potentials also can give the same level structure in one dimension. (See refs. [58] and [65, part I] for a discussion.)

The squares of s-wave wavefunctions at $r = 0$ are easily evaluated with the help of (4.21):

$$|\Psi_n(0)|^2 = \frac{1}{2\pi^2}\left(\frac{2\mu\lambda}{\hbar^2}\right)^{3/(2+\nu)} \frac{\nu}{2+\nu} [A(\nu)]^{3\nu/(2+\nu)} (n - \tfrac{1}{4})^{2(\nu-1)/(2+\nu)}, \tag{4.35}$$

with $n - \frac{1}{4} \to n$ for $\nu = \infty$. In table 3 we show how well eq. (4.35) reproduces the exact results for the linear, harmonic oscillator, and infinite square well potentials. It is clear from Stirling's formula that the two expressions for the oscillator agree in the large-n limit. The degree to which they coincide even for small n is striking.

4.2. Singular potentials

4.2.1. Power-law potentials

When $V(0) = -\infty$, as occurs for negative-power-law or logarithmic potentials, certain of the above discussions no longer are valid. In particular, the form (4.18) does not represent the wavefunction correctly near $r = 0$. As long as $|E_n| \to 0$ for $n \to \infty$, however, we may adopt a simple approximation to obtain the wavefunction near $r = 0$, and then deduce the appropriate quantization condition and normalization by joining this wavefunction onto the WKB solution (4.5) for larger r. The approximation we shall make is to neglect E_n†36. In this limit the (scaled) Schrödinger equation (3.12) takes the form

$$w''(\rho) + [\rho^\nu - l(l+1)/\rho^2] w(\rho) = 0, \tag{4.36}$$

where ρ is defined in eq. (3.8). An appropriate change of dependent and independent variables permits this to be cast in the form of Bessel's equation. First defining

$$q \equiv (2+\nu)^{-1}, \tag{4.37}$$

Table 3
Semiclassical and exact results for $|\Psi_n(0)|^2$ in potentials $V(r) = \lambda r^\nu$, $\nu > 0$. Here $2\mu\lambda/\hbar^2 = 1$

	$\lvert\Psi_n(0)\rvert^2$ (semi-classical, eq. (4.35))	$\lvert\Psi_n(0)\rvert^2$ (exact)
$\nu = 1$ (linear)		
	$1/4\pi$	$1/4\pi$ [eq. (3.16)]
$\nu = 2$ (harmonic oscillator)		
n	$\frac{2}{\pi^2}(n - \frac{1}{4})^{1/2}$	$\frac{2}{\pi^2}\frac{\Gamma(n+\frac{1}{2})}{\Gamma(n)}$ [eqs. (2.43), (3.62)]
1	0.17549	0.17959
2	0.26807	0.26938
3	0.33604	0.33673
4	0.39242	0.39285
5	0.44165	0.44195
$\nu \to \infty$ (infinite square well, radius R: $\lambda = R^{-\nu}$)		
	$\pi n^2/2R^3$	$\pi n^2/2R^3$

†36 This method is discussed, for example, in ref. [56, pp. 129–131] and in refs. [57] and [66]. It is valid for potentials of the form (3.1) with $\lambda < 0$ and $\nu < 0$, all of which have an infinite number of bound states with $\lim_{n\to\infty} E_n \to 0^-$.

we let

$$\rho = (z/2q)^{2q}, \tag{4.38}$$

and

$$w(\rho) = z^q v(z), \tag{4.39}$$

whereupon (4.36) can be cast as

$$v''(z) + \frac{1}{z} v'(z) + \left[1 - \frac{q^2(2l+1)^2}{z^2}\right] v(z). \tag{4.40}$$

The solution of this equation which is regular at $z = 0$ is

$$v(z) = cJ_{q(2l+1)}(z). \tag{4.41}$$

The wavefunction $w(\rho)$ is proportional to ρ^{l+1} as $\rho \to 0$, as required.

The constant c is evaluated by demanding the correct asymptotic behavior as $z \to \infty$: since

$$J_\sigma(z) \sim \sqrt{2/\pi z} \cos\{z - \tfrac{1}{2}\sigma\pi - \tfrac{1}{4}\pi\}, \tag{4.42}$$

we find

$$w(\rho) \simeq \frac{c(2q)^q}{\sqrt{\pi q}} \rho^{-\nu/4} \cos\left\{\int_0^\rho \mathrm{d}x\, (x^\nu)^{1/2} - \frac{q(2l+1)\pi}{2} - \frac{\pi}{4}\right\}. \tag{4.43}$$

Upon restoring dimensions, we see that this is the appropriate generalization of (4.18) as long as

$$c(2q)^q/\sqrt{\pi q} = \pm(\hbar^2/2\mu|\lambda|)^{q/2} N/\sqrt{\hbar} \tag{4.44}$$

and

$$\int_0^{r_c} \mathrm{d}r\, [2\mu(E_{nl} - V(r))]^{1/2} = \left(n - \frac{1}{2} + \frac{q(2l+1)}{2}\right)\pi\hbar = \left[n - \frac{1}{2}\left(\frac{1+\nu-2l}{2+\nu}\right)\right]\pi\hbar \tag{4.45}$$

for $n = 1, 2, 3, \ldots$. The quantization condition (4.45) is the appropriate replacement for (4.20), for power-law potentials (3.1) with $\lambda < 0$, $\nu < 0$. The left-hand side can be evaluated in closed form: we find

$$|E_{nl}| = |\lambda|^{2/(2+\nu)} \left(\frac{2\mu}{\hbar^2}\right)^{-\nu/(2+\nu)} \left\{\tilde{A}(\nu)\left[n - \frac{1}{2}\left(\frac{1+\nu-2l}{2+\nu}\right)\right]\right\}^{2\nu/(2+\nu)}, \tag{4.46}$$

with

$$\tilde{A}(\nu) \equiv \left[2|\nu|\sqrt{\pi}\,\Gamma\left(1 - \frac{1}{\nu}\right)\right] \Big/ \Gamma\left(-\frac{1}{2} - \frac{1}{\nu}\right), \qquad (-2 < \nu < 0). \tag{4.47}$$

This expression is exact for the Coulomb potential and is a useful approximation for s-waves in the potential $V = -r^{-1/2}$, as shown in table 4.

The square of the s-wave wavefunction at $r = 0$ now is easily evaluated since we have wavefunctions $u(r)$ which behave properly at $r = 0$. We find

Table 4
Semiclassical and exact results for energy levels in potentials $V(r) = \lambda r^\nu$, $-2 < \nu < 0$. Here $2\mu/\hbar^2 = -\lambda = 1$

	E_n(semiclassical, eq. (4.46))	E_n(exact)
$\nu = -1/2$		
n	$-[4(n-1/6)]^{-2/3}$	numerical calculation
1	−0.448	−0.438
2	−0.265	−0.263
3	−0.198	−0.198
4	−0.162	−0.162
5	−0.139	−0.139
$\nu = -1$ (Coulomb)		
	$-1/4n^2$	$-1/4n^2$ [eq. (3.71)]

$$|\Psi(0)|^2 = \frac{N^2}{4}\{q^{-\nu q}/[\Gamma(q)]^2\}\left(\frac{2\mu|\lambda|}{\hbar^2}\right)^q \tag{4.48a}$$

$$= \frac{1}{4\pi}\frac{2|\nu|}{(2+\nu)}\left(\frac{2\mu|\lambda|}{\hbar^2}\right)^{3/(2+\nu)}\{[\tilde{A}(\nu)]^2(2+\nu)\}^{\nu/(2+\nu)}\left[n - \frac{1}{2}\frac{(1+\nu-2l)}{(2+\nu)}\right]^{(\nu-2)/(\nu+2)}\Big/[\Gamma(1/(2+\nu))]^2 \tag{4.48b}$$

with N given by eq. (4.15). Notice that eq. (4.48a) does not contain an explicit factor of $E_{nl}^{1/2}$, in contrast to eq. (4.21). The expression (4.48b) for $|\Psi(0)|^2$ is exact for the Coulomb potential and is reasonably accurate for $\nu = -\frac{1}{2}$, as demonstrated in table 5.

In analogy with the discussion [63] of eqs. (4.22)–(4.24) for nonsingular potentials, we may also evaluate the behavior of the radial wavefunction for $l > 0$ near the origin for power-law potentials with $\nu < 0$:

$$|R_{nl}^{(l)}(0)|^2 \equiv \left|\frac{\mathrm{d}^l R_{nl}(r)}{\mathrm{d}r^l}\bigg|_{r=0}\right|^2 = q\left[\frac{l!\,q^{q(2l+1)}}{\Gamma\{q(2l+1)+1\}}\right]^2 \frac{\mathrm{d}(2\mu E_{nl}/\hbar^2)}{\mathrm{d}n}\left(\frac{2\mu|\lambda|}{\hbar^2}\right)^{1/(2+\nu)}. \tag{4.49}$$

Table 5
Semiclassical and exact results for $|\Psi_n(0)|^2$ in potentials $V(r) = \lambda r^\nu$, $-2 < \nu < 0$. Here $2\mu/\hbar^2 = -\lambda = 1$

	$\lvert\Psi_n(0)\rvert^2$ (semiclassical, eq. (4.48b))	$\lvert\Psi_n(0)\rvert^2$ (exact)
$\nu = -1/2$		
n	$1/[4\pi\, 3^{4/3}[\Gamma(2/3)]^2(n-1/6)^{5/3}]$	numerical calculation
1	0.01359	0.01123
2	0.00365	0.00333
3	0.00177	0.00167
4	0.00107	0.00102
5	0.00073	0.00071
$\nu = -1$ (Coulomb)		
	$\frac{1}{8\pi n^3}$	$\frac{1}{8\pi n^3}$ [eqs. (2.43), (3.72)]

The ratio of this expression to the true expression for the Coulomb potential (ref. [33, p. 15]) yields

$$(R_{nl}^{(l)}(0)|_{\text{approx.}})/(R_{nl}^{(l)}(0)|_{\text{exact}}) = (n-1)!(n+l)^{2l+1}/(n+2l)! \tag{4.50}$$

which approaches unity as $n \to \infty$ for fixed l. Eq. (4.49), obtained here by direct solution of eq. (4.36), also may be found by applying the transformation described in section 3.2 to a power-law potential with $\nu > 0$, and using the result (4.22).

The transformation of section 3.2 also permits a powerful generalization of eq. (4.33) which is valid for s-waves in power-law potentials with $\nu > 0$, to all values of l. Starting from eq. (4.46) for negative powers, we find that for $\nu > 0$

$$E_{nl} = \lambda^{2/(2+\nu)}\left(\frac{2\mu}{\hbar^2}\right)^{-\nu/(2+\nu)}\left[A(\nu)\left(n+\frac{l}{2}-\frac{1}{4}\right)\right]^{2\nu/(2+\nu)}, \tag{4.51}$$

with $A(\nu)$ given by eq. (4.34). This result is exact for the harmonic oscillator. Note that the appropriate quantization variable is $n + l/2$ for *all* values of $\nu > 0$, and we expect this also to be so for $\nu = 0 (V \sim \ln r)$ by comparing the limits $\nu \to 0^+$ in (4.51) and $\nu \to 0^-$ in (4.46).

4.2.2. Behavior of $\langle r^k \rangle_n$ for power-law potentials

Moments of the spatial probability distribution of an s-wave bound state may be written approximately as

$$\langle r^k \rangle_n \approx \int_0^{r_c} \mathrm{d}r \frac{r^k}{p(r)} \Big/ \int_0^{r_c} \frac{\mathrm{d}r}{p(r)}, \tag{4.52}$$

where we have neglected oscillations of the wavefunction as in eq. (4.13). For power-law potentials of the form (3.1), the integrals lead to beta functions and

$$\langle r^k \rangle_n \approx |E_n/\lambda|^{k/\nu} Z(\nu), \tag{4.53}$$

where

$$Z(\nu) = \begin{cases} B\left(\frac{k+1}{\nu}, \frac{1}{2}\right) \Big/ B\left(\frac{1}{\nu}, \frac{1}{2}\right), & \nu > 0 \quad \text{(4.54a)} \\ B\left(\frac{1}{2} - \frac{k+1}{\nu}, \frac{1}{2}\right) \Big/ B\left(\frac{1}{2} - \frac{1}{\nu}, \frac{1}{2}\right), & \nu < 0. \quad \text{(4.54b)} \end{cases}$$

Since according to eqs. (4.33) and (4.46) $|E_n| \propto n^{2\nu/(2+\nu)}$ for large values of the principal quantum number n, we obtain

$$\langle r^k \rangle_n \propto n^{2k/(2+\nu)}. \tag{4.55}$$

In a Coulomb potential ($\nu = -1$), the Bohr radius behaves as n^2; in an infinite square well ($\nu = \infty$), moments of the probability distribution are independent of n.

The semiclassical expression (4.53) is exact for the mean radius for a Coulomb potential, $V(r) = \lambda/r$, reproducing

$$\langle r \rangle_n = 3\lambda/4E_n, \tag{2.37}$$

and for a linear potential, $V(r) = \lambda r$, in agreement with

$$\langle r \rangle_n = 2E_n/3\lambda. \tag{2.36}$$

For the harmonic oscillator potential, $V(r) = \lambda r^2$, for which

$$\langle r \rangle = (1/2\lambda)\langle V' \rangle = (\pi\hbar^2/\mu\lambda)|\Psi(0)|^2, \tag{4.56}$$

we may use the exact form of $|\Psi(0)|^2$ given in table 3 together with the scaling law (3.15), to compute

$$\langle r \rangle_n = \frac{4}{\pi}\left(\frac{2\mu\lambda}{\hbar^2}\right)^{-1/4} \frac{\Gamma(n+\frac{1}{2})}{\Gamma(n)}. \tag{4.57}$$

This is to be compared with the semiclassical result

$$\langle r \rangle_n \approx \frac{2}{\pi}\left(\frac{E_n}{\lambda}\right)^{1/2} = \frac{4}{\pi}\left(\frac{2\mu\lambda}{\hbar^2}\right)^{-1/4} (n-\tfrac{1}{4})^{1/2}. \tag{4.58}$$

The excellent agreement between $\Gamma(n+\frac{1}{2})/\Gamma(n)$ and $(n-\frac{1}{4})^{1/2}$ has already been noted in connection with table 3.

4.2.3. The logarithmic potential

Although the potential

$$V = C \ln (r/r_0) \tag{3.21}$$

is singular at $r = 0$, there is a certain sense in which it may be regarded as the limit of either a nonsingular ($\nu > 0$) or singular ($\nu < 0$) potential. The quantization conditions (4.46) and (4.51) become identical in the limit $\nu = 0$, indicating that $n + l/2 - \frac{1}{4}$ is very likely the optimal variable for the problem. We then find

$$E_{nl} = C \ln \left[\frac{2\sqrt{\pi}(n + l/2 - \frac{1}{4})}{(2\mu C/\hbar^2)^{1/2} r_0}\right]. \tag{4.59}$$

The accuracy of eq. (4.59) for the energy eigenvalues is shown in table 6. The approximation is seen to deteriorate for fixed n and increasing l but to improve for fixed l and increasing n. It is considerably better for s-waves than for $l \neq 0$. Improved approximations for $l \neq 0$ are given in ref. [47]. They do not appear to have the simple form quoted here.

Positive moments of the probability distribution also are easily computed for s-waves. When $r_0 = 1$,

Table 6
Exact and semiclassical levels in a potential $V(r) = C \ln (r/r_0)$. The WKB eigenvalues, shown in parentheses, are based on eq. (4.59). Here $C = \hbar^2/2\mu r_0^2 = 1$

n \ l	0	1	2	3	4
1	1.0443	1.643	2.015	2.286	2.499
	(0.9778)	(1.489)	(1.825)	(2.076)	(2.277)
2	1.8474	2.151	2.388	2.581	2.742
	(1.8251)	(2.076)	(2.277)	(2.444)	(2.587)
3	2.2897	2.491	2.663	2.811	2.941
	(2.2771)	(2.444)	(2.587)	(2.712)	(2.824)
4	2.5957	2.744	2.880	2.999	3.107
	(2.5873)	(2.712)	(2.824)	(2.924)	(3.015)
5	2.8299	2.948	3.060	3.159	3.251
	(2.8237)	(2.924)	(3.015)	(3.098)	(3.175)

$$\langle r^k\rangle_n \simeq \int_0^{r_c} \frac{dr\, r^k}{\sqrt{E_n - C\ln r}} \Big/ \int_0^{r_c} \frac{dr}{\sqrt{E_n - C\ln r}} = \frac{e^{kE_n/C}}{\sqrt{k+1}}, \tag{4.60}$$

where $E_n \equiv E_{n0}$ so that with $2\mu C/\hbar^2 = 1$, we have

$$\langle r^k\rangle_n = \frac{(4\pi)^{k/2}}{\sqrt{k+1}}(n-\tfrac{1}{4})^k. \tag{4.61}$$

This agrees with the dependence upon k and n anticipated from the $\nu \to 0$ limits of eqs. (4.53)–(4.55). In table 7 we have checked the accuracy of eq. (4.61) for $\langle r\rangle_n$ and have quoted values of $|\Psi_n(0)|^2$, which behave approximately as $0.06/n$. The behavior of $|\Psi_n(0)|^2$ can be anticipated from the $\nu \to 0$ limits of eqs. (4.35) and (4.48), but we have not found a satisfactory closed form.

4.3. Summary of approximate results

In this subsection we summarize and test the accuracy of semiclassical results regarding the principal-quantum-number dependence of bound state energies and normalizations. These will find application in the discussions of experimental data in section 5 and beyond.

For power-law potentials (3.1) the energy eigenvalues are given by

$$|E_{nl}| \approx (n - \gamma_l(\nu))^{2\nu/(2+\nu)}, \tag{4.62}$$

where

$$\gamma_l(\nu) = \begin{cases} -l/2, & \text{for } \nu = \infty, \\ \dfrac{1-2l}{4}, & \text{for } 0 < \nu < \infty, \\ \dfrac{\nu+1-2l}{2(2+\nu)}, & \text{for } -2 < \nu < 0. \end{cases} \tag{4.63}$$

The corresponding result for the logarithmic potential is eq. (4.59). The connection (4.62) implies that for power-law potentials the s-wave levels $E_n \equiv E_{n0}$ obey

$$\frac{E_3 - E_2}{E_2 - E_1} \approx \frac{[3-\gamma(\nu)]^s - [2-\gamma(\nu)]^s}{[2-\gamma(\nu)]^s - [1-\gamma(\nu)]^s}, \tag{4.64}$$

where $\gamma(\nu) = \gamma_0(\nu)$ and

$$s \equiv 2\nu/(2+\nu). \tag{4.65}$$

Table 7
Semiclassical and exact results for $\langle r\rangle_n$ and $|\Psi_n(0)|^2$ of s-wave levels in a potential $V(r) = C\ln(r/r_0)$. Here $C = \hbar^2/2\mu = r_0^2 = 1$

n	$\langle r\rangle_n$ (semiclassical, eq. (4.61))	$\langle r\rangle_n$ (exact)	$\lvert\Psi_n(0)\rvert^2$ (exact)	$n\lvert\Psi_n(0)\rvert^2$
1	1.88	1.97	0.0549	0.0549
2	4.39	4.46	0.0280	0.0560
3	6.89	6.95	0.0191	0.0574
4	9.40	9.46	0.0146	0.0583
5	11.91	11.97	0.0118	0.0592
6	14.41	14.47	0.0100	0.0600

For the logarithmic potential,

$$\frac{E_3-E_2}{E_2-E_1}\approx\frac{\ln(11/7)}{\ln(7/3)}=0.533. \tag{4.66}$$

The ratios (4.64) and (4.66) are plotted in fig. 9 together with points corresponding to the exact ratios. Agreement is excellent for all the examples we have studied.

The ratio $(E_{2S}-E_{2P})/(E_{2S}-E_{1S})$ is also characteristic of the power ν. Although exact for $\nu=-1$ and $\nu=2$, the WKB approximation is rather crude in between. We shall discuss exact results in section 5.3.1.

Another simple relation which has been derived semiclassically is

$$|\Psi_n(0)|^2\propto(n-\gamma(\nu))^t, \tag{4.67}$$

where

$$t=\begin{cases}2(\nu-1)/(2+\nu), & \text{for } 0<\nu<\infty\\ (\nu-2)/(2+\nu), & \text{for } -2<\nu<0.\end{cases} \tag{4.68}$$

Thus we find

$$\frac{|\Psi_2(0)|^2}{|\Psi_1(0)|^2}\approx\left[\frac{2-\gamma(\nu)}{1-\gamma(\nu)}\right]^t. \tag{4.69}$$

We show in fig. 10 the close correspondence between eq. (4.69) and the exact ratios.

It has been pointed out [67] that in a wide class of power-law potentials the quantity

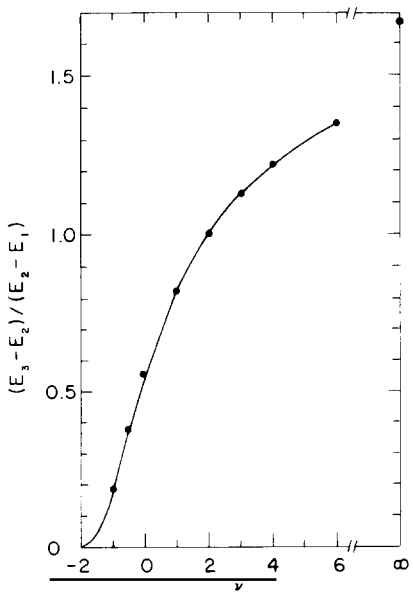

Fig. 9. Semiclassical (curve) and exact (points) ratios $(E_3-E_2)/(E_2-E_1)$ for s-wave levels in potentials $V(r)=\lambda r^\nu$.

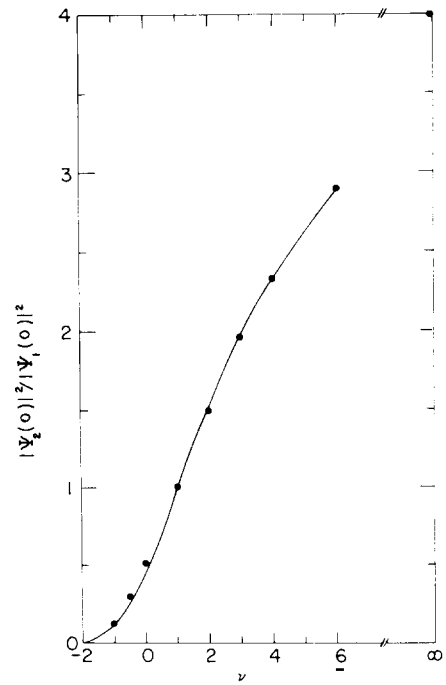

Fig. 10. Semiclassical (curve) and exact (points) ratios $|\Psi_2(0)|^2/|\Psi_1(0)|^2$ for s-wave levels in potentials $V(r)=\lambda r^\nu$.

$$R \equiv \frac{\ln[|\Psi_3(0)|/|\Psi_2(0)|]}{\ln[|\Psi_2(0)|/|\Psi_1(0)|]} \tag{4.70}$$

varies within restrictive bounds. This remark stemmed in part from the observation that eq. (4.67) implies that

$$R = \frac{\ln(11/7)}{\ln(7/3)} = 0.533 \tag{4.71}$$

for $\gamma(\nu) = \frac{1}{4}$, which is appropriate for $\nu > 0$. In table 8 we quote the exact and semiclassical results for R for several of the potentials we have been discussing.

4.4. Mass dependence of wavefunctions

For s-wave bound states we may write the classical probability that a particle is located within a spherical shell of radius R as

$$P_c(R) \equiv \frac{\int_0^R dr/v(r)}{\int_0^{r_c} dr/v(r)} = \frac{\int_0^R dr\,[E - V(r)]^{-1/2}}{\int_0^{r_c} dr\,[E - V(r)]^{-1/2}} \tag{4.72}$$

where

$$v(r) \equiv p(r)/\mu \tag{4.73}$$

is the classical velocity of the particle at the position r, and at the classical turning point $v(r_c) = 0$. The expression (4.72) is approximately equal to the corresponding quantum mechanical probability if we neglect the oscillatory factors in the semiclassical wavefunctions (4.18).

We may study the dependence of $P_c(R)$ on E instead of μ. Since

$$\frac{\partial P_c(R)}{\partial \mu} = \frac{\partial P_c(R)}{\partial E} \cdot \frac{dE}{d\mu} = -\frac{\langle T \rangle}{\mu} \frac{\partial P_c(R)}{\partial E}, \tag{4.74}$$

the signs of $\partial P_c(R)/\partial\mu$ and $\partial P_c(R)/\partial E$ are opposite.

Table 8
The ratio $R \equiv \ln(|\Psi_3(0)|/|\Psi_2(0)|)/\ln(|\Psi_2(0)|/|\Psi_1(0)|)$ for several simple potentials

Potential	$R_{\text{semiclassical}}$	R_{exact}	Remarks
$-r^{-1}$	0.585	0.585	$\ln(3/2)/\ln 2$ [eq. (3.72)]
$-r^{-1/2}$	0.552	0.57	Table 4
$\ln r$	0.533	0.57	Table 6
r	0.533	0.56	Limiting value for $V(r) = r^\nu$, $\nu \to 1$
r^2	0.533	0.550	$\ln(5/4)/\ln(3/2)$ [eq. (3.62)]
Infinite square well	0.585	0.585	$\ln(3/2)/\ln 2$ [table 3]

The classical probability $P_c(R)$ provides some insight into the types of potentials for which probability will flow inward as μ is increased. Consider the nested square well example of section 3.4. If the energy of the particle slightly exceeds the value that permits it to move classically in the outer well, it will move slowly there and spend most of its time in the outer well. As the energy is decreased, a limit is approached in which the particle spends a fraction approaching 1 of its time in the outer region, until E is lowered sufficiently to classically forbid its presence there. Thus for this situation, $\partial P_c(R)/\partial E$ is not always negative. An additional condition beyond the monotonicity of $V(r)$ is needed to guarantee that $\partial P_c(R)/\partial\mu > 0$.

An example of such a condition has been proposed by Martin [68]: if $V''(r) < 0$, and $V'(r) > 0$, then $\partial P_c(R)/\partial E > 0$. To prove this statement we note that the numerator of (4.72) decreases as E increases. We must therefore show that the denominator

$$D \equiv \int_0^{r_c} dr\,[E - V(r)]^{-1/2} \tag{4.75}$$

is an increasing function of E, so that

$$\partial D/\partial E > 0. \tag{4.76}$$

To do so we write

$$D = \int_{V=V(0)}^{V=E} dV/V'\sqrt{E-V} = -\frac{2\sqrt{E-V}}{V'}\bigg|_{V(0)}^{E} - 2\int_{V(0)}^{E} dV\frac{V''\sqrt{E-V}}{(V')^2}$$

$$= \frac{2\sqrt{E-V(0)}}{V'(0)} - 2\int_{V(0)}^{E} dV\,V''\sqrt{E-V}/(V')^2, \tag{4.77}$$

so that

$$\frac{\partial D}{\partial E} = \frac{1}{V'(0)\sqrt{E-V(0)}} - \int_{V(0)}^{E} dV\,V''/(V')^2\sqrt{E-V} > 0. \tag{4.78}$$

Further classical examples in which $\partial P_c(R)/\partial\mu$ can be investigated are under study [66]. These examples have applications to the determination of new quark charges, as reviewed in section 7.

5. Quarkonium applications: Scaling laws

Until now, we have discussed bound-state quantum mechanics in a general context. For the remainder of this article we shall concentrate increasingly on the problem that kindled our interest in these methods, the nonrelativistic description of states composed of heavy quarks. For these applications, it is convenient to set $\hbar = 1$.

In this section we shall apply some of the scaling laws derived in sections 3 and 4 to general features of the ψ and Υ families. The mass and principal-quantum-number dependence of level spacings and of wavefunctions at the origin will be treated in some detail, and we shall relate branching ratios in the ψ and Υ systems.

5.1. Experimental preliminaries

Some attributes of the charmonium (ψ) family have already been discussed in the introduction. The ψ/J(3095) was discovered as a resonance in the reactions [17]

$$p + Be \to (e^+e^-) + \text{anything} \tag{5.1}$$

at Brookhaven National Laboratory and [18]

$$e^+e^- \to \text{hadrons} \tag{5.2}$$

at the Stanford Linear Accelerator Center in November, 1974. Within ten days, a companion, $\psi(3684)$, often denoted ψ', was found [69] at SLAC. Since the initial discoveries, a rich spectrum of related states has been uncovered in the study of electron–positron annihilations†$_7$. The present knowledge of the charmonium spectrum is summarized in fig. 3(a). As the spectroscopic assignments in fig. 3(b) indicate, these levels have been interpreted with considerable success as nonrelativistic bound states of a charmed quark and charmed antiquark. The ψ and ψ' are assigned as the 1S and 2S levels with parallel quark spins.

In the spring of 1977 the heavy meson Υ was discovered at Fermilab [70] in the reaction

$$p + N \to (\mu + \mu^-) + \text{anything}. \tag{5.3}$$

What we now recognize as the first hints of the ψ family had been seen in this same reaction some seven years before [71]. Although the Υ mass is more than three times that of the ψ, there are obvious parallels between the two states. Because it was observed in an electromagnetic decay mode, and had an intrinsic width consistent with zero, the Υ appeared, like the ψ, to be extraordinarily stable. The stability of Υ was confirmed by subsequent experiments [72–74] at DESY, which indicate a total width†$_{37}$

$$\Gamma(\Upsilon \to \text{all}) \approx 50\ \text{keV}. \tag{5.4}$$

Finally, the upsilon was observed to be accompanied by at least one partner [77], about $0.6\ \text{GeV}/c^2$ more massive. These similarities to the psions suggested at once that Υ and Υ′ could be regarded as 1S and 2S levels of a new quark Q bound with its antiquark $\bar{\text{Q}}$.

Some comparisons between the ψ and Υ families are made in fig. 11. The Υ–Υ′ mass splitting is closely equal to the ψ–ψ' spacing, and the interval between Υ and Υ″ is approximately equal to the ψ–ψ'' separation. This important regularity will be discussed in section 5.2.

In one respect the ψ and Υ families of vector mesons bear a remarkable resemblance to the light, short-lived vector mesons ρ^0, ω^0, and ϕ^0. Both the light vector mesons and the heavy vector mesons have partial decay widths into lepton pairs

$$\Gamma(\mathcal{V}^0 \to \ell^+\ell^-) = \mathcal{O}(1\ \text{keV}). \tag{5.5}$$

The experimental data are summarized in table 9. In the nonrelativistic picture that appears appropriate for the description of heavy vector mesons, leptonic decay widths are connected with the wavefunction at the origin through eq. (3.18). The systematics of leptonic widths as a function of quark mass are discussed in section 5.2. The principal quantum number dependence of observables including leptonic widths will be taken up in section 5.3.

The scaling arguments of sections 3 and 4, when applied to the rich spectroscopy of charmonium, can

†$_{37}$ This estimate is an average [75] based upon measurements of the muonic width and branching ratio reported in ref. [76].

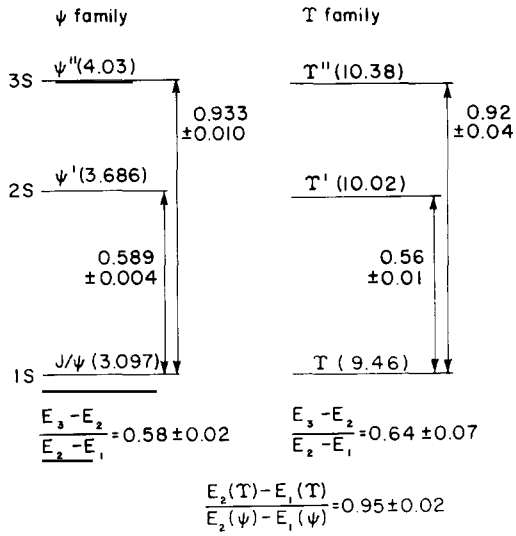

Fig. 11. Comparison of $^3S_1$ levels of the ψ and Υ families. Masses of the psions are from ref. [6]. The Υ–Υ′ splitting is taken from refs. [74] and [78], and the Υ″ mass is from ref. [79].

Table 9
Partial decay widths of vector mesons into e^+e^-

Meson (mass, MeV/c^2)	Quark content	Principal quantum number	$\Gamma_{e^+e^-}$(keV)	Ref.
$\rho(776)$	$(u\bar{u}-d\bar{d})/\sqrt{2}$	1	6.7 ± 0.8	6
$\rho(1649)$		2	3.1 ± 0.2	80
$\omega(783)$	$(u\bar{u}+d\bar{d})/\sqrt{2}$	1	0.77 ± 0.17	6
$\phi(1020)$	$s\bar{s}$	1	1.27 ± 0.07	6
$\psi(3095)$		1	4.8 ± 0.6	81
$\psi(3684)$		2	2.1 ± 0.3	81
$\psi(4040)$	$c\bar{c}$	3	0.75 ± 0.10	20
$\psi(4159)$		4?	0.77 ± 0.20	20
$\psi(4414)$		5 or 4	0.44 ± 0.14	81
Υ(9460)	$b\bar{b}$	1	1.2 ± 0.2	75
Υ(10020)		2	0.33 ± 0.10	75

be used to construct a hypothetical table of branching ratios for the Υ spectrum. The outlines of this exercise are reported in section 5.4.

5.2. *Mass dependence of observables*

5.2.1. *Level spacings*

The weak dependence of E_2-E_1 upon quark mass for the ψ and Υ levels may carry important

implications for the interquark potential. For a power-law potential, the scaling law (3.13) indicates that

$$\Delta E \propto \mu^{-\nu/(2+\nu)}. \tag{5.6}$$

Hence if a common power-law potential is to describe both families, the effective power ν must be close to zero†38. The value obtained for ν depends upon the ratio m_Q/m_c, where m_Q and m_c are the masses of the quark bound in the Υ and the charmed quark bound in the ψ, respectively. If we take this ratio to lie in the range $3 \leq m_Q/m_c \leq 4$, we find

$$\nu = 0.08 \pm 0.05. \tag{5.7}$$

5.2.2. Leptonic decay widths

The dependence of $|\Psi(0)|^2$ upon the quark mass provides another measure of the effective power-law form of the potential. Unless the potential is exactly power-behaved, the effective power determined in this manner need not be the same as the effective power implied by the level spacings, because the wavefunction at the origin probes shorter distances†39. Likewise, the effective power inferred from the leptonic widths may be different for different radial excitations. The leptonic widths of ψ and ψ' have been measured in several experiments. We take as representative the values measured at SPEAR [81],

$$\Gamma(\psi \to e^+e^-) = 4.8 \pm 0.6\,\text{keV},$$
$$\Gamma(\psi' \to e^+e^-) = 2.1 \pm 0.3\,\text{keV}. \tag{5.8}$$

Recently, the Υ and Υ′ have been observed at the storage ring DORIS in e^+e^- annihilations into hadrons [72–74, 78]. The mean values of the leptonic widths are [75]

$$\Gamma(\Upsilon \to e^+e^-) = 1.2 \pm 0.2\,\text{keV},$$
$$\Gamma(\Upsilon' \to e^+e^-) = 0.33 \pm 0.10\,\text{keV}. \tag{5.9}$$

As we shall see in section 7, the DESY experiments make compelling the conclusion that the charge of the (fifth) quark which is the constituent of Υ is $e_Q = -1/3$. With this knowledge, we can extract the values of $|\Psi(0)|^2$ for Υ and Υ′, and use (3.15) to explore the shape of the potential. The wavefunctions at the origin of the $n = 1$ and $n = 2$ levels of ψ and Υ are displayed in fig. 12. Because the masses of the c-quark and the fifth quark are poorly known, we have indicated a plausible range for the quantity m_Q/m_c. With such a limited set of data, this exercise can only be illustrative. The effective powers of the potential deduced from these data are shown in table 10. Obviously they do not reliably fix the potential form, but with more precise data from still more families of heavy mesons, we may hope to find this analysis more incisive.

5.3. Quantum-number dependence

5.3.1. Level spacings

The level density of a bound system provides further information about the nature of the potential. In the semiclassical approximation, the energy levels go as

$$E_n \sim (n - \gamma(\nu))^{2\nu/(2+\nu)} \tag{4.62}$$

†38 This circumstance motivated the introduction of the logarithmic potential in ref. [49].
†39 This is illustrated in figs. 1 and 2 of the second paper of ref. [65].

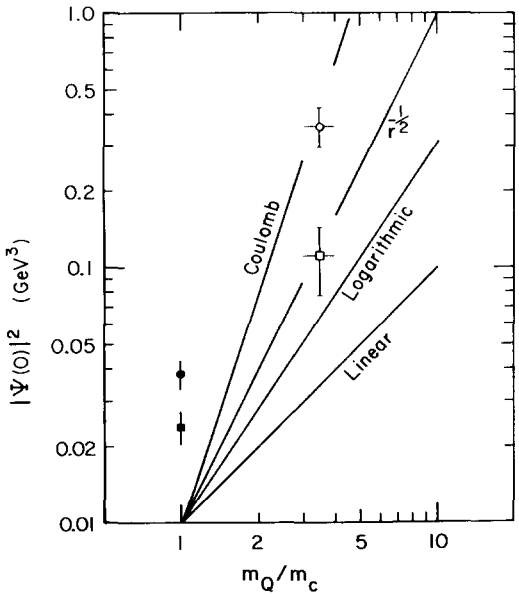

Fig. 12. Quark-mass-dependence of the wavefunction at the origin for the $n = 1$ and $n = 2$ quarkonium levels. The data are from table 9 for the ψ(3.095)●, ψ'(3.684)■, Υ(9.46)○, and Υ'(10.02)□. The mass dependence characteristic of several simple potentials is indicated by the slopes of the straight lines.

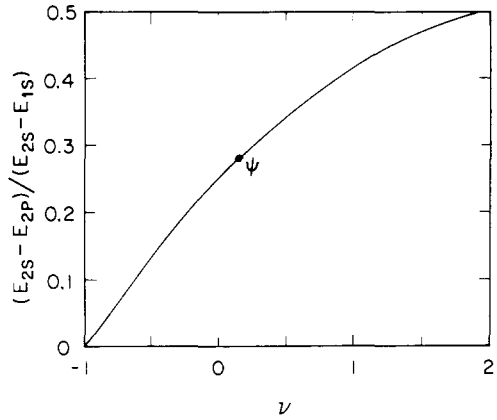

Fig. 13. The quantity $(E_{2S}-E_{2P})/(E_{2S}-E_{1S})$ for power-law potentials $V(r) = \lambda r^\nu$, $-1 \le \nu \le 2$. The datum is the value in the charmonium system [6].

Table 10
Effective power-law potentials deduced from ψ and Υ leptonic widths

n \ m_Q/m_c	3	4
1	-0.53 ± 0.14	-0.14 ± 0.17
2	$+0.15 \pm 0.47$	$+0.72 \pm 0.59$

for a power-law potential, where $\gamma(\nu) = \gamma_0(\nu)$ is given by (4.63). Thus the quantity $(E_3 - E_2)/(E_2 - E_1)$, which has been determined for the ψ and Υ systems, can be used to determine the shape of the potential. For the ψ family we find

$$\nu(\psi) = 0.20 \pm 0.06 \tag{5.10}$$

while for the Υ family we conclude that

$$\nu(\Upsilon) = 0.33 \pm 0.23. \tag{5.11}$$

The two determinations of the effective power are compatible, as is to be expected from the similarity of $(E_3 - E_2)/(E_2 - E_1)$ for the two families. It is interesting that present data on level densities do not by themselves support the idea that the Υ system is more Coulombic than the ψ system. Such a trend might be expected if the short-range interquark force were a Coulomb force.

The ratio $(E_{2S} - E_{2P})/(E_{2S} - E_{1S}) = 0.28$ for the charmonium family is compared with exact cal-

culations for power-law potentials in fig. 13. A value $\nu(\psi) \approx 0.15$ is implied, consistent with the determinations given above.

5.3.2. Leptonic widths of the psions

Within a quarkonium family, the principal-quantum-number dependence of observables is another source of information about the nature of the potential. With the aid of the WKB results

$$|\Psi_n(0)|^2 \sim (n - \tfrac{1}{4})^{2(\nu-1)/(2+\nu)}, \qquad 0 < \nu < \infty, \tag{4.35}$$

$$|\Psi_n(0)|^2 \sim \left(n - \frac{(1+\nu)}{2(2+\nu)}\right)^{(\nu-2)/(2+\nu)}, \qquad -2 < \nu < 0, \tag{4.67}$$

for power-law potentials, we may investigate the implications of the leptonic widths of the psions. Although the quantum number assignments listed in table 9 are not unambiguous, and multichannel effects are cause for concern above charm threshold, we make use here of all the data. Two alternative assignments are portrayed in fig. 14.

In fig. 14(a), we regard $\psi(3095)$, $\psi(3684)$, $\psi(4040)$, and $\psi(4414)$ as the $n = 1, 2, 3, 4$ levels. In fig. 14(b), we identify $\psi(4159)$ as the $n = 4$ level and $\psi(4414)$ as the $n = 5$ level. The effective power of the potential is determined as

$$\nu = 0.00 \pm 0.09 \tag{5.12}$$

in the four-level case, and as

$$\nu = 0.06 \pm 0.08 \tag{5.13}$$

in the five-level case†$_{40}$.

5.3.3. Leptonic widths of 1S and 2S levels

Finally, we may investigate how the quantity $|\Psi_2(0)|^2/|\Psi_1(0)|^2$ varies from one quarkonium system to another. This ratio is shown in fig. 15 for the ψ and Υ families, together with the behavior expected for

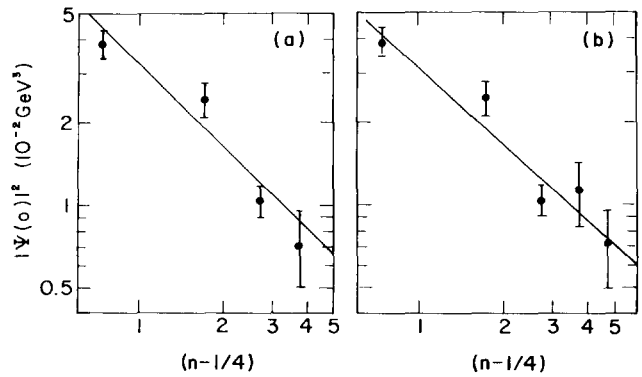

Fig. 14. Square of the wavefunction at the origin deduced from leptonic widths of the psions. Possible mixing between the $2\,^3S_1(3684)$ and $3\,^3D_1(3772)$ levels has been neglected. (a) a best fit proportional to $(n-\frac{1}{4})^p$, with $p = -1.00 \pm 0.15$, assuming the conventional 4S assignment for $\psi(4414)$. (b) an alternative 5S assignment for $\psi(4414)$, which corresponds to $p = -0.91 \pm 0.11$. In plotting the data against $n - \frac{1}{4}$, we have anticipated the result $p > -1$ ($\nu > 0$).

†$_{40}$ The principal-quantum-number dependence of psion leptonic widths led to the investigation in ref. [82] of potentials which rise less rapidly than a linear potential.

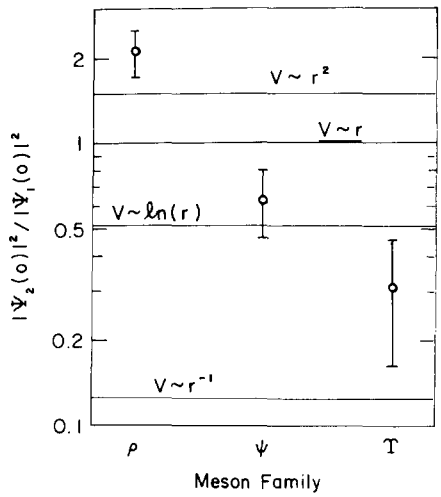

Fig. 15. The ratio $|\Psi_2(0)|^2/|\Psi_1(0)|^2$ is indicated for various potentials: 3/2 for harmonic oscillator, 1 for linear, ~0.51 for logarithmic, and 1/8 for Coulomb. The experimental points refer to the ρ, ψ, and Υ families. Data are from table 9.

a number of simple potentials. On this basis, the Υ family is seen to be somewhat more Coulomb-like than the ψ family. Although light mesons cannot reasonably be described in nonrelativistic terms, it is of at least passing interest to examine $|\Psi_2(0)|^2/|\Psi_1(0)|^2$ for the ρ^0 family. For these light mesons, the ratio is decidedly un-Coulombic. Therefore, we may cautiously see in fig. 15 a trend toward a more singular effective potential with increasing quark mass.

5.4. Crystal gazing

Although the exercises we have just reviewed cannot be said to fix precisely an effective power-law potential, we may conclude that an effective power close to $\nu = 0$ is compatible with what is known experimentally. This contention is supported by the relative success of the logarithmic potential (3.2) in reproducing ψ and Υ spectroscopy, which will be detailed in section 6. With a specific choice such as $\nu = 0$, the scaling laws of section 3 may be used to anticipate other properties of the upsilons, or of heavier mesons. A number of more or less detailed applications have been made to the Υ family [22, 27, 46, 83].

To illustrate the arguments involved in these analyses, let us consider the radiative and leptonic decays of the 2S levels ψ' and Υ′. The scaling laws (3.19b) and (3.23) yield†41

$$\Gamma(\mathrm{E1})/\Gamma(\mathcal{V} \to \ell^+\ell^-) \sim \mu^{-(1+\nu)/(2+\nu)}, \qquad -1 \le \nu \le \infty. \tag{5.14}$$

Consequently, with $\nu = 0$, we anticipate that

$$\frac{\Gamma(\Upsilon' \xrightarrow{\mathrm{E1}} \chi_b\gamma)}{\Gamma(\Upsilon' \to \ell^+\ell^-)} \Big/ \frac{\Gamma(\psi' \xrightarrow{\mathrm{E1}} \chi_c\gamma)}{\Gamma(\psi' \to \ell^+\ell^-)} \approx \left(\frac{m_c}{m_b}\right)^{1/2} \approx (0.5 \text{ to } 0.6), \tag{5.15}$$

†41 In making this illustrative estimate, we assume that binding energy is negligible compared with quark mass, so that μ sets the scale of vector meson masses, and we ignore the effect of fine structure splitting on the Q-value of the decay.

in other words, that radiative decays are relatively less important for Υ′ than for ψ'. A more thorough exploration of the decay channels of ψ, ψ', Υ, and Υ′ leads to the expectation that†42

$$\frac{\Gamma(\Upsilon' \to \ell^+\ell^-)}{\Gamma(\Upsilon' \to \text{all})} \Big/ \frac{\Gamma(\Upsilon \to \ell^+\ell^-)}{\Gamma(\Upsilon \to \text{all})} \approx 4 \frac{\Gamma(\psi' \to \ell^+\ell^-)}{\Gamma(\psi' \to \text{all})} \Big/ \frac{\Gamma(\psi \to \ell^+\ell^-)}{\Gamma(\psi \to \text{all})} \approx \frac{1}{2}. \tag{5.16}$$

No direct measurement of the leptonic branching ratio of Υ′ has yet been made, and the leptonic branching ratio of Υ is known only crudely†43. However, eq. (5.16) plays an important role in explaining the observation that in 400 GeV/c proton–nucleus collisions

$$\left.\frac{d\sigma(\Upsilon' \to \mu^+\mu^-)/dy}{d\sigma(\Upsilon \to \mu^+\mu^-)/dy}\right|_{y=0} = 0.31 \pm 0.03 \text{ [79]}, \tag{5.17}$$

whereas

$$\left.\frac{d\sigma(\psi' \to e^+e^-)/dy}{d\sigma(\psi \to e^+e^-)/dy}\right|_{y=0} = 0.018 \pm 0.006 \text{ [84]}. \tag{5.18}$$

6. Two specific potentials – An illustration

The scaling arguments of section 5 have led in several circumstances to an effective power $\nu \approx 0$ if the charmonium and upsilon families are to be described by a common potential of the form $V(r) = \lambda r^\nu$. The reader will recall that one is led to $\nu \approx 0$ by considering mass splittings in both families and leptonic widths in the charmonium family. A simple potential with $\nu_{\text{effective}} = 0$ is $V \sim \ln r$. In this section we shall review some properties of this potential as applied to the charmonium and upsilon families. It can be considered to interpolate between the two, but no one would be more surprised than we if it should continue to describe families of still heavier quarks. Quantum chromodynamics (QCD), the candidate theory of the strong interactions, predicts that $\nu_{\text{effective}}$ should continue to fall toward -1 as the quark mass is increased. We shall thus compare the logarithmic potential with a simplified "QCD-like" potential consisting of fixed Coulomb + linear terms†44.

6.1. Description of mass splittings

6.1.1. The logarithmic potential

Stimulated by the approximate equality

$$M(\Upsilon') - M(\Upsilon) \approx M(\psi') - M(\psi), \tag{6.1}$$

we asked: For what form of the quark-antiquark potential is the level spacing ΔE independent of the reduced mass μ? The answer [49] which has been given in section 3, is that the potential

$$V(r) = C \ln (r/r_0) \tag{3.2}$$

is the *unique form* for which level spacings do not depend upon μ. Whether or not the potential (3.2) applies to the real world of quarkonium, it is in some sense special, and its properties were examined further. The low-lying energy levels of the logarithmic potential are summarized in table 6 and fig. 4.

†42 An up-to-date evaluation appears in ref. [27].

†43 An average of measurements made at DESY is $\Gamma(\Upsilon \to \mu^+\mu^-)/\Gamma(\Upsilon \to \text{all}) = 2.6 \pm 1.4\%$ (ref. [75], based upon data of refs. [76]).

†44 In this section we adopt "natural" units, with $\hbar = c = 1$.

In the context of the logarithmic potential, we may express the masses of quarkonium states as

$$M_{nl} = CE_{nl} + E_0(\mu), \tag{6.2}$$

where n and l denote the principal quantum number and orbital angular momentum (in units of $\hbar$) of the bound state, and E_{nl} is the eigenvalue appearing in table 6. The parameter E_0 depends upon r_0 and μ, which need not be specified separately at this point. By fitting (6.2) to the masses of ψ, ψ' and Y, we determine

$$C = 0.733\ \text{GeV}, \tag{6.3}$$

$$E_0(\psi\ \text{family}) = 2.329\ \text{GeV}, \tag{6.4}$$

$$E_0(\Upsilon\ \text{family}) = 8.694\ \text{GeV}. \tag{6.5}$$

According to the virial theorem of eqs. (2.18) and (3.5), the mean kinetic energy is

$$\langle T\rangle = \tfrac{1}{2}C \approx 0.37\ \text{GeV} \tag{6.6}$$

so that in the nonrelativistic limit the mean squared velocity of a quark of mass m is

$$\langle\beta^2\rangle \approx \langle p^2/m^2\rangle = (1/m)\langle p^2/2\mu\rangle = \langle T\rangle/m = C/2m. \tag{6.7}$$

For a quark mass $m \gtrsim 1.5\ \text{GeV}$, $\langle\beta^2\rangle \lesssim \frac{1}{4}$, so a nonrelativistic description is expected to make sense. Since in the logarithmic potential $\langle\beta^2\rangle$ is the same for all bound states, the quality of the nonrelativistic approximation does not deteriorate for excited states. Moreover, the justification for a nonrelativistic description improves markedly with increasing quark mass. Equations (6.6) and (6.7) indicate that a nonrelativistic description of the ρ, ω, and ϕ families as light quark pairs bound in a logarithmic potential is unthinkable. As a consequence, we do not expect the ρ'–ρ, ω'–ω, and ϕ'–ϕ intervals to be equal to the ψ'–ψ splitting†45.

The predictions of eqs. (6.2)–(6.5) for masses of members of the charmonium and upsilon families are presented in table 11. (Throughout this section the predictions are for spin-triplet levels, and we neglect differences in hyperfine level shifts.) The masses tabulated for orbital excitations are for weighted averages that eliminate spin–orbit splittings, namely

$$M(^3\mathrm{L}) = \sum_{J=L-1}^{J=L+1} (2J+1)M(^3\mathrm{L}_J)/3(2L+1). \tag{6.8}$$

The positions of the 3S levels in the ψ and Y families (fig. 11) are reproduced satisfactorily, as is the position of the $2\,^3$P (charmonium) center of gravity.

The logarithmic potential produces an extremely crowded spectrum for large principal quantum numbers, as indicated in fig. 4. The unusual feature of exponentially rising Regge trajectories, already suggested by eq. (4.59), may be interpreted†46 in terms of a limiting hadronic temperature equal to $\langle T\rangle = C/2 = 0.37\ \text{GeV}$. The high density of excited states means that any agreement between predicted and observed levels could be coincidental. The $\psi(4414)$ must be regarded as the 5S level in the logarithmic potential. The nearest candidate for the 4S level is $\psi(4160)$, which lies about 70 MeV below the predicted mass. We regard charmonium states above the 3S level as neither supporting nor rejecting the logarithmic

†45 Lipkin has conjectured that the scaling laws of the logarithmic potential may nevertheless apply to light hadron systems. See refs. [85].
†46 We thank R. Hagedorn for this remark. The limiting temperature of the logarithmic potential was discussed by Rumer [86].

Table 11
Levels in two potentials

	Charmonium family			Upsilon family		
	Predicted mass (GeV/c^2)			Predicted mass (GeV/c^2)		
	$V \sim \ln r$	$V = -A/r + Br$	Observed	$V \sim \ln r$	$V = -A/r + Br$	Observed
1S	3.097*	3.097*	3.097[a]	9.46*	9.46*	9.46 ± 0.01[d]
2P	3.53	3.51	3.522[a]	9.90	9.93	
2S	3.686*	3.686*	3.686[a]	10.049	10.02*	10.016 ± 0.020[d]
3D	3.87	3.80	3.772 ($^3D_1$)[a]	10.24	10.17	
3P	3.91	3.97		10.27	10.27	
4F	4.01	4.05		10.37	10.35	
3S	4.01	4.12	4.04 ± 0.01[b]	10.37	10.35	10.38 ± 0.04[e]
4D	4.08	4.20	[c]4.16 ± 0.01[b]	10.45	10.45	
→						
4S	4.23	4.49	[c]4.41 ± 0.01[b]	10.60	10.62	
→						
5S	4.41	4.83		10.77	10.85	

* input.
→ levels omitted.
[a] Ref. [6].
[b] Ref. [20].
[c] Assignments differ in the two models.
[d] Ref. [75].
[e] Ref. [79].

potential.†$_{47}$ Further tests will be noted in section 6.2, after we have introduced a second potential which reproduces the Υ′–Υ splitting.

6.1.2. *A Coulomb-plus-linear potential*

Although the logarithmic potential is unique in giving level spacings independent of the quark mass, it is by no means alone in reproducing the equal spacing rule (6.1).

There are theoretical reasons, as mentioned in the introduction, for believing that the short-range quark–antiquark force arises from a Coulomb-like strong interactions of the form

$$V_1(r) = -\tfrac{4}{3}\alpha_s/r, \tag{6.9}$$

in which the strong coupling constant α_s is weakly dependent on the mass of the system in question. (The factor 4/3 has a group-theoretic origin which is not important for the present discussion.)

The *long-range* quark–antiquark force often is assumed to be of the form

$$V_2(r) = r/a^2, \tag{6.10}$$

a linearly rising potential which is capable of confining quarks permanently. Such a potential can give rise to a spectrum of particles containing light quarks in rough accord with experiment [30, 87].

The specific parameters adopted to describe the charmonium and Υ families in one study which preceded the discovery of the latter were [88]

$$\alpha_s(\psi) \approx 0.19, \qquad \alpha_s(\Upsilon) \approx 0.15, \qquad a \approx 2.2\ \text{GeV}^{-1}. \tag{6.11}$$

†$_{47}$ Here we are neglecting coupled-channel effects which may have an important influence on levels above the charm threshold. The multichannel problem has been discussed by Eichten et al. [26, 112].

With these parameters, both the ψ and Υ families are primarily sensitive to the linear component of the potential

$$V(r) = -4\alpha_s/3r + r/a^2, \tag{6.12}$$

for which, according to (3.13), energy level spacings scale with mass as

$$\Delta E_{\text{linear}} \sim \mu^{-1/3}. \tag{6.13}$$

In a purely linear potential a 2S–1S spacing of 0.6 GeV for the charmonium family then would imply a spacing of $3^{-1/3} \cdot 0.6\,\text{GeV} \approx 0.4\,\text{GeV}$ for a family composed of quarks three times as massive as the charmed quark. Explicit calculations using (6.11) and (6.12) led to the prediction that

$$M(\Upsilon') - M(\Upsilon) \approx 420\,\text{MeV}, \tag{6.14}$$

which disagrees with subsequent experimental observations. As the quark mass is further increased, the levels fall deeper into the potential as required by the Feynman–Hellmann theorem (2.16), and the scaling behavior

$$\Delta E_{\text{Coulomb}} \sim \mu\alpha_s^2 \tag{6.15}$$

characteristic of the Coulomb component will set in. If α_s is a slowly-decreasing function of μ, as suggested by asymptotic freedom arguments, the resulting increase in level spacings will be slower than a linear growth with μ.

This discussion suggests that it must be possible to choose a potential of the Coulomb-plus-linear form (6.12) for which the spacing between the 1S and 2S levels is 0.59 GeV at precisely two levels of the quark mass. This was accomplished in ref. [49] with the choices $\alpha_s = 0.42$, $a = 2.48\,\text{GeV}^{-1}$, and numerous comparisons were made there with the logarithmic potential.

The new values of Υ and Υ′ masses quoted in table 9 change this picture quantitatively but not qualitatively. The observed 1S and 2S levels of charmonium and upsilon families are reproduced by a potential of the form (6.12), with

$$\alpha_s = 0.38, \qquad a = 2.43\,\text{GeV}^{-1}, \tag{6.16}$$

and the quark masses†48

$$m_c = 1.37\,\text{GeV}/c^2, \qquad m_Q = 4.79\,\text{GeV}/c^2. \tag{6.17}$$

Level spacings in the potential specified by (6.12) and (6.16) are compared with the experimental data in fig. 16. The 2S–1S spacing passes through a minimum between the quark masses given by (6.17), then rises for larger quark masses as the effects of the Coulomb potential become more pronounced. For a quark mass of $15\,\text{GeV}/c^2$, which is the highest value accessible with present accelerators†49, the expected 2S–1S splitting is 0.9 GeV. Recall that by construction it would be ~0.6 GeV in the logarithmic potential. Preliminary attempts [89] to extrapolate from the upsilons to a family composed of $15\,\text{GeV}/c^2$ quarks using the inverse scattering approach of ref. [65] give 2S–1S splittings that range from just under 0.6 GeV to 0.8 GeV.

The predicted masses for the ψ and Υ families in the potential (6.16) are shown in table 11. The

†48 Unlike the authors of refs. [26] and [88], we do not shift the zero of energy. Particle masses are given by twice the quark mass plus the eigenvalues of the Schrödinger equation (2.1).

†49 The electron–position storage rings PETRA (Hamburg) have recently attained c.m. energies in excess of 30 GeV. Similar performance is expected of the PEP (Stanford) machine in 1980.

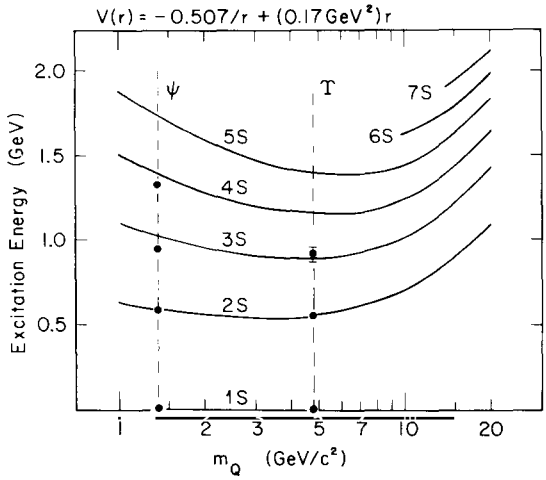

Fig. 16. Level spacings in the potential $V(r) = -0.507/r + (0.17\ \mathrm{GeV}^2)r$. Points denote observed masses of members of ψ and Υ families.

principal difference with respect to the logarithmic potential is the assignment of $\psi(4414)$ as the 4S, rather than 5S, level. The peak at 4.16 GeV must then be identified as a 4D level.

6.2. Leptonic widths

A crucial parameter of an s-wave bound state is $|\Psi(0)|^2$, the square of the wavefunction at the origin. Several experimental quantities are sensitive to $|\Psi(0)|^2$. Of these, the one best measured and freest from theoretical ambiguities is the rate for vector meson decay into lepton pairs. In a nonrelativistic treatment the leptonic decay width is given by

$$\Gamma(\mathscr{V}^0 \to \ell^+\ell^-) = 16\pi e_Q^2 |\Psi(0)|^2 / M_{\mathscr{V}}^2. \tag{3.18}$$

Unlike the level spacings, leptonic widths predicted in the logarithmic potential depend upon a choice of quark mass. We rescale the values of $|\Psi(0)|^2$ tabulated in table 7, which are appropriate for $m = 2\mu = 1$, to the physical situation according to eq. (3.15) as

$$|\Psi(0)|^2_{m,C} = (mC)^{3/2} |\Psi(0)|^2_{m=C=1}. \tag{6.18}$$

Thus, for example, we find†$_{50}$

$$\Gamma(\psi \to e^+e^-) = 4.28\ \mathrm{keV}\ (m_c/1\ \mathrm{GeV})^{3/2} \tag{6.19}$$

which leads, using the measured leptonic width quoted in table 9, to a charmed quark mass

$$m_c = 1.08\ \mathrm{GeV}/c^2. \tag{6.20}$$

The leptonic widths of remaining members of the ψ family may now be computed directly.

Having fixed the value of m_c, we may use eqs. (6.4) and (6.5) to determine the parameter r_0 and the mass m_Q of the quark that forms the Υ family. From eqs. (3.31)–(3.33) we may conclude that

$$E_0(\psi\ \text{family}) = 2.329\ \mathrm{GeV} = 2m_c - \tfrac{1}{2}C \ln (Cm_c r_0^2), \tag{6.21}$$

†$_{50}$ The numerical coefficient on the right-hand side of eq. (6.19) corrects a misprint in ref. [49].

and

$$E_0(\Upsilon \text{ family}) = 8.694\ \text{GeV} = 2m_Q - \tfrac{1}{2}C \ln (Cm_Q r_0^2), \tag{6.22}$$

which implies that

$$r_0 = 0.89\ \text{GeV}^{-1}, \tag{6.23}$$

and

$$m_Q = 4.52\ \text{GeV}/c^2. \tag{6.24}$$

With this information in hand we may compute $|\Psi(0)|^2$ and hence leptonic widths for all the $^3S_1$ levels of the Υ family.

The calculation of leptonic widths in the Coulomb-plus-linear potential of eqs. (6.12) and (6.16) is straightforward. Predictions for the ψ and Υ states derived from both potentials are given in table 12. The large values for leptonic widths predicted by the Coulomb-plus-linear potential specified by (6.16) favor the smaller values of α_s often adopted. However, it has been argued [90] that relativistic corrections might substantially reduce the predicted widths of the psions. Applied to the case of the logarithmic potential, this suppression would allow a corresponding increase in the rather small charmed quark mass quoted in eq. (6.20).

The potentials discussed in this section make definite predictions for the sizes of bound states. For the logarithmic potential (3.2) we need only to scale the values of $\langle r_n \rangle$ given in table 7 according to eq. (3.8). A numerical computation is required for the Coulomb-plus-linear case. The results for the ψ and Υ families are given in table 13. They show the members of the Υ family to be about half the size of the corresponding ψ levels.

We conclude this comparison of the logarithmic and Coulomb-plus-linear potentials by emphasizing that neither of these informative examples is expected to describe the real world in complete detail. The

Table 12
Calculated and observed leptonic widths of vector mesons in two potentials

		$\Gamma_{e^+e^-}$(keV)			
Meson mass (GeV/c^2)	n	Predicted, logarithmic	Predicted, modified Coulomb	Observed	Ref.
Charmonium family					
3.095	1	4.80	7.82	4.8 ± 0.6	81
3.684	2	1.73	3.83	2.1 ± 0.3	81
4.04	3	0.98	2.79	0.75 ± 0.10	20
4.16	4	0.71	–	0.77 ± 0.20	20
4.41	5	0.51	2.19 (n = 4)	0.44 ± 0.14	81
Upsilon family					
9.460	1	1.10	2.85	1.2 ± 0.2	75
10.02	2	0.50	1.07	0.33 ± 0.10	75
10.38	3	0.32	0.76		
[10.60][a]	4	0.23	0.63		

[a]predicted mass.

Table 13
Mean radii $\langle r \rangle$ of ψ and Υ states in two potentials

	Logarithmic potential [eqs. (3.2), (6.3)]	Modified Coulomb potential [eqs. (5.18)–(5.20)]
ψ	2.2 GeV^{-1}	2.0 GeV^{-1}
ψ'	5.0	4.1
Υ	1.1	1.0
Υ′	2.5	2.4

logarithmic potential was motivated by a drastic generalization of the observed equal 2S–1S spacing of the ψ and Υ families, and the Coulomb-plus-linear form yields leptonic widths larger than those observed. We have restricted our attention to spin-triplet states, neglecting fine-structure, hyperfine-structure, and other relativistic effects†$_{51}$. Asymptotic freedom would prescribe a slow (logarithmic) decrease in the value of the strong coupling "constant" which will postpone to higher masses the onset of Coulomb-like behavior of the observables†$_{52}$.

7. Measuring quark charges

Some of the methods we have described have been used [27, 38, 74, 78] to determine that the Υ family is composed of quarks with electric charge $|e_Q| = 1/3$. In this section we review the assumptions and reasoning that led to this conclusion.

At the present time, the observables most directly related to the charge of the quarks within upsilons are the leptonic decay rates of Υ and Υ′. In a nonrelativistic description, the leptonic width of a massive vector meson is given by

$$\Gamma(\mathcal{V}^0 \to \ell^+\ell^-) = 16\pi\alpha^2 e_Q^2 |\Psi(0)|^2 / M_{\mathcal{V}}^2. \tag{3.18}$$

This expression contains two unknown quantities: the quark charge e_Q and the square of the wavefunction at the origin, $|\Psi(0)|^2$. The latter can usefully be bounded with the aid of data on other quarkonium families in a relatively model-independent fashion, as we shall now explain.

A plausibility argument for the assignment $|e_Q| = 1/3$ for the quark constituent of the upsilons may be based on fig. 17 where the quantity $\Gamma(\mathcal{V}^0 \to \ell^+\ell^-)/e_Q^2$ has been plotted for the known vector mesons. For the ground states ρ, ω, ϕ and ψ, a common value of about 12 keV is obtained. The Υ(9.46) conforms to this pattern if the assignment $|e_Q| = 1/3$ is adopted. For the first excited states ρ', ψ', and Υ′, one may divine a smoother trend if the Υ constituent has $|e_Q| = 1/3$ than if it has $|e_Q| = 2/3$ or larger†$_{53}$.

To go beyond this qualitative discussion, we can invoke the theorem on mass dependence of Schrödinger wavefunctions introduced in sections 2.4, 3.4 and 4.4. Under plausible general assumptions, lower bounds on the leptonic widths of Υ and Υ′ follow from this theorem. The observed leptonic widths are incompatible with these bounds for $|e_Q| \geq 2/3$.

For the special case of a power-law potential $V(r) = \lambda r^\nu$, eq. (3.15) implies that for a fixed principal quantum number

$$|\Psi_Q(0)|^2 = (m_Q/m_c)^{3/(2+\nu)} |\Psi_c(0)|^2. \tag{7.1}$$

†$_{51}$ A recent contribution in this respect is that of ref. [91]. See ref. [27] for reference to earlier works.
†$_{52}$ Several authors [92] have explored this possibility for Coulomb-like potentials of the form $V \sim 1/[r \ln(r)]$.
†$_{53}$ The pattern of constant Γ_{ee}/e_Q^2 has been emphasized, for example, in ref. [93]. See also ref. [94].

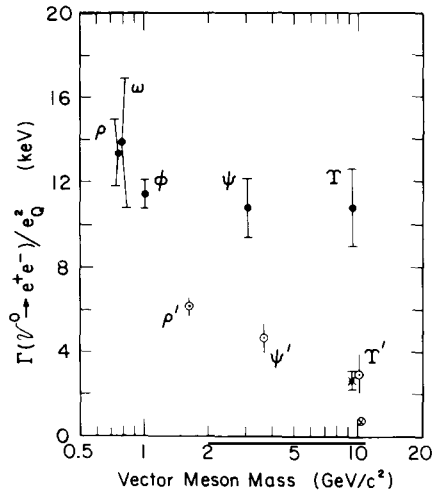

Fig. 17. Leptonic widths $\Gamma(V^0 \to e^+e^-)$ (table 9) normalized by squares of quark charges e_Q^2, as functions of vector meson mass. The solid points correspond to the ground states. Open circles correspond to 2S levels. For the Y and Y' a quark charge $|e_Q| = 1/3$ has been assumed. The crossed points refer to the alternative assignment $|e_Q| = 2/3$.

If the potential is concave downward†54,

$$d^2V/dr^2 \leq 0, \tag{7.2}$$

i.e. if $\nu \leq 1$, the scaling law (7.1) may be expressed as a lower bound

$$|\Psi_Q(0)|^2 \geq (m_Q/m_c)|\Psi_c(0)|^2, \tag{7.3}$$

if $m_Q > m_c$. This in turn implies that

$$\Gamma(\Upsilon_n \to e^+e^-) \geq \frac{e_Q^2}{e_c^2}\frac{m_Q}{m_c}\frac{M(\psi_n)^2}{M(\Upsilon_n)^2}\Gamma(\psi_n \to e^+e^-). \tag{7.4}$$

We shall prove that eq. (7.4) holds for the ground state in any monotonically increasing potential which is concave downward, and will argue that it is also valid for excited states in any reasonably smooth potential. We shall then discuss the application of eq. (7.4) to the determination of the fifth quark's charge.

To establish (7.3) for the ground state, we recall that

$$|\Psi(0)|^2 = \frac{\mu}{2\pi\hbar^2}\left\langle\frac{dV}{dr}\right\rangle = \frac{m}{4\pi\hbar^2}\left\langle\frac{dV}{dr}\right\rangle, \tag{2.19}$$

where $m = 2\mu$ is the quark mass. It is elementary to compute

$$4\pi\hbar^2\frac{\partial}{\partial m}\left[\frac{1}{m}|\Psi(0)|^2\right] = 2\int_0^\infty dr\, u(r)\frac{\partial u(r)}{\partial m}V'(r). \tag{7.5}$$

†54 The influence of d^2V/dr^2 on the relative sizes of ψ and ψ' leptonic widths is discussed by Martin in ref. [95]. This result has been generalized to higher excitations within a semiclassical approximation in the second of refs. [95].

Using

$$G'(r) = 2u(r)\frac{\partial u(r)}{\partial m}, \tag{2.92}$$

we find

$$4\pi\hbar^2 \frac{\partial}{\partial m}\left[\frac{1}{m}|\Psi(0)|^2\right] = \int_0^\infty dr\, G'(r)\, V'(r) = -\int_0^\infty dr\, G(r)\, V''(r). \tag{7.6}$$

It was proved in section 2.4 that for the ground state the function

$$G(r) \equiv \frac{\partial}{\partial m}\int_0^r dr'\,[u(r')]^2 \geq 0. \tag{2.84}$$

Hence, if $V''(r) \leq 0$, eq. (7.6) implies that

$$\frac{\partial}{\partial m}\left[\frac{1}{m}|\Psi(0)|^2\right] \geq 0, \tag{7.7}$$

which is equivalent to eq. (7.3).

We have not succeeded in constructing a general proof of eq. (7.3) for excited states. It is rigorously true for logarithmic and power-law potentials with $\nu \leq 1$, as already remarked. It also holds in the classical limit for potentials with $V' \geq 0$ and $V'' \leq 0$, as the discussion in section 4.4 implies. At the present time, then, we are forced to conjecture the validity of eq. (7.4) for excited states such as Υ'. The fact that an effective power-law potential (with $\nu \approx 0$) seems to interpolate well between the ψ and Υ families may be taken as support for this assumption.

To make eq. (7.4) useful for the Υ family, we must estimate (or bound) m_Q/m_c. In specific potential models†55, we find

$$3 \leq m_Q/m_c \leq 4. \tag{7.8}$$

It is possible to argue more generally: as the quark mass increases, the Feynman–Hellmann theorem (2.18) implies that states become more tightly bound, so that

$$M_\Upsilon - 2m_Q \leq M_\psi - 2m_c, \tag{7.9}$$

and

$$M_{\Upsilon'} - 2m_Q \leq M_{\psi'} - 2m_c. \tag{7.10}$$

These lead to nearly identical restrictions on m_Q/m_c, namely†56

$$m_Q/m_c \geq 1 + \frac{(M_\Upsilon - M_\psi)}{2m_c} \approx 1 + \frac{(M_{\Upsilon'} - M_{\psi'})}{2m_c} \approx 1 + \frac{3.15\ \mathrm{GeV}/c^2}{m_c}. \tag{7.11}$$

All charmonium calculations known to us employ $m_c \leq 2\ \mathrm{GeV}/c^2$. This implies

$$m_Q/m_c \geq 2.6, \tag{7.12}$$

†55 The second of refs. [65] is representative.

†56 A more restrictive bound, $m_Q - m_c > 3.29\ \mathrm{GeV}/c^2$, is obtained in ref. [96].

which we shall adopt hereafter. The rather conservative lower bounds

$$\Gamma(\Upsilon \to e^+e^-)/e_Q^2 \geq 2.6\,\text{keV} \tag{7.13}$$

$$\Gamma(\Upsilon' \to e^+e^-)/e_Q^2 \geq 1.4\,\text{keV} \tag{7.14}$$

follow from eqs. (7.4) and (7.12), together with the central values minus one standard deviation for the psion leptonic widths given in table 9.

The bounds (7.13) and (7.14) are shown in fig. 18 together with predictions derived from twenty potentials [65] that reproduce the ψ and ψ' masses and leptonic widths. The bounds are plotted for $|e_Q| = 1/3$ and 2/3, but the model calculations are given only for $|e_Q| = 1/3$. The experimental values (from table 9) are shown as well. The leptonic width of Υ' is incompatible with the lower bound (7.14) for $|e_Q| \geq 2/3$. The leptonic width of Υ, while in comfortable agreement with the explicit potential model predictions for $|e_Q| = 1/3$, is (just) within the range allowed for $|e_Q| = 2/3$. This circumstance was anticipated [38]. The explicit potential predictions show that the model uncertainty in $|\Psi(0)|^2$ is far greater for Υ than for Υ'. The Υ' lies in a region of space already well-probed by the charmonium states, whereas the deeper-lying Υ explores a terra incognita of the quark-antiquark interaction. Thus it is $\Gamma(\Upsilon' \to e^+e^-)$ that decisively excludes the assignment $|e_Q| \geq 2/3$.

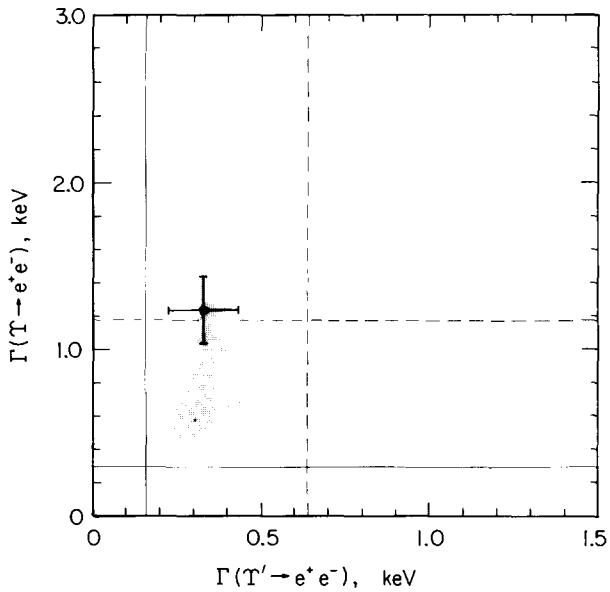

Fig. 18. Lower bounds for leptonic widths of Υ and Υ' [38], together with data (table 9). The shaded area represents the range of predictions of twenty potentials reproducing the ψ and ψ' masses and leptonic widths, for $e_Q = -1/3$. Solid and dashed lines correspond to lower bounds for $e_Q = -1/3$ and 2/3, respectively.

8. Counting narrow quarkonium levels

In the cross section for e^+e^- annihilation into hadrons, two extraordinarily narrow spikes, $\psi(3095)$ and $\psi'(3684)$, are observed below the onset of charmed meson production at $E_{c.m.} = 2M_D \approx 3.73\,\text{GeV}$. This was indicated in fig. 3(a). The narrowness [6] of ψ,

$$\Gamma(\psi \to \text{all}) = (67 \pm 12)\,\text{keV}, \tag{8.1}$$

and of ψ',

$$\Gamma(\psi' \to \text{all}) = (228 \pm 56)\,\text{keV}, \tag{8.2}$$

was a prime factor in their discovery. It can be understood if the mechanism for the decay of psions into uncharmed hadrons is dynamically suppressed. This suppression reflects the operation of the Okubo [97]–Zweig [98]–Iizuka [99] rule. It is believed that violations of the OZI rule occur through the mechanism depicted in fig. 2(c). Suppression of OZI-violating decays is attributed to the weakness of the strong interaction at the short distances characterized by the Compton wavelength of the charmed quark [13]. Vector mesons above charm threshold can dissociate into charmed particle pairs as shown in fig. 2(b), and are found to be correspondingly broader, with total widths on the order of tens of MeV.

It is clearly of interest to know whether a similar pattern is to be expected for the upsilon family, and for more massive quarkonium families: How many narrow $^3S_1$ Υ levels lie below the new-flavor threshold? At what energy does the flavor threshold occur?

One would expect the question of flavor threshold to involve the relativistic bound state dynamics of light quark (q)–heavy quark (Q) systems. However, by taking as given the relation of charm threshold to the ψ and ψ' positions we may sidestep many details of the binding of light quarks to heavy ones. This is an approach taken by Eichten and Gottfried [88] for a specific potential, but we shall see that it has general validity.

We shall show that the number of n of $^3S_1$ levels of a $Q\bar{Q}$ system which lie below the threshold for OZI-allowed decays grows as [100]

$$n - \tfrac{1}{4} \approx a(m_Q/m_c)^{1/2}, \tag{8.3}$$

where m_Q and m_c are the masses of the heavy quark Q and of the charmed quark. The proportionality constant a will have a value near 2 because charm threshold lies just above the ψ'. The expression (8.3) and the value $a \approx 2$ are supported by explicit potential models. For the upsilon system, with $m_Q/m_c \approx 3$ to 4, we then expect three or four quasistable $^3S_1$ levels below the flavor threshold. For a quarkonium family composed of quarks with $m_Q/m_c \approx 10$, roughly the largest quark mass accessible in the present generation of e^+e^- storage rings, we may anticipate six or seven such levels – indeed a rich spectroscopy. Interleaved with the narrow $^3S_1$ levels one may expect a number of orbital excitations, all of which should have narrow widths (no more than a few MeV) below flavor threshold.

Key to the result (8.3) is the observation [88, 100] that although the dynamics of the $Q\bar{q}$ system cannot be expected to yield to a nonrelativistic analysis, the dependence upon m_Q of the $Q\bar{q}$ mass becomes simple as m_Q becomes large. The mass of the lowest-lying $^1S_0$ $Q\bar{q}$ state depends upon m_Q in three ways: (i) the additive contribution m_Q; (ii) the hyperfine ($^3S_1$–$^1S_0$) splitting which decreases monotonically as $m_Q \to \infty$; and (iii) the binding which has a feeble dependence through reduced mass effects. Thus the quantity

$$\delta(m_Q) \equiv 2M(Q\bar{q}) - 2m_Q \tag{8.4}$$

is expected to approach a finite limit δ_∞ as $m_Q \to \infty$.

Let us at first assume that

$$\delta(m_Q)/\delta_\infty \approx 1 \text{ for } m_Q \geq m_c, \tag{8.5}$$

which we will attempt to justify momentarily, and define the zero of energy in the $Q\bar{Q}$ system to be at $2m_Q$. The threshold for dissociation of a $Q\bar{Q}$ state into $Q\bar{q} + \bar{Q}q$ then lies $\delta(m_Q)$ above this zero of energy. We now consider any potential $V(r)$ which binds $Q\bar{Q}$ states rising at least $\delta(m_Q)$ above $2m_Q$.

This condition is satisfied by any confining potential. Then the number n of bound states which lie below $\delta(m_Q)$ is given in the semiclassical approximation by†57

$$\int_0^{r_\delta} \mathrm{d}r[m_Q(\delta(m_Q)-V(r))]^{1/2} \approx (n-\tfrac{1}{4})\pi, \tag{8.6}$$

where the classical turning point is specified by

$$V(r_\delta) = \delta(m_Q). \tag{8.7}$$

The radius r_δ becomes independent of m_Q as $m_Q \to \infty$. If we adopt the approximation (8.5), the left-hand side of (8.6) is simply proportional to $m_Q^{1/2}$, as in eq. (8.3). The constant of proportionality a can be expressed as

$$a \approx (1/\pi) \int_0^{r_\delta} \mathrm{d}r\,[m_c(\delta_\infty - V(r))]^{1/2}, \tag{8.8}$$

but it is more useful to determine a from the charmonium system. Since the charm threshold lies approximately 40 MeV above the ψ' and the $3\,^3S_1$ level $\psi(4.03)$ lies approximately 350 MeV above the ψ', we estimate†58

$$n(m_c) \approx 2.1 = a + \tfrac{1}{4}, \tag{8.9}$$

so that

$$a \approx 1.9. \tag{8.10}$$

The relation (8.3), it will be noted, is independent of the form of the potential. It is interesting to examine how this comes to pass in various potentials. The issue before us is how many levels lie below a certain energy (δ_∞ in the present application). This can be studied in fig. 5, where energy levels are plotted as functions of 2μ for three potentials. For the linear potential $V(r) = r$, which vanishes at the origin, the levels approach each other as $\Delta E \propto (2\mu)^{-1/3}$, as shown in fig. 5(a). Thus more of them fall below a certain energy as the mass increases. For the logarithmic potential $V = \ln(r)$ which corresponds to fig. 5(b), all the levels descend into the well at the common rate given by eq. (3.43), $E_n(2\mu) = E_n(1) - \frac{1}{2}\ln(2\mu)$, maintaining the initial level spacing. In the case of the potential $V(r) = -r^{-1/2}$, the level spacings grow as $\Delta E \propto (2\mu)^{+1/3}$, but the levels fall so rapidly into the well that eq. (8.3) is fulfilled. As we have seen in section 4, the WKB approximation yields highly accurate energy eigenvalues in many cases, so we would expect eq. (8.6) to provide a reliable count of the number of bound states below threshold.

Let us now examine more critically the assumption (8.5) that $\delta(m_Q)$ is essentially independent of m_Q, for $m_Q \geq m_c$. The magnitude of the hyperfine splitting that contributes to $\delta(m_Q)$ is determined by the charmed mesons, for which [6] $M_{D^*} - M_D = 142\,\mathrm{MeV}/c^2$. We assume [31] that $Q\bar{q}$ hyperfine splittings are described by quantum chromodynamics and are inversely proportional to m_Q†59. The $1\,^1S_0(Q\bar{q})$

†57 The shifted variable $n - \frac{1}{4}$ is appropriate for a nonsingular potential. For a specific singular power-law potential, the best choice is given by eq. (4.45).

†58 We have used a shifted variable $(n - \frac{1}{4})$ and a linear interpolation which may not be optimal. The uncertainty arising from this procedure will be smaller when the coefficient in eq. (8.3) can be determined from the Y family.

†59 We neglect a small variation in $|\Psi(0)|^2$ for the $Q\bar{q}$ mesons which will arise from slight changes in the reduced mass as $m_Q \to \infty$.

state is therefore expected to lie a distance

$$-\tfrac{1}{2}\delta(m_Q)_{HFS} = (m_c/m_Q)^3_4(M_{D^*} - M_D) = 107\ \text{MeV}\ (m_c/m_Q) \tag{8.11}$$

below the 1S($Q\bar{q}$) center of gravity†60. The contribution (8.11) to $\delta(m_Q)$ is a negative one, already small in the charmonium system and diminishing in importance as m_Q increases. A small positive contribution to $\delta(m_Q)$ arises from the dependence of the binding energy upon the reduced mass

$$\mu(m_Q) = m_q m_Q/(m_q + m_Q). \tag{8.12}$$

The reduced mass increases slowly as m_Q increases. This variation leads, according to the Feynman–Hellmann theorem (2.16), to deeper binding. A crude estimate of the change in binding energy can be had by treating the $Q\bar{q}$ system nonrelativistically and adopting for simplicity the logarithmic potential

$$V(r) = C \ln (r), \qquad C = 0.733\ \text{GeV} \tag{8.13}$$

which describes the ψ and Υ spectra. Using eq. (3.43), we find that

$$\frac{1}{2}[\delta(m_c) - \delta(m_Q)]_{\text{reduced mass}} = \frac{C}{2} \ln \left[\frac{1 + m_q/m_c}{1 + m_q/m_Q}\right]. \tag{8.14}$$

By combining (8.11) and (8.14) we obtain for $m_q \ll m_c$

$$\delta(m_Q) - \delta(m_c) \approx (213\ \text{MeV} - C m_q/m_c)(1 - m_c/m_Q). \tag{8.15}$$

As a numerical illustration, we take [31] $m_q/m_c = 1/5$, which leads to

$$\delta(m_Q) - \delta(m_c) \approx 66\ \text{MeV}\ (1 - m_c/m_Q). \tag{8.16}$$

This 10% correction to δ_∞ cannot be expected to make an appreciable difference in the prediction (8.3).

The proportionality between the number of narrow $^3S_1$ levels and $m_Q^{1/2}$ depends only on the assumption of a universal interquark potential and on the validity of a nonrelativistic description of quarkonium spectroscopy. Serious violations of (8.3) for heavier families of vector mesons would be a strong indication of new physics.

9. Summary

In this article we have presented a number of elementary scaling techniques and semiclassical methods of nonrelativistic quantum mechanics. Although general in their applicability, these methods have been employed here to explore how systems composed of heavy quarks behave when the quark mass, interaction strength, or excitation level is varied.

The appropriate formalism has been presented in a manner independent of the details of elementary particle physics in sections 2–4. The specific applications presented in sections 5–8 are more narrowly focused. Let us review some of the accomplishments of the nonrelativistic quantum mechanics description of quarkonium systems.

We have found the "effective power" ν characterizing a potential $V(r) = \lambda r^\nu$ to be a powerful tool for investigating the nature of the interquark interaction. Properties of the ψ and Υ families indicate that this effective power is close to zero. One consequence of this result is the prediction that leptonic

†60 For the highly excited $Q\bar{Q}$ states we shall neglect hyperfine effects. (This amounts to rejecting the interpretation of X(2830) as the $^1S_0$ partner of the ψ(3095).) The inclusion of such hyperfine effects for $Q\bar{Q}$ states would tend to raise slightly our estimate of $n(m_Q)$ as long as these effects are becoming smaller for increasing m_Q.

decays of vector mesons should grow in importance compared to radiative decays as the mass of the constituents increases.

The similar level spacings observed in the ψ and Υ families are one manifestation of an effective power near zero. This has suggested that the potential $V(r) \sim \ln(r)$ would interpolate between the two families. Predictions of the logarithmic potential have been compared with those of a Coulomb plus linear form.

The present methods played a key role in determining the charge of the fifth quark, the constituent of Υ, to be $|e_Q| = 1/3$. Quantum mechanical considerations make it possible to separate the effects of quark charge from those of the bound-state wavefunction on the leptonic decays of Υ and Υ'. This allowed us to place useful lower bounds on leptonic widths of the Υ states by extrapolating from the ψ states. The observed leptonic widths of the upsilons exclude a quark charge $|e_Q| \geq 2/3$.

A semiclassical argument leads to the prediction that the number of narrow $^3S_1$ $Q\bar{Q}$ states below flavor threshold grows as the square root of the heavy quark mass, independent of the specific form of the interquark potential.

We foresee a number of additional applications of the present methods to the data on quarkonium states that will soon be forthcoming. Encouraged by the satisfactory extrapolations over a factor of three in mass from the ψ to Υ families which our methods have permitted, one may anticipate similar success in passing from upsilon properties to those of heavier $Q\bar{Q}$ families accessible at PETRA and PEP. A popular guess [101] is that the next quark, denoted t, will have charge $e_t = 2/3$ and mass $m_t \approx 15\,\mathrm{GeV}/c^2$. What would be the characteristics of a hypothetical ζ family of $t\bar{t}$ bound states?

We would expect six or seven narrow $^3S_1$ ζ states below the t-flavor threshold. Leptonic widths of the vector states would decrease with principal quantum number at least as rapidly as

$$\Gamma(\zeta_n \to \ell^+\ell^-) \sim n^{-1}, \tag{9.1}$$

if the potential may be characterized by an effective power $\nu \lesssim 0$. The leptonic width of the ground state must respect the lower bound†$_{61}$:

$$\Gamma(\zeta \to e^+e^-) \geq \frac{(2/3)^2}{(1/3)^2}\frac{M_\Upsilon}{M_\zeta}\Gamma(\Upsilon \to e^+e^-) \approx 1.6\,\mathrm{keV}. \tag{9.2}$$

Of course we do not know in advance the charge and mass of the next quark (assuming it exists). The quark charge may be established by comparing the leptonic widths of ζ, ζ', ζ'' with those of Υ, Υ' and Υ'', if our experience with the Υ system is a reliable guide. Leptonic widths of the excited ζ states may be almost completely determined (up to the quark charge) by details of the interquark potential already fixed by the ψ and Υ families. This is certainly the case in the inverse scattering approach to the interaction [65, 89].

Our discussion of the nonrelativistic quantum mechanics of bound states is by no means exhaustive. Many of our general conclusions about quarkonium properties would not have been reached without the pathfinding calculations based on explicit potentials [102]. We have mentioned only in passing the inverse scattering methods [65] which lie beyond the scope of this review, although we believe them to offer great promise and freedom from theoretical biases†$_{62}$. A number of useful constraints on radiative decay rates of the psions have been derived using quantum mechanical sum rules [104] and related applications of the sum rules derived in section 2.5 have been made to light-hadron spectroscopy [105].

†$_{61}$ The result (9.2) follows from (7.3) if the quark masses and vector meson masses are in the same ratio. Larger values of $\Gamma(\zeta \to e^+e^-)$ would be expected if $\nu_{\mathrm{eff}} \approx 0$ or if Γ/e_Q^2 is universal.

†$_{62}$ The relative strengths and weaknesses of the inverse scattering method are assessed in ref. [103].

Finally, rigorous inequalities on the order of energy levels and other properties of bound systems have been derived by Martin and collaborators [106].

As fruitful as the nonrelativistic approach to quarkonium physics appears to be, we must bear in mind that it has not been given a firm theoretical basis. Within the framework of QCD, it is believed [107] that a static, flavor-independent potential will emerge as a correct description of the interactions of infinitely massive quarks. This has not been proved, however, and it is conceivable that no sensible static limit exists. For quarks of finite mass, relativistic corrections are present in principle. These may be estimated for the psions to be small but not insignificant. A self-consistent and fully relativistic treatment of the charmonium system is a worthwhile goal. For the moment, the best justification of the nonrelativistic approach derives from its experimental success.

What more can we expect to learn from the study of more massive quarkonium families? We believe the physics revealed by $Q\bar{Q}$ states near the flavor threshold to be largely independent of the quark mass because, as we have argued in section 8, dissociation into pairs of flavored mesons occurs at a fixed size, or classical turning point. The lowest-lying levels of heavier quarkonium systems will, however, probe the interquark potential at increasingly short distances. We do not expect quarkonium physics to provide particular insights into the nature of the confining force which operates at long distances. At interquark distances of a fermi or less, we expect that the nonrelativistic methods will at the least give qualitative insight into the character of the interaction, while providing useful mnemonics for the variation of observables with quark mass and excitation energy. Quantitatively reliable predictions appear to be nearly within reach. We eagerly await the experimental measurements and discoveries that will judge the ultimate worth of quarkonium quantum mechanics.

Acknowledgments

We are grateful to many of our colleagues for their interest, comments, questions, and wise insights. We wish especially to thank J.S. Bell, R.N. Cahn, U. Fano, S. Gasiorowicz, K. Gottfried, J.D. Jackson, C.N. Leung, H.J. Lipkin, A. Martin, P. Moxhay, J.J. Sakurai, J. Schonfeld and H.B. Thacker for instructive and enjoyable discussions. Members of Fermilab Experiment 288, the discoverers of the upsilons, first stimulated our interest in the subject of this review. Among them, C.N. Brown, S. Herb, W.R. Innes, L.M. Lederman and T. Yamanouchi deserve our special thanks. J.L.R. wishes to acknowledge the generous hospitality of Fermilab during the preparation of this article. We thank Trudi Legler for typing the lengthy manuscript with speed and good humor.

Notes added in proof

(1) The situation of the pseudoscalar charmonium states remains unsettled. Two recent experiments at SPEAR have presented evidence against the candidates depicted in fig. 3(a). Both the Mark II experiment [108] and the Crystal Ball experiment [109] report upper limits for the cascade

$$\begin{array}{l}\psi'(3684)\to\gamma+\chi(3454)\\ \qquad\qquad\quad\big\lfloor\!\!\to\gamma+\psi(3097)\end{array}$$

which are inconsistent with the previous world average [19]

$$B(3454)\equiv\Gamma(\psi'\xrightarrow{\gamma}\chi(3454)\xrightarrow{\gamma}\psi)/\Gamma(\psi'\to\text{all})=(0.6\pm0.4)\%.$$

The Mark II experiment gives $B(3454) < 0.12\%$, while the Crystal Ball experiment yields $B(3454) < 0.044\%$. The Crystal Ball experiment also reports

$$B(3591) \equiv \Gamma(\psi' \xrightarrow{\gamma} \chi(3591) \xrightarrow{\gamma} \psi)/\Gamma(\psi' \to \text{all}) < 0.05\%,$$

in conflict with the earlier observation [21] of $B(3591) = (0.28 \pm 0.12)\%$, and provides a limit on transitions from ψ to X(2830):

$$\frac{\Gamma(\psi \to \gamma + \text{X}(2830))\Gamma(\text{X}(2830) \to \gamma\gamma)}{\Gamma(\psi \to \text{all})\Gamma(\text{X}(2830) \to \text{all})} \lesssim 5 \times 10^{-5}$$

which is incompatible with the previous value [19] of $(1.4 \pm 0.4) \times 10^{-4}$. Finally, the Crystal Ball reports evidence for a new state U(2976) seen as a 5 standard deviation effect in the inclusive spectrum of photons in the decay $\psi' \to \gamma +$ anything. The U(2976) is a promising candidate for the η_c, and would imply a hyperfine splitting easily accommodated by the quarkonium theory.

(2) Measurements of the ratio $\sigma(e^+e^- \to \text{hadrons})/\sigma(e^+e^- \to \mu^+\mu^-)$ at the new PETRA storage rings in Hamburg [110] support the assignment $e_b = -\frac{1}{3}$ for the charge of the quark constituents of Y. In addition, the PETRA experiments indicate that the mass of the next quark with charge $e_Q = \frac{2}{3}$ (usually called the t-quark) must exceed approximately 15 GeV/c^2.

(3) Attention should be drawn to three theoretical contributions which have appeared since the submission of this report. The derivation of quantum mechanical sum rules has been discussed by Burnel and Caprasse [111]. A detailed comparison of the Coulomb-plus-linear potential model with data has been presented by the Cornell group [112]. Voloshin [113] has given a critical discussion of the applicability of potential models to quarkonium.

References

[1] Max Born, My life (Scribner's, New York, 1978) p. 225ff.
[2] V. de Alfaro and T. Regge, Potential scattering (North-Holland, Amsterdam, 1965).
[3] H. Harari, Beyond charm, in: Weak and electromagnetic interactions at high energies, eds. R. Balian and C.H. Llewellyn-Smith (North-Holland, Amsterdam, 1977) p. 613;
C. Quigg, Lectures on charmed particles, FERMILAB-Conf-78/37-THY.
[4] O.W. Greenberg, Quarks, Ann. Rev. Nucl. Part. Sci. 28 (1978) 327;
A.W. Hendry and D.B. Lichtenberg, Rep. Prog. Phys. 41 (1978) 1707.
[5] L.W. Jones, Rev. Mod. Phys. 49 (1977) 717.
[6] Particle Data Group, Phys. Lett. 75B (1978) 1.
[7] G.S. LaRue, W.M. Fairbank and A.F. Hebard, Phys. Rev. Lett. 38 (1977) 1011;
G.S. LaRue, W.M. Fairbank and J.D. Phillips, Phys. Rev. Lett. 42 (1979) 142;
G. Gallinaro, M. Marinelli, and G. Morpurgo, Phys. Rev. Lett. 38 (1977) 1255.
[8] R.P. Feynman, Photon-hadron interactions (Benjamin, New York, 1972).
[9] W. Marciano and H. Pagels, Phys. Rep. 36C (1978) 137.
[10] H.D. Politzer, Phys. Rep. 14C (1974) 129.
[11] J. Ellis, Deep hadronic structure, in: Weak and electromagnetic interactions at high energies, eds. R. Balian and C.H. Llewellyn-Smith (North-Holland, Amsterdam, 1977) p. 1.
[12] A. Buras, FERMILAB-Pub-79/17-THY, Rev. Mod. Phys., to be published.
[13] T. Appelquist and H.D. Politzer, Phys. Rev. Lett. 34 (1975) 43.
[14] M. Deutsch, Adv. Exp. Phys. 4 (1975) 63.
[15] G.T. Bodwin and D.R. Yennie, Phys. Rep. 43C (1978) 267.
[16] J.M. Jauch and F. Rohrlich, Theory of photons and electrons (Addison-Wesley, Reading, Mass., 1955) §12-6.
[17] J.J. Aubert et al., Phys. Rev. Lett. 33 (1974) 1404.
[18] J.E. Augustin et al., Phys. Rev. Lett. 33 (1974) 1406.

[19] G.J. Feldman and M.L. Perl, Phys. Rep. 33C (1977) 285.
[20] B. Wiik and G. Wolf, DESY Report No. 78/23.
[21] W. Bartel et al., Phys. Lett. 79B (1978) 492.
[22] K. Gottfried, in: Proc. 1977 Int. Symp. on Lepton and photon interactions at high energies, August, Hamburg, ed. F. Gutbrod (DESY, Hamburg) p. 667.
[23] J.D. Jackson, New particle spectroscopy, in: Proc. 1977 European Conf. on Particle physics, July, Budapest, Hungary, eds. L. Jenik and I. Montvay (Central Res. Inst. for Physics, Budapest) Vol. I, p. 603.
[24] V.A. Novikov, L.B. Okun, M.A. Shifman, A.I. Vainshtein, M.B. Voloshin and V.I. Zakharov, Physics Reports 41C (1978) 1.
[25] T. Appelquist, R.M. Barnett and K. Lane, Charm and beyond, Ann. Rev. Nucl. Part. Sci. 28 (1978) 387.
[26] E. Eichten et al., Phys. Rev. D17 (1978) 3090.
[27] J.D. Jackson, C. Quigg and J.L. Rosner, in: Proc. XIX Intern. Conf. on High energy physics, Tokyo, 1978, eds. S. Homma, M. Kawaguchi and H. Miyazawa (Physical Society of Japan, Tokyo, 1979) p. 391.
[28] Y. Hara, Proc. XIX Intern. Conf. on High energy physics, Tokyo, 1978, eds. S. Homma, M. Kawaguchi and H. Miyazawa (Physical Society of Japan, Tokyo, 1979) p. 824.
[29] J. Rosner, Phys. Rep. 11C (1974) 189;
R.H. Dalitz, in: Fundamentals of quark models, eds. I.M. Barbour and A.T. Davies (Scottish Universities Summer School in Physics, Edinburgh, 1977) p. 151.
[30] R.L. Jaffe and K. Johnson, Comments Nucl. Part. Phys. 7 (1977) 107.
[31] A. De Rújula, Howard Georgi and S.L. Glashow, Phys. Rev. D12 (1975) 147.
[32] Erwin Schrödinger, Ann. d. Physik 79 (1926) 361, 489; 80 (1926) 437; 81 (1926) 109. Translated in: Schrödinger, Collected Papers on Wave mechanics, by J.F. Shearer and W.M. Deans (Blackie and Son, London, 1928) pp. 1–12.
[33] Hans A. Bethe and Edwin E. Salpeter, Quantum mechanics of one- and two-electron atoms (Springer-Verlag, Berlin, 1957).
[34] H. Hellmann, Acta Physicochimica URSS I, 6 (1935) 913; IV, 2 (1936) 225; Einführung in die Quantenchemie (F. Denticke, Leipzig and Vienna, 1937) p. 286;
R.P. Feynman, Phys. Rev. 56 (1939) 340.
[35] E. Eichten et al., Phys. Rev. Lett. 34 (1975) 369.
[36] Albert Messiah, Quantum mechanics, transl. by G.M. Temmer (North-Holland, Amsterdam, 1961–62).
[37] M. Abramowitz and I.A. Stegun, eds., Handbook of mathematical functions (Dover Publications, New York, 1965).
[38] J.L. Rosner, C. Quigg and H.B. Thacker, Phys. Lett. 74B (1978) 350.
[39] C.N. Leung and J.L. Rosner, J. Math. Phys. 20 (1979) 1435.
[40] Harry J. Lipkin, Quantum mechanics: New approaches to selected topics (North-Holland, Amsterdam, 1973) pp. 322–324.
[41] W. Thomas, Naturwiss. 13 (1925) 627;
F. Reiche and W. Thomas, Z. Phys. 34 (1925) 510;
W. Kuhn, Z. Phys. 33 (1925) 408.
[42] J.C. Slater, Quantum theory of atomic structure (McGraw-Hill, New York, 1960).
[43] W. Heisenberg, Z. Phys. 33 (1925) 879.
[44] C. Quigg and J.L. Rosner, Comments Nucl. Part. Phys. 8 (1978) 11.
[45] Howard J. Schnitzer, Phys. Rev. D13 (1976) 74;
J. Kandaswamy, J. Schechter and M. Singer, Phys. Rev. Lett. 38 (1977) 933.
[46] T. Sterling, Nucl. Phys. B141 (1978) 272.
[47] Gordon Feldman, Thomas Fulton and Alberto Devoto, Nucl. Phys. B 154 (1979) 441
[48] R. Van Royen and V.F. Weisskopf, Nuovo Cim. 50 (1967) 617; 51 (1967) 583.
[49] C. Quigg and J.L. Rosner, Phys. Lett. 71B (1978) 153.
[50] J.M. Jauch and E.L. Hill, Phys. Rev. 57 (1940) 641;
D. Bergmann and Y. Frishman, J. Math. Phys. 6 (1965) 1855;
James D. Talman, Special functions: A group theoretic approach, based on lectures by Eugene P. Wigner (W.A. Benjamin, New York, 1968) ch. 13.
[51] S. Flügge, Practical quantum mechanics (Springer-Verlag, Berlin, 1971).
[52] P.M. Morse and H. Feshbach, Methods of theoretical physics (McGraw-Hill, New York, 1953).
[53] L.D. Landau and E.N. Lifshitz, Quantum mechanics, non-relativistic theory, transl. by J.B. Sykes and J.S. Bell (Pergamon Press, Oxford; Addison-Wesley, Reading, Mass., 1965).
[54] C.N. Leung and J.L. Rosner (unpublished).
[55] N. Fröman and P.O. Fröman, JWKB approximation: Contributions to the theory (North-Holland, Amsterdam. 1965).
[56] A.B. Migdal and V. Krainov, Approximation methods in quantum mechanics, transl. by A.J. Leggett (W.A. Benjamin, New York, 1969).
[57] A.B. Migdal, Qualitative methods in quantum theory, transl. by A.J. Leggett (W.A. Benjamin, New York, 1977).
[58] J.A. Wheeler, in: Studies in Mathematical physics: Essays in honor of Valentine Bargmann, eds. E.H. Lieb, B. Simon and A.S. Wightman (Princeton University Press, Princeton, 1976) p. 351.

[59] E.C. Kemble, The fundamental principles of quantum mechanics with elementary applications (Dover, New York, 1958);
R.E. Langer, Phys. Rev. 51 (1937) 669;
H.A. Kramers, Z. Phys. 39 (1926) 836.
[60] I.I. Gol'dman and V.D. Krivchenkov, Problems in quantum mechanics, transl. by E. Marquit and E. Lepa (Addison-Wesley, Reading Mass., 1961).
[61] M. Krammer and P. Léal Ferreira, Rev. Bras. Fis. 6 (1976) 7.
[62] C. Quigg and J.L. Rosner, Phys. Rev. D17 (1978) 2364.
[63] J.S. Bell and J. Pasupathy, Phys. Lett. 83B (1979) 389 and CERN-TH-2649.
[64] L.D. Landau and E.M. Lifshitz, Mechanics, transl. by J.B. Sykes and J.S. Bell (2nd ed., Pergamon Press, Oxford, 1969).
[65] H.B. Thacker, C. Quigg and J.L. Rosner, Phys. Rev. D18 (1978) 274, 287.
[66] P. Moxhay and J.L. Rosner (unpublished).
[67] R. Bertlmann, H. Grosse and A. Martin, Phys. Lett. 81B (1979) 59.
[68] A. Martin, private communication.
[69] G.S. Abrams et al., Phys. Rev. Lett. 34 (1974) 1453.
[70] S.W. Herb et al., Phys. Rev. Lett. 39 (1977) 252.
[71] J.H. Christenson, G.S. Hicks, L.M. Lederman, P.J. Limon, B.G. Pope and E. Zavattini, Phys. Rev. Lett. 25 (1970) 1523; Phys. Rev. D8 (1973) 2016.
[72] C.W. Darden et al., Phys. Lett. 76B (1978) 246.
[73] Ch. Berger et al., Phys. Lett. 76B (1978) 243.
[74] J.K. Bienlein et al., Phys. Lett. 78B (1978) 360.
[75] G. Flügge, in: Proc. XIX Intern. Conf. on High energy physics, Tokyo, 1978, eds. S. Homma, M. Kawaguchi and H. Miyazawa (Physical Society of Japan, Tokyo, Japan, 1979) p. 793.
[76] H. Spitzer, in: Proc. XIX Intern. Conf. on High energy physics, Tokyo, 1978, eds. S. Homma, M. Kawaguchi and H. Miyazawa (Physical Society of Japan, 1979) p. 255;
W. Schmidt-Parzefall, ibid., p. 260.
[77] W.R. Innes et al., Phys. Rev. Lett. 39 (1977) 1240, 1640(E).
[78] C.W. Darden et al., Phys. Lett. 78B (1978) 364.
[79] K. Ueno et al., Phys. Rev. Lett. 42 (1979) 486;
L.M. Lederman, private communication.
[80] G.P. Murtas, in: Proc. XIX Intern. Conf. on High energy physics, Tokyo, 1978, eds. S. Homma, M. Kawaguchi and H. Miyazawa (Physical Society of Japan, Tokyo, 1979) p. 269.
[81] P.A. Rapidis et al., Phys. Rev. Lett. 39 (1977) 526, 974(E).
[82] M. Machacek and Y. Tomozawa, Ann. Phys. (NY) 110 (1978) 407.
[83] R.N. Cahn and S.D. Ellis, Phys. Rev. D16 (1977) 1484.
[84] H.D. Snyder et al., Phys. Rev. Lett. 36 (1976) 1415;
B.C. Brown et al., FERMILAB-Pub-77/54-EXP (unpublished).
[85] H.J. Lipkin, Phys. Lett. 74B (1978) 399; Phys. Rev. Lett. 41 (1978) 1629.
[86] Yu.B. Rumer, Zh. Eksp. i Teor. Fiz. 38 (1960) 1899 [Sov. Phys.-JETP 11 (1960) 1365].
[87] Y. Nambu, Phys. Rev. D10 (1974) 4262.
[88] E. Eichten and K. Gottfried, Phys. Lett. 66B (1977) 286.
[89] C. Quigg, J.L. Rosner and H.B. Thacker, FERMILAB-Pub-79/52-THY.
[90] R. Barbieri, R. Gatto, R. Kögerler and Z. Kunszt, Phys. Lett. 57B (1975) 455;
E. Poggio and H.J. Schnitzer, Brandeis preprint (1979, unpublished).
[91] D. Beavis, S.Y. Chu, B. Desai and P. Kaus, UCR-78-6, Phys. Rev. D, to be published.
[92] B. Margolis, R. Roskies and N. DeTakacsy, submitted to IVth European Antiproton Conference, Barr, France, June 1978;
John L. Richardson, Phys. Lett. 82B (1979) 272;
P. Ditsas, N.A. McDougall and R.G. Moorhouse, Nucl. Phys. B146 (1978) 191.
[93] D. Yennie, Phys. Rev. Lett. 34 (1975) 239;
J.J. Sakurai, Physica 96A (1979) 300.
[94] J.D. Jackson, Lectures on the New Particles, in: Proc. Summer Institute on Particle Physics, 1976, ed. M.C. Zipf, Stanford Linear Accelerator Center Report SLAC-198, November 1977, p. 147.
[95] A. Martin, Phys. Lett. 70B (1977) 192;
V. Gupta and R. Rajaraman, Phys. Rev. D19 (1979) 697.
[96] H. Grosse and A. Martin, Phys. Lett. 79B (1978) 103.
[97] S. Okubo, Phys. Lett. 5 (1963) 165.
[98] G. Zweig, CERN reports TH-401 and TH-412 (1964), unpublished.
[99] J. Iizuka, K. Okada and O. Shito, Prog. Theor. Phys. 35 (1966) 1061;
J. Iizuka, Suppl. Prog. Theor. Phys. 37–38 (1966) 21.

[100] C. Quigg and J.L. Rosner, Phys. Lett. 72B (1978) 462.
[101] S. Meshkov, in: New frontiers in high energy physics, eds. Arnold Perlmutter and Linda F. Scott (Plenum, New York, 1978) p. 221.
[102] E. Eichten et al., Phys. Rev. Lett. 34 (1975) 369; 36 (1976) 500;
J.S. Kang and H.J. Schnitzer, Phys. Rev. D12 (1975) 841, 2791;
J. Gunion and R.S. Willey, Phys. Rev. D12 (1975) 174.
[103] C. Quigg, in: New frontiers in high energy physics, eds. Arnold Perlmutter and Linda F. Scott (Plenum, New York, 1978) p. 263.
[104] J.D. Jackson, Phys. Rev. Lett. 37 (1976) 1107;
T.N. Pham and T.N. Truong, Phys. Lett. 64B (1976) 51.
[105] H.J. Lipkin, FERMILAB-Conf-78/73-THY, to appear in Proc. 1978 Advanced Study Institute in Nuclear Theory, Banff, Alberta, Canada.
[106] A. Martin, Phys. Lett. 67B (1977) 330;
H. Grosse, Phys. Lett. 68B (1977) 343;
H. Grosse and A. Martin, CERN preprint TH. 2674.
[107] F. Feinberg, Phys. Rev. Lett. 39 (1977) 316;
T. Appelquist, M. Dine and I.J. Muzinich, Phys. Lett. 69B (1977) 231;
W. Fischler, Nucl. Phys. B129 (1977) 157.
[108] G.S. Abrams et al., SLAC-PUB-2350 (1979, unpublished).
[109] E. Bloom, invited talk at the 1979 Intern. Symp. on Lepton and Photon Interactions at High Energies, Fermilab.
[110] H. Newman, Ch. Berger, G. Wolf and S. Orito, invited talks presented at the 1979 Intern. Symp. on Lepton and Photon Interactions at High Energies, Fermilab.
[111] A. Burnel and H. Caprasse, Sum Rules for the Quarkonium Systems, Liège preprint (1979, unpublished).
[112] E. Eichten et al., Cornell preprint CLNS-425 (1979, unpublished).
[113] M.B. Voloshin, ITEP-86 (1978, unpublished).